Deanship of Graduate Studies

Al – Quds University

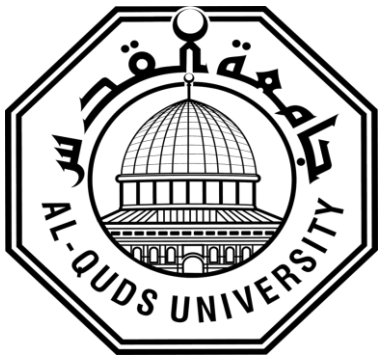


# Complexation of a linear polyelectrolyte with charged dendrimers: Polyelectrolyte length effect.

Nab’a Adnan Zahran

M.Sc. Thesis

Jerusalem – Palestine

1436/2015

Deanship of Graduate Studies

Al – Quds University

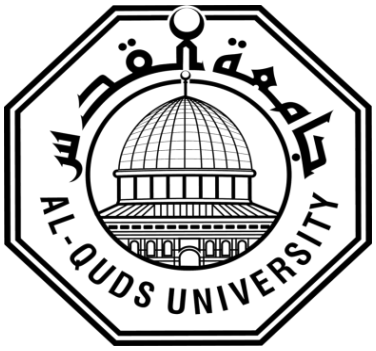


# Complexation of a linear polyelectrolyte with charged dendrimers: Polyelectrolyte length effect.

Prepared by:

Nab'a Adnan Zahran

Supervisor:

Dr. Khawla Qamhieh

A thesis submitted in partial fulfillment of requirement
for the degree of Master of Science in Physics

Jerusalem – Palestine
1436/2015

Deanship of Graduate Studies

Al – Quds University

Thesis Approval

# Complexation of a linear polyelectrolyte with charged dendrimers: Polyelectrolyte length effect.

Prepared by: Nab'a Adnan Zahran
Registration No: 21310180

Supervisor: Dr. Khawla Qamhieh

Master thesis submitted and accepted, date / /2015

The name and signature of examining committee member are as follows:

1. Head of the committee: Dr. Khawla Qamhieh Signature: ...……..…
2. Internal Examiner: Dr. Musa Abu Tair Signature: .....
3. External Examiner: Dr. Mohammad Abu Ja'far Signature: .....

Jerusalem – Palestine
1436/2015

## Dedication

Every challenging work needs self efforts as well as guidance of elders especially those who were very close to our hearts. My humble effort I dedicate to my parents who have always been my nearest and reverse nearest neighbors, and have been so close to me that I found them with me whenever I needed. It is their unconditional love that motivates me to set higher targets. Also, I dedicate this thesis to my sweet and loving husband Salem Ta'amrah , whose affection, love, encouragement and prays of day and night make me able to get such success and honor--- to my sisters and brothers who taught me that the best kind of knowledge to have is that which is learned for its own sake, and even the largest task can be accomplished if it is done one step at a time.Finally; I dedicate this thesis to my little fetus Ahmad.

## Declaration

I herewith declare that this thesis is based on the results found by myself. Materials of works found by other researchers are mentioned by references. This thesis, neither in whole or in part, has been previously submitted for any degree.

The work was done under the supervision of Dr. Khawla Qamhieh, at Al – Quds University, Palestine.

Name: Nab'a Adnan Zahran.

Sign:

Date: / /2015

## Acknowledgements

I would like to express my deepest appreciation to my thesis advisor, Dr. Khawla Qamhieh. I would like to thank her for giving the opportunity to work on this field of research and giving me support and technical advice, from fundamental research directionto last step in writing this thesis, throughout this time. I admire her broad spectrum ofknowledge in both theoretical physics and simulation methods and technique for biophysics. Without her guidance and persistent help this thesis would not have been possible.

I would like to thank my committee members, Dr. Mohammad Abu Ja'far (external examiner) and Dr. Musa Abu Tair (internal examiner) .

My gratitude also goes to the teacher assistant Doa' Hawamdeh from Berzuit University for her assistance in working on the simulation part by using Brawnain Dynamic technique.

I would also like to thank my family, my husband, friends, who stood beside me and encouraged me constantly.

I am also indebted many thanks to my department, to all doctors and techears who have made my experience as master thesis a truly memorable one.

Finally, I wish to express my gratitude to the Almighty Allah for providing the grant to make this thesis possible.

Nab'a Adnan Zahran

## Abstract

The complex formation between the positive charge spherical macroions (PAMAM dendrimers) and linear polyelectrolyte (LPE) chain has been studied using a new developed theoretical model describing the interaction between linear polyelectrolyte (LPE) chain with multible hard spheres. It was found that the wrapping length of LPE around macroions in alone, two and three spheres cases increases considerably by increasing the chain length until reaching a maximum value to become slightly constant at the end. The developed theory predicts that there are two regimes for a complex configuration as a function of the LPE length. Below some critical length, the chain is wound around two or three macroions which are close to each other. The overcharging increases with the lengthening of LPE. When the maximum overcharging degree is achieved, the linker appears and macroions start to separate from each other. All nonadsorbed LPE monomers are in the linker, and the tail appearance is unfavorable for the complexation with two or three macroions, but it is favorable to appear in the case of the complexation with one macroion.The developed model has been proved to be a suitable one to describe the complexation between the LPE and the macroions. The effect of the length of LPE chain, on the linker formed between three macroions-LPE chain complexes have been found, such that the optimal wrapping length increases with increasing LPE length until it reach to the critical value of the chain length. Above this critical length, the linker appears and then increases with the increasing of chain length.

In addition to the theoretical model, Brownian Dynamic simulation method is used to investigate how the negatively charged LPE interacts with three positively charged macroions. The simulation helps in studying the radius of gyration of the complex, which is found to increase at the beginning with small values and then at the end becoms slightly constant. The dynamics of the LPE-dendrimer complexes is studied by analyzing the distances between the dendrimer and each monomer of the LPE chain participating in the complex all the time; this shows that during the first μs, the LPE becomes closer to the dendrimer without wrapping around it. After that the LPE makes several energetic and random movements to find its optimal wrapping patterns on the dendrimer surface.

## Table of Contents

## List of Tables

## List of Figures

## List of Abbreviations

| | |
|---|---|
| DNA | Deoxyribonucleic acid |
| LPE | Linear Polyelectrolyte |
| PAMAM | Poly(amido amine) |
| $N_{ch}$ | Number of the monomers on the chain |
| $Z_{dend}$ | Number of functional groups of dendrimer |
| EDA | Ethylenediamine |
| MD | Molecular Dynamic |
| BD | Brownian Dynamic |
| bp | base – pair |
| $l_{opt}$ | The optimal wrapping length of chain around dendrimer |
| $l_{iso}$ | The length of the chain needed to neutralized the charge of dendrimer |
| dsDNA | Double strand DNA |
| ssDNA | Single strand DNA |
| $l_B$ | Bjerrum length |
| Cs | Salt concentration |
| G | Generation of dendrimer |
| CG | Coarse – grained |
| MRI | Magnetic Resonance Imiging |

# Chapter One

# Introduction

## 1.1 Introduction

The complextion of negatively charged LPE (Linear Polyelectrlyte) interacts with opositly charged macroions takes place in many studies in order to help us to understand some of the fundemental questions about the complexes formed between DNA (Deoxyribos Nuclic Acid). There have been numerous experimental, theoretical, and computer simulation studies on LPE compaction on various nanoscale objects, below we have many previous studies on spherical macroions with LPE chain complexation.

### 1.1.1 Experimental studies of spherical Macroions – LPE complexation.

Potentiometric titration experiments of poly(propylene imine) dendrimers (up to the fifth generation) were carriedout at salt concentrations of 0.1, 0.5 and 1.0 M KCl and NaCl, was done by Duijuenbode, Borkovec, and Koper [1]. The experiments were performed at two different locations on different instruments and were converted to titration curves using two different methods, resulting in a consistent experimental data set for the dendrimers measured. The titration curves feature two distinct steps around pH 6 and 10 with an intermediate plateau at 2/3 of the total ionizable groups.

The binding interaction between salmon sperm DNA of 2000bp ($L$ = 680nm) and PAMAM (Polyamido amine) dendrimers of G4 has been investigated by Örberg [2] Results based on dynamic light scattering (DLS) and steady-state fluorescence spectroscopy has made it possible to propose a binding model.

An experimental study carried by using cryo-TEM, dynamic light scattering (DLS) and fluorescence spectroscopy was done by Ainalem [3] showed that the morphologies of the aggregate formed between DNA and PAMAM dendrimers of different generations are affected by dendrimer size and charge at low charge ratio in dilute solution.

A recent experimental study performed by Carnerup and co-workers [4] They studied the condensation of DNA by dendrimer of generations G1, G2, G4, G6, and G8 as a function of salt concentration, and they observed there was an increase in the size of the aggregate formed by lower generations (G1, G2, and G4) when the salt concentration increases.

### 1.1.2 Computer simulation studies of spherical Macroions – LPE complexation

Cao and Bachmann [5] usedLangevin molecular dynamics simulations to study the complexation of a linear polyelectrolyte (LPE) chain with an oppositely charged soft nanoparticle, modeled by a spherical polyelectrolyte brush (SPB). By changing core radius of the SPB and length of polyelectrolyte (GPE) chains grafted at it, a structural transition from a

charged, LPE-covered sphere via a softer nanobrush toward a star-like polyelectrolyte is identified. As a result, the LPE chain develops various wrapping conformations around the SPB.

Jonsson and Linse [6]studied The complexation between a linear flexible polyelectrolyte and one or several oppositely charged macroions which was examined by employing a simple model system with focus on the electrostatic interactions. The complexation between a linear flexible polyelectrolyte and one or several oppositely chargedmacroions was examined by employing a simple model system with focus on the electrostaticinteractions.

The complexation of a PAMAM dendrimer with an oppositely charged LPE has been motivated many simulation studies aimed at understand the atomistic details of the process. Luylin and co-workers [7] performed Brownian dynamics computer simulations of complexes formed by charged dendrimer and oppositely charged linear polymer chain of different degree of polymerization (different number of monomers on the chain $N_{ch}$). They showed that when the monomers of the linear chains with$N_{ch}$ equal to number of dendrimer's terminal charged groups are located very close to these terminal groups.

A recent MD simulation study, Luylin and co-workers [8], showed that the maximum of the LPE chain adsorption occurs at some critical length of LPE chain. The first order phase transition from completely coiled conformation to the conformation with released tails takes place upon increasing the linear-chain length above the critical length. The one-long-tail conformation becomes energetically preferable.

Jonsson and Linse[9] again investigated a simple model with focus on the electrostatic interaction which has been used to examine thecomplexation of a linear polyelectrolyte possessing variable flexibility with one or severaloppositely charged macroions. Composition, structure, and thermodynamic properties of thecomplexes were obtained by using Monte Carlo simulations.

### 1.1.3 Theoretical studies of spherical Macroions – LPE complexation

Complexation of a polyelectrolyte with an oppositely charged spherical macroionis studied for both salt-free and salty solution was studied by Shklovskii and co-workers [10]. When a polyelectrolyte winds around the macroion, its turns repel each other and form an almost equidistant solenoid. It is shown that this repulsive correlations of turns lead to the charge inversion: more polyelectrolyte winds around the macroion than it is necessary to neutralize it. The charge inversion becomes stronger with increasing concentration of salt and can exceed 100%.

The condensation of DNA and poly(amido amine) dendrimers of generation 1, 2, 4, 6, and 8 as a function of salt concentration in order to reveal the forces that control the aggregate size and morphology was studied by Carnerup, Ainalem and Alfredsson [11]. For the lower generation dendrimers (1, 2, and 4) a dramatic increase in aggregate size occurs as a result of an increase in salt concentration.

The interaction between positively charged poly(amido amine) (PAMAM) dendrimers of generation 4 and DNA has been investigated by Qamhieh, Nylander, and Ainalem[12]. For two DNA lengths; 2000 basepairs (bp; *L* ) 680 nm) and 4331 bp (*L* ) 1472.5 nm) using a theoretical model by Schiessel for a semiflexible polyelectrolyte and hard spheres. The model was modifiedto take into account that the dendrimers are to be regarded as soft spheres, that is, the radius is not constant whenthe DNA interact with the dendrimer.

The interaction of a charged, semiflexible polymer with an oppositely charged sphere was studied by Nets and Joanny [13]. Both the effects of added salt (leading to a finite screening length) and of a bare stiffnessof the polymer are taken into account. For intermediate salt concentration and high enough sphere charge they obtain a strongly bound complex where the polymer completely wraps around the sphere.

Schiessel and co-workers[14] considered complexes formed between positively charged macroion and a persistence LPE. They studied first the case of complexation with a single hard sphere and calculated the wrapping length of the chain. Then they extended their consideration to complexes of many wrapped spheres.

Qamhieh and Abu Khaleel [15] investigated a theoretical model describing a linear polyelectrolyte (LPE) and ion-penetrable spheres has been developed and applied to investigate the interaction between linearized DNA and positively charged dendrimer of different generations. Through out the study, they emphasized on the effect of the medium's environments on the complexation of LPE chainwith one dendrimer.

### 1.2 Statement of the problem

Shklovskii and co-workers [16] studied the complexation of a polyelectrolyte with one cationic hard sphere. It was shown that the repulsive correlation of polyelectrolyte turns lead to charge inversion of dendrimers. Lyulin and co-workers [17] modefied the model to describe the interaction between LPE and two cationic hard spheres.

In our study we modified these two models to investigate the complexation of LPE with three cationic hard spheres. This is done to study the case of overcharging and so we can investigate charge inversion.

Beside to the calculations depends on the theoretical model, I did simulation to study the complexation of LPE with three macroions by Brownian dynamics silmulation.

As a note we have to take into account that all cationic hard spheres (macroions) used in this work are assumed to be PAMAM dendrimers, by using dendrimers charges and radii of different generations.

# Chapter Two

# Model and Method

## Chapter Two

### 2.1 Introduction

The method of study is mainly based on using a new theoretical model developed to study the complexation of LPE with three cationic macroions, in which some modifications has been made to a model that was developed by Shklovskii and co-workers [18], and expanding all of the parameters into this model to study their effect on the complex taking into account that the macroions are regarded as hard spheres.

### 2.2 Theoretical background

Gene therapy was first proposed nearly forty years ago as a method of manipulating cells at the molecular level in order to cure rare genetic diseases like cystic fibrosis, phenylketonuria and cancers. Researchers are testing several approaches to gene therapy, including:

- Replacing a mutated gene that causes disease with a healthy copy of the gene.
- Inactivating, or "knocking out," a mutated gene that is functioning improperly.
- Introducing a new gene into the body to help fight a disease [19,20].

Gene therapy takes place where drugs or genes are delivered into a cell in order to correct the genetic defects of damaged sites. Here the challenge is to be able to transport DNA, which generally is a very large, stiff and therefore bulky polyelectrolyte (PE), through the cell walls. This can be achieved by condensing DNA with an oppositely charged specimen, such as positively charged surfactants or PEs [21,22].

There are two main approaches to gene therapy, in vivo and ex-vivo. in vivo, which means interior (where genes are changed in cells still in the body). This form of gene therapy is called in vivo, because the gene is transferred to cells inside the patient's body. ex vivo, which means exterior (where cells are modified outside the body and then transplanted back in again). In some gene therapy clinical trials, cells from the patient's blood or bone marrow are removed and grown in the laboratory. The cells are exposed to the virus that is carrying the desired gene. The virus enters the cells and inserts the desired gene into the cells' DNA. The cells grow in the laboratory and are then returned to the patient by injection into a vein. This type of gene therapy is called ex vivo because the cells are treated outside the body [23-26].

There have been numerous experimental, theoretical, and computer simulations studies on DNA compaction on various nanoscale objects, these nanoscale objective can help us to understand some of the fundamental questions, namely, how the complex conformation depends on the various system parameters such as charge of the sphere and LPE chain( such as DNA), LPE chain length and sphere diameter and salt concentration of the surrounding medium[27]. Various nanoscale objects can be used in these studies, such as dendrimers [28-42] also, others used macroions[43-47] they showed that the overcharging phenomena of dendrimers or macroions

was observed when the length of LPE chain exceeds the length that is needed to neutralize the total charge of dendrimers or macroions. In the case of using dendrimers, the overcharging degree depends on dendrimer generation (size and charge) and salt concentration, also they concluded that the morphology and binding model of dendrimer – LPE chain depends on the generation. Dendrimer can mimic biological macromolecules such as enzymes, viral protein, antibodies, histone, and polyamine such as spermine and spermidine[48-50], as a consequence dendrimers form stable complexes with DNA and protect DNA against degradation, such properties make dendrimer excellent tools for gene delivery[51].

### 2.3 Macroions

The word macroion is a very large ion, especially a colloidal particle carrying an electric charge. Electrostatic interaction between macroions in aqueous solution containing macroions are ubiquitous in all living cells. The macroions maybe appears as charges lipid membrane, DNA, colloidal particle, proteins, viruses, and even entire cells. Macroions such as multivalent metal ions, dendrimers, charged micelles, and polyelectrolytes mediate electrostatic interactions between macroions. For example, divalent diamin ions induce the aggregation of rod-like M13 viruses, multivalent ions mediate network formation in action solution, multivalent counterions condense DNA, and positively charged collides form complexes with DNA[52]. The interaction between macroions can be illustrated in figure 2.1 bellow, which shows Electrostatic Interactions BetweenMacroions. DNA used as an example of negatively charged macroin, where protein as an example of positively charged macroion[53].

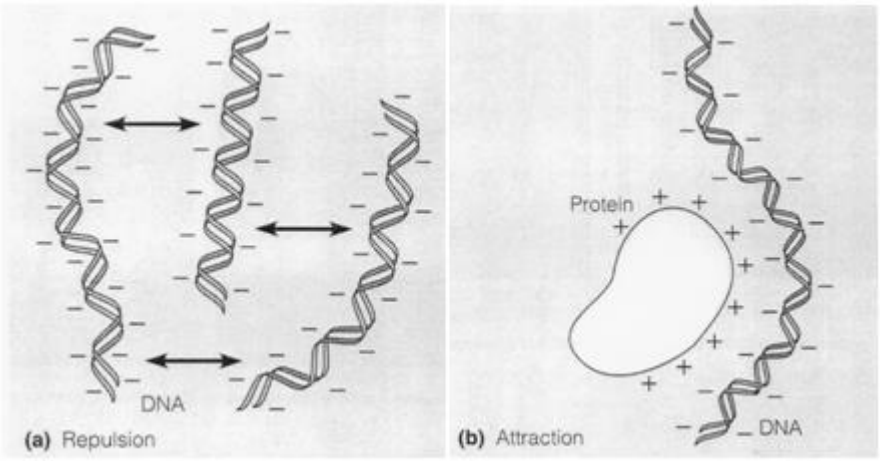


Figure 2.1: Electrostatic Interactions Between Macroions. DNA used as an example of negatively charged macroin, where protein as an example of positively charged macroion[53].

### 2.4 Dendrimers

Dendrimers are hyper-branched macromolecules comprising a multifunctional core denoted by C, several branching points denoted by B, and outer surface moieties denoted by O, so one can understand the word dendrimer which is derived from the Greek words dendron (‘tree’ or ‘branch’) and meros (‘part’) these shown in figure 2.2. Dendrimers are spherical polymeric

molecules which have several characteristics, such as size, weight, shape. Dendrimer size is classified by 'generation', wherein each generation corresponds to a layer of branching units unlike traditional linear polymer synthesis that produces a mixture of materials ranging in molecular weight. An opportunity to control dendrimer size, shape, and surface reactivity has brought these molecules to the forefront of biomedicine and drug delivery in particular.

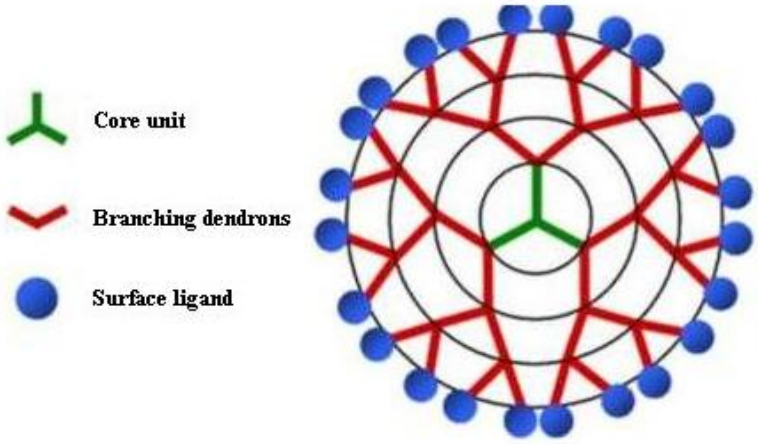


Figure 2.2 : Basic dendrimer components[54].

A dendrimer consists of a core, repeated iterations surrounding the core called dendrons, and the periphery groups which can be modified for ligand attachment. The number of branches emanating from the core can be counted as subsequent "generations." The chemistries of the dendrimers vary greatly to affect solubility, degradability, and biological activity; however, some of the more common building blocks used arepolyamidoamines (PAMAM), polyamines, polyamides, poly (aryl esters), polyesters, carbohydrates, and DNA. Dendrimers have a wide variety of applications, including drug delivery vesicles, therapeutic agents, imaging contrast agents, scaffold materials for tissue engineering, and artificial enzymes. The utility of dendrimers stems from the capability of tuning dendrimer characteristics, such as size, shape, and composition and the synthesis of dendrimers in a highly reproducible and consistent fashion. A useful property of dendrimers is that as the generation number increases, the dendrimer size increases and the terminal groups become more tightly packed together to regulate release rates from the dendrimer interior. The increased number of terminal groups allows for multiple ligand attachment sites and increases the probability of an affinity interaction. Also, the terminal groups are important because they can be hydrophobic or hydrophilic, anionic or cationic, all which determine its interactions in the solvent [55-57].

The dendrimer size linearly increases with every addition of a new branch point (generation, G), and the number of functional primary amine groups ($Z$) increases exponentially by $Z = N_c N_b^G$ where $N_c$represents the core multiplicity (for ethylenediamine$N_c$ =4, and ammonia $N_c$= 3), $N_b$is the branch cell multiplicity and equals to 2 in both cases, and G is the generation[58].

Table 2.1: Theoretical properties of Ethylenediamine cored PAMAM dendrimer (EDA core)[59].

| generation | Molecular weight | Measured diameter($A^0$) | Surface groups |
|---|---|---|---|
| 0 | 517 | 15 | 4 |
| 1 | 1430 | 22 | 8 |
| 2 | 3256 | 29 | 16 |
| 3 | 6909 | 36 | 32 |
| 4 | 14215 | 45 | 64 |
| 5 | 28826 | 54 | 128 |
| 6 | 58048 | 67 | 256 |
| 7 | 116493 | 81 | 512 |
| 8 | 233383 | 97 | 1024 |
| 9 | 467162 | 114 | 2048 |
| 10 | 934720 | 135 | 4096 |

For dendrimers, the interest of using them arises from their ease of synthesis with controlled structure and size, minimal cytotoxicity, biodegradability and high transfection efficiencies[60]. They enhance cytosolic and nuclear availability as indicated by Confocal microscopy as well as cell uptake and transfection efficiency of plasmid DNA.

### 2.4.1 Properties of dendrimers

Dendrimers are monodisperse macromolecules, unlike linear polymers. The classical polymerization process which results in linear polymers is usually random in nature and produces molecules of different sizes, whereas size and molecular mass of dendrimers can be specifically controlled during synthesis. Because of their molecular architecture, dendrimers show some significantly improved physical and chemical properties when compared to traditional linear polymers.

In solution, linear chains exist as flexible coils; in contrast, dendrimers form a tightly packed ball. This has a great impact on their rheological properties. Dendrimer solutions have significantly lower viscosity than linear polymers[61]. When the molecular mass of dendrimers increases, their intrinsic viscosity goes through a maximum at the fourth generation and then

begins to decline [62]. Such behavior is unlike that of linear polymers. For classical polymers the intrinsic viscosity increases continuously with molecular mass.

The presence of many chain-ends is responsible for high solubility and miscibility and for high reactivity [63]. Dendrimers' solubility is strongly influenced by the nature of surface groups. Dendrimers terminated in hydrophilic groups are soluble in polar solvents, while dendrimers having hydrophobic end groups are soluble in nonpolar solvents. In a solubility test with tetrahydrofuran (THF) as the solvent, the solubility of dendritic polyester was found remarkably higher than that of analogous linear polyester. A marked difference was also observed in chemical reactivity. Dendritic polyester was debenzylated by catalytic hydrogenolysis whereas linear polyester was unreactive.

Dendrimers have some unique properties because of their globular shape and the presence of internal cavities. The most important one is the possibility to encapsulate guest molecules in the macromolecule interior. It is possible to create dendrimers which can act as extremely efficient light-harvesting antennae [64,65]. Absorbing dyes are placed at the periphery of the dendrimer and transfer the energy of light to another chromophore located in the core. The absorption spectrum of the whole macromolecule is particularly broad because the peripheral chromophores cover a wide wavelength range. The energy transfer process converts this broad absorption into the narrow emission of the central dye. The light harvesting ability increases with generation due to the increase in the number of peripheral chromophores.

Biological properties of dendrimers are crucial because of the growing interest in using them in biomedical applications. "Cationic" dendrimers (e.g., amine terminated PAMAM and poly(propylene imine) dendrimers that form cationic groups at low pH) are generally haemolytic and cytotoxic. Their toxicity is generation-dependent and increases with the number of surface groups [66]. PAMAM dendrimers (generation 2, 3 and 4) interact with erythrocyte membrane proteins causing changes in protein conformation. These changes increase with generation number and the concentration of dendrimers. The interactions between proteins and half-generation PAMAM dendrimers are weakerAnionicdendrimers, bearing a carboxylate surface, are not cytotoxic over a broad concentration range [67]. Incubation of human red blood cells in plasma or suspended in phosphate-buffered saline with PAMAM dendrimers causes the formation of cell aggregates. No changes in aggregability of nucleated cells such as Chinese hamster fibroblasts are observed.

### 2.4.2 Applications of dendrimers

#### 2.4.2.1 Drug Delivery

Dendrimers are used for drug delivery because the carrier can improve solubility, increase circulation half-life, and improve drug transit across biological barriers. Polyamidoamine

(PAMAM) dendrimers have carried the antitumor drug methotrexate and fluorescein for tracking [68]. The peripheral amines were coated with acetyl groups to reduce charge at the dendrimer surface. The acetylated dendrimer was derivatized with folate as the target ligand to attach to the overexpressed folate receptors in KB tumors. The concentration of the dendrimer was 5-10 times higher than the control group with dendrimers without folate ligands. In mice, treatment with 15 biweekly intravenous injections showed reduced tumor growth rate when compared to mice treated with saline. The diameter of the dendrimers was less than 5 nm, which means that the drug could be quickly eliminated by the renal system. This results in a double-edged sword of reduced toxicity concomitant with reduced drug efficacy.

Gene therapy could also benefit from the use of positively charged dendrimerscomplexed to negatively charged DNA. Studies have shown reduced toxicity in transfected cells when compared to traditional polyamine agents [69]. However, to be useful in clinical applications, the issues surrounding the use of a positively charged carrier must be addressed because cationic substances are associated with toxic and hemolytic effects. We can see the use of dendrimer in this field in figure 2.3.

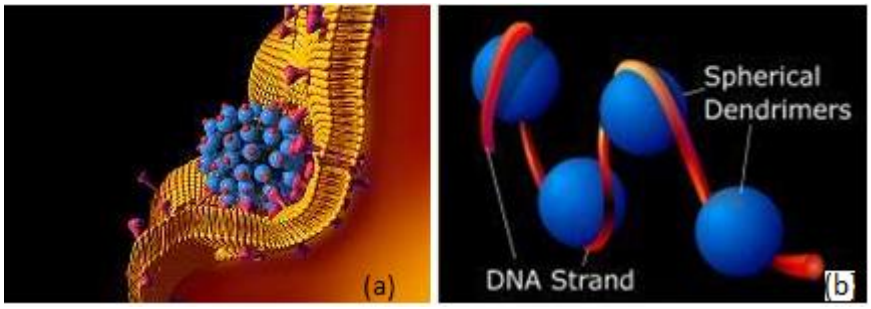


Figure 2.3: Using of dendrimers in drug delivery, Dendrimer attachment to cellular membrane (a) and Dendrimer conjugation to DNA strand (b) [70].

### 2.4.2.2 Therapeutics

While dendrimers can be used as drug carriers, they themselves can be used as therapeutic agents. One group exploited the branching properties of the dendrimers to induce removal of prion proteins in infected cells, which proved to be more effective than linear or small polyamines [71]. The multivalency of surface ligands on dendrimers was further used to demonstrate that this property could inhibit foreign agents, such as bacteria, viruses, and proteins from binding to the cell. Another study showed a G-4 poly(L-lysine) dendrimer with sulfate groups at the surface could bind electrostatically to viral envelope proteins and block viral entry into the cell [72].

### 2.4.2.3 Imaging

Dendrimers have been used as MRI (Magnetic Resonance Imiging) contrast agent and oxygen-tumor sensing agents. In tumors, the oxygen levels can be a measure or how well the tumor will respond to treatment. Consequently, dendrimers made of poly(glutamic acid), poly(aryl esther) or poly(ether amide) can be encapsulated with metallopolyphorins. These dendrimers are water-soluble, and the metallopolyphorins' phosphorescence is quenched upon collision with oxygen [73,74]. In vivo or in vitro measurements can be made by phosphorescence excitation with visible or IR light.

Dendrimers have also been recently used in the functional magnetic resonance imaging of the kidney which uses low-molecular weight contrast agents that can be filtered at the glomerulus but not absorbed or secreted by the tubules. Gadolinium-bound dendrimers are used in specific renal parenchymal diseases and its uptake is indicative of damage to the proximal straight tubule in the outer medulla [75]. Figure 1.4 below shows the use of dendrimers in medical imaging.

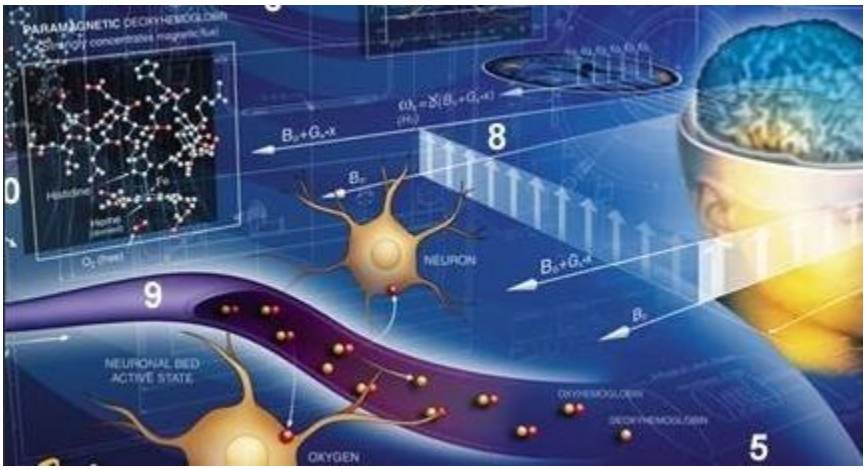


Figure 2.4: Using of dendrimers in medical imaging[77].

## 2.5 Polyelectrolyte

Polyelectrolytes are charged molecules that display a high solubility in water and strong adsorbing capacity on surfaces bearing an opposite charge, as shown in Figure 2.5. An interesting feature is that they can act both as a stabilizing and as a destabilizing agent in particle suspensions [78,79]. The long-range character of the electrostatic interactions gives polyelectrolytes very specific properties which are only partially understood from the theoretical point of view[80,81].

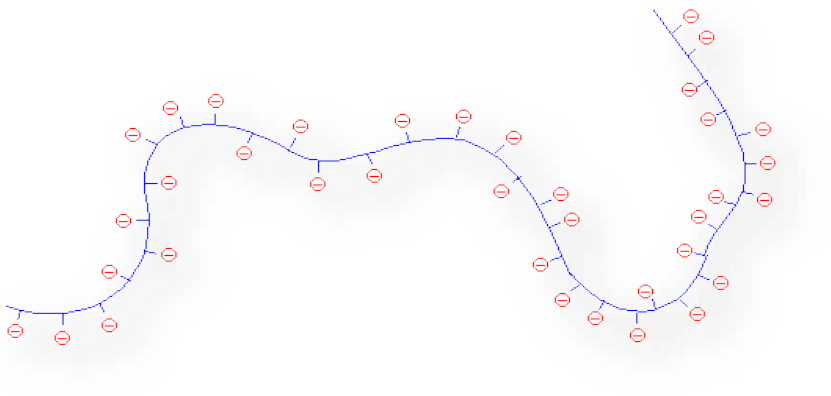

Figure 2.5 A polyelectrolyte expands because it's like charges repel each other[82].

In aqueous solution, polyelectrolyte chains strongly interact with other charged mesoscopic objects, and in particular, they tend to associate with charged objects of opposite sign and form complexes[83]. The complexing agent can be a flexible or a rigid polyelectrolyte, a small colloidal particle, a protein, or a surfactant aggregate such as a micelle or a vesicle. Apart from being interesting for a variety of applications, they are simple models for the complexation between a polyelectrolyte (such as DNA) and proteins or, more specifically, for histone-DNA complexes in nucleosomal core particles and for the interaction between polyelectrolytes and charged surfactant micelles or charged vesicles; in an extreme limit, these complexes can also be viewed as a model for the interaction between a polyelectrolyte and multivalent counterions [84-89]. Note that these examples are differentiated by the size of the spherical objects which varies over several orders of magnitude.

### 2.5.1 General characteristics of DNA

Deoxyribonucleic acid : the nucleic acid in which the sugar is deoxyribose, constituting the primary genetic material of all cellular organisms and the DNA viruses, and occurring predominantly in the nucleus. It is a linear or circular polymer with a backbone composed of deoxyribose moieties that are linked by phosphate groups attached to their 5' and 3' hydroxyls, with side chains composed of purine (adenine, guanine) and pyrimidine (cytosine, thymine) bases attached to the sugars. The strands are twisted to form a double helix and are antiparallel. DNA is duplicated by replication, and it serves as a template for synthesis of ribonucleic acid.

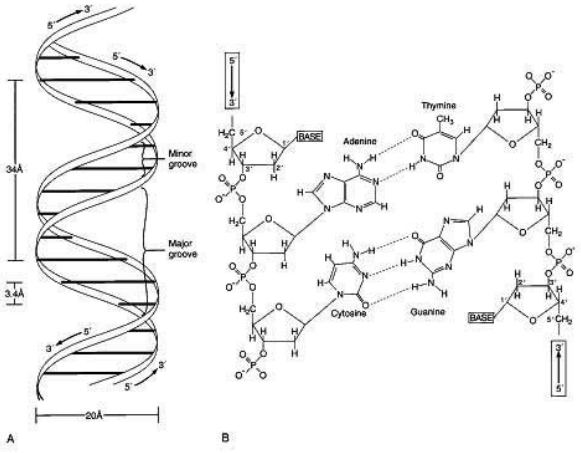


Figure 2.6: (a) Structure and dimention of B-form DNA, (b) Structure of a nucleotide[90].

The most important and most abundant form in which DNA can be found in nature is the double-helical B-form as it shown in Figure 2.6.a The double helix consists of two tightly associated polymer chains, each being a string of four interchangeable types of basic repeating units called nucleotides (see Figure 2.6.b). Each nucleotide unit contains a sugar-phosphate backbone element, which carries one negative charge. Attached to each sugar is one of four types of bases. These bases are classified into two types: cytosine (C) and thymine (T) are six-membered heterocyclic, organic compounds called pyrimidines (see Figure 2.7.a), while adenine (A) and guanine (G) are fused five- and six-membered rings called purines (see Figure 2.7.b). The length of each DNA backbone unit is about 0.34nm. The DNA double helix is mainly stabilized by hydrogen bonds between complementary bases on opposite strands forming base pairs (bp), which lie horizontally between the two spiraling strands. Adenine (A) forms a base pair with thymine (T), as guanine (G) does with cytosine (C) in DNA .

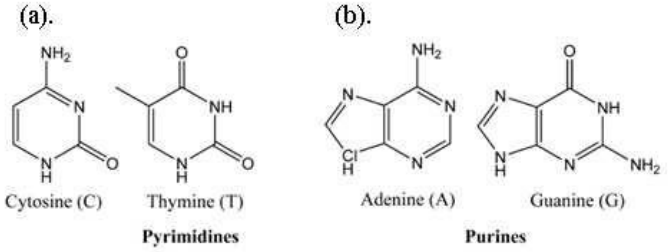


Figure 2.7: Major pyrimidine and purine bases of nucleic acids[90].

### 2.5.2 Importance of charge inversion

To deliver a LPE chain such as DNA from outside to the living cell, the charge of the DNA has to be screened or inverted, because the cell membrane possesses the potential of the same sign as DNA, which prevents the penetration of the DNA through the cell membrane if it is not overcharged, DNA has to be overcharged via complexation with oppositely charged macroion to penetrate through the membrane. As a vehicle for DNA such objects as proteins, dendrimers, micelles, etc. can be used. The formation of complexes DNA - cationic liposomes, when the

nucleic acids are completely encapsulated within the positively charged lipid bilayers, is another example of the overcharging [90]. Around 90% of the negative charges on the DNA need to be neutralized in order to overcome the intramolecular electrostatics repulsion[91], for this reason the cationic nature of the condensing agents is important in order to decreases the repulsion between the anionic phosphate groups of the DNA backbone, allowing condensation to occur.

## 2.6 Analytical model of the system

Consider a LPE of a linear charge density $\boldsymbol{\eta}$, and a radius of a, interacts with N spherical spheres each has a radius of R and a positive charge of Q. It is assumed that the LPE length L is greater than the neutralizing length $\boldsymbol{\mathcal{L}} = \frac{\boldsymbol{NQ}}{\boldsymbol{\eta}}$. The part of LPE $\boldsymbol{L_1 = NL_{s_i}}$ ,$\boldsymbol{i = 1, 2, \dots, N}$, is tightly wound around spheres. The rest of the chain with length $\boldsymbol{L_2 = L - L_1}$ can form (N-1) linkers with the length $\boldsymbol{L_{x_i}, i = 1, 2, \dots, N-1}$, which is the length of LPE chain formed between two succesive macroions, and two tails with length $\boldsymbol{L_{T_i}}$ ,$\boldsymbol{i = 1 or 2}$. as in figure 2.8.

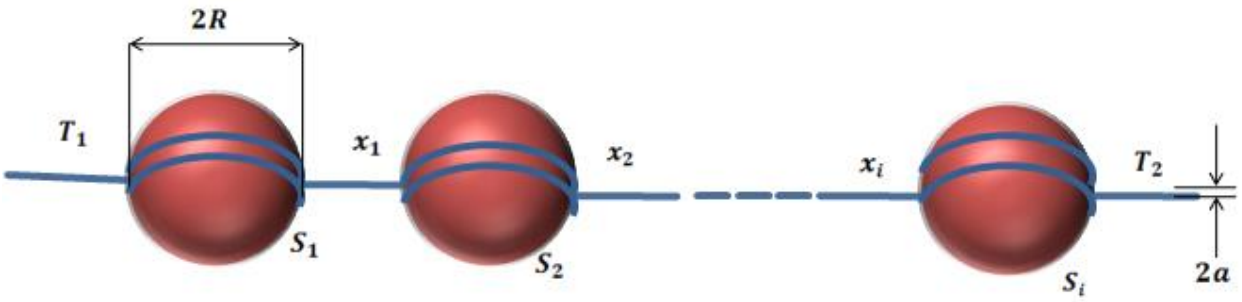


Figure 2.8 LPE wound around N spherical macroions. The nonadsorbed part of LPE forms (N-1) linkers and two tails.

The total energy of the system is presented in a similar way to Lyulin and co-workers [92] as a sum of self energies of nonadsorbed parts of LPE and spherical complexes (the hard sphere with wound LPE) and the interaction energies of complexes constitute with each other.

$$E = E_{self} + E_{int} \tag{2.1}$$

$$E_{self} = NE_{s_i} + (N-1)E_{x_i} + 2E_{T_i} \tag{2.2}$$

$E_{s_i}$is the self-energy of the sphere with wound LPE, $E_{T_i}$is the self energy of the straight tail, which is equal to $E_{T_i} = (L_T)\ln(\frac{L_T}{a})$,and have two of them, each one has a length of $L_T = \frac{L-L_1}{N-1}$, and $E_{x_i}$ is the self energy of the linker.

The interaction energy $E_{int}$ is a sum of energies of interaction of different parts of a complex.

$$E_{int} = E_{s_i s_j} + E_{x_i s_j} + E_{x_i x_j} + E_{T_i s_j} + E_{T_i x_j} + E_{T_1 T_2} \tag{2.3}$$

Where $\boldsymbol{i, j = 1, 2, 3}$ .... $\boldsymbol{. i \neq j}$.

The first term in eq. (2.3) is the interaction energy of the sphere with the wrapping length of the LPE wound. The second and fourth terms correspond to the interaction energies of tails or linkers with spherical complex. The remaining terms correspond to the interaction energy of tails with each other or with linkers.

Substitute all terms for self energy to give:

$$E_{self} = N(L_1 \ln\left(\frac{R}{a}\right) - L_1 \ln\left(\frac{L_1}{R}\right) + \frac{(L_1 - \mathcal{L})^2}{2R}) + (N-1)(L_x)\ln(\frac{L_x}{a}) + 2(L_T)\ln(\frac{L_T}{a}) \tag{2.4}$$

Where $L_x$ is the linker length.

And $E_{int}$ is the sum of the following terms:

The interaction energy of many spherical complexes is equal to

$$E_{s_i s_j} = \sum_{q=1}^{N} \frac{(N-q)(L_1 - \mathcal{L})(L_1 - \mathcal{L})}{q(2R+l) + (q-1)L_x} \tag{2.5}$$

Where $q = 1,2, \ldots N$.

The interaction energy of linkers with a spherical complex is given by

$$E_{x_i s_j} = \sum_{q=1}^{N-1} (2N - 2q)(L_1 - \mathcal{L}) \ln\left(\frac{L_x + (2q-1)R + (q-1)L_x}{(2q-1)R + (q-1)L_x}\right) \tag{2.6}$$

The energy of interaction of linkers of LPE with each other is written as

$$\begin{aligned} E_{x_i x_j} = \sum_{q=1}^{N-1} & (N - q - 1)(2L_x + 2qR + (q-1)L_x)\ln(2L_x + 2qR + (q-1)L_x) \\ & - (L_x + 2qR + (q-1)L_x)\ln(L_x + 2qR + (q-1)L_x) \\ & - (L_x + 2qR + (q-1)L_x)\ln(L_x + 2qR + (q-1)L_x) + (2qR + (q \\ & - 1)L_x)\ln(2qR + (q-1)L_x) \end{aligned} \tag{2.7}$$

The energy of interaction of tails of LPE with a spherical complex is given by

$$E_{T_i s_j} = \sum_{q=1}^{N}(2)(L_1 - \mathcal{L}) \ln\left(\frac{L_T+(2q-1)R+(q-1)L_T}{(2q-1)R+(q-1)L_T}\right) \quad (2.8)$$

The interaction energy of linkers with tails

$$\begin{aligned} E_{T_i x_j} = \sum_{q=1}^{N-1} & 2(L_x + L_T + 2qR + (q-1)L_x)\ln(L_x + L_T + 2qR + (q-1)L_x) \\ & - (L_T + 2qR + (q-1)L_x)\ln(L_T + 2qR + (q-1)L_x) \\ & - (L_x + 2qR + (q-1)L_x)\ln(L_x + 2qR + (q-1)L_x) + (2qR + (q \\ & - 1)L_x)\ln(2qR + (q-1)L_x) \end{aligned} \quad (2.9)$$

The interaction energy of tails with each other is written as

$$\begin{aligned} E_{T_1 T_2} = & (2L_T + 2NR + (N-1)L_T)\ln(2L_T + 2NR + (N-1)L_T) \\ & - (L_T + 2NR + (N-1)L_T)\ln(L_T + 2NR + (N-1)L_T) \\ & - (L_T + 2NR + (N-1)L_T)\ln(L_T + 2NR + (N-1)L_T) + (2NR + (N \\ & - 1)L_T)\ln(2NR + (N-1)L_T) \end{aligned} \quad (2.10)$$

Thus, by substituting these equations in equation(2.1), this equation represents the total free energy of the system in units of $\frac{\eta^2}{D}$, where D is the dielectric constant of water. Thus, the energy has a dimensionality of length, so we should multiply this equation by the factor of $\frac{K_B T L}{b^2}$ so the equation then becomes in unit of $k_B T$.We conclude this factor since $b = \frac{1}{\eta}$, and D is a constant (dielectric constant of water), so this factor is appeared.

### 2.7 Brownian Dynamic Simulation (BD):

BD is a dynamic simulation method that can be used to model the time-dependent behavior of a given molecular system[93,94]. Because of the large number of individual objects, it is impossible to include every atom in the solvent and the large molecules in molecular simulations. Therefore, in BD simulation the solvent is modeling using continuum models, along with a simplified description of the macromolecules. This model is known also as Implicit solvation model which is a method of representing solvent as a continuous medium instead of individual "explicit" solvent molecules. The thermal motion and hydrodynamic drag of the solvent are replaced by a suitable stochastic force on the macromolecules. Also, the ion concentration and dielectric properties of water are used in a continuum-based models for computation of the electrostatic forces between the macromolecules. The Brownian model assumed that the solvent damping is very large compared to inertial effects.

A scalable Brownian dynamics package, BD_BOX, written by using Fortran languge was developed to perform multiscale simulations of systems containing significant numbers of various molecular species. BD_BOX uses coarse-grained models of molecules, a coarse-grained description of a system regards large subcomponents as we see in figure 2.9 below. Each molecule consists of a number of spherical beads in various levels of resolution[93]. The potential energy of a system of spherical subunits is given as a sum of terms describing bonded and nonbonded interactions.

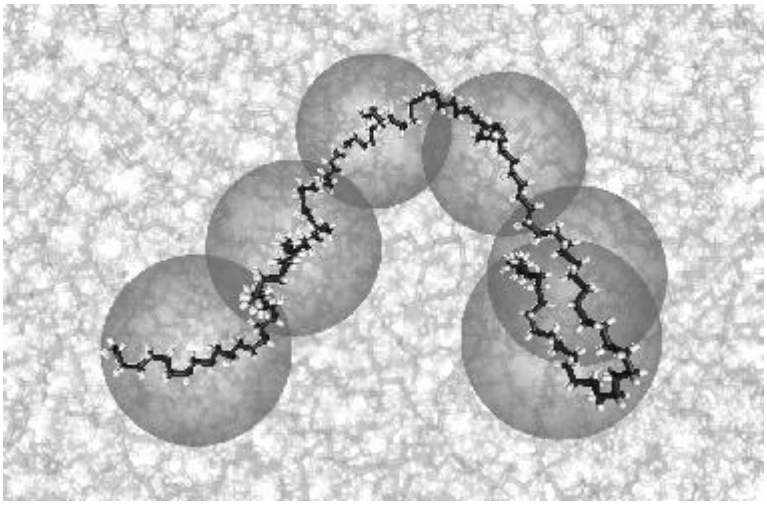

Figure 2.9 Illustrative figure of Coarse-graining system of molecules.[93]

### 2.7.1 Bonded Interactions

1) The potential which describes the connection between spherical subunits $i$ and $j$ is given by:

$$V_{ij}^{bond} = -\frac{1}{2}Hr_{max}^2 \ln\left(\frac{r_{max}^2 - r_{ij}^2}{r_{max}^2 - r_0^2}\right) - \frac{1}{2}Hr_{max}r_0 ln\left(\frac{(r_{max}+r_{ij})(r_{max}-r_0)}{(r_{max}-r_{ij})(r_{max}+r_0)}\right) \quad (2.11)$$

Where $H$ is the force constant, $r_0$ Is the equilibrium bond length, and $r_{max}$ is the maximal bond length[93].

2) The potential characterizing deformations of planar angles, which are the angles between the bonds connecting subunits $i, j$ and $j, k$ can be either:

$$V_{ijk}^{angle} = \frac{1}{2}k_{\varphi ijk}(cos\varphi_{ijk} - cos\varphi_{ijk}^0)^2 \quad (2.12)$$

Or

$$V_{ijk}^{angle} = \frac{1}{2}k_{\varphi ijk}(\varphi_{ijk} - \varphi_{ijk}^0)^2 \quad (2.13)$$

With $k_\varphi$ being the force constant and $\varphi^0$ the equilibrium angle.

3) Dihedral angles potential: the deformations of dihedral angles defined by four subunits $i, j, kand$are currently modeled either using simple harmonic functions:

$$V_{ijkl}^{dihe} = \frac{1}{2} k_{\theta ijkl} (\theta_{ijkl} - \theta_{ijkl}^{0})^2 \quad (2.14)$$

Where $k_\theta$ is the force constant and $\theta_0$ is the equilibrium angle, or with:

$$V_{ijkl}^{dihe} = \frac{1}{2} k_{\theta ijkl} \left(1 + \cos\left(\delta_{ijkl}\right) \cos\left(m_{ijkl}\theta_{ijkl}\right)\right) \quad (2.15)$$

Where $\delta_{ijkl} = 0$ or $\delta_{ijkl} = \pi$ and $m = 1,2, \ldots ,6$.

### 2.7.2 Nonbonded Interactions

Nonbonded interactions in BD_BOX include electrostatics and repulsive-attractive Lennard-Jones interactions. The Debye-Huckel approximation is used to model screened electrostatic interactions. Two spherical subunits with radii $R_i$ and $R_j$ and central charges $Q_i and Q_j$ interact via pairwise additive potentials of the form[93]:

$$V_{ij}^{el} = \frac{Q_i Q_j}{4\pi\epsilon_0 \epsilon (1+\kappa R_i)(1+\kappa R_j) r_{ij}} e^{-\kappa(r_{ij} - R_i - R_j)} \quad (2.16)$$

where $\epsilon_0$ is the vacuum permittivity, $\epsilon$ is the dielectric constant of the immersing medium, $\kappa$ is the inverse of the Debye screening length, and $r_{ij}$ is the separation of charges.

The repulsive interactions between subunits at small separations and attractive interactions at large separations, are evaluated using standard Lennard-Jones potentials:

$$V_{ij}^{LJ} = 4\epsilon_{ij}^{LJ} \left[ \left( \frac{\sigma_{ij}^{LJ}}{r_{ij}} \right)^{12} - \left( \frac{\sigma_{ij}^{LJ}}{r_{ij}} \right)^{6} \right] \quad (2.17)$$

Where $\epsilon_{ij}^{LJ} = \sqrt{\epsilon_i^{LJ} \epsilon_j^{LJ}}$ is the well depth and $\sigma_{ij}^{LJ} = R_i + R_j$. E It is also possible to model only purely repulsive interactions, without the long-range term.

### 2.7.3 Properties of the system

In our Brownian dynamics simulations of LPE-macroion we represent LPE by using a bead-spring model where each any two beads are connected together by elastic springs. While, a dendrimer is modeled by a positively charged sphere. This model of LPE is based on a linear flexible polyelectrolyte model used to study the complexation between a linear flexible polyelectrolyte and macroions. This model described LPE as a freely jointed chain of charged hard spheres each of them has a radius of 2.0Å and a charge of –e connected by harmonic bonds of spring constant of 0.576 kcal/(mol.Å$^2$). An illustrative figure of the system of LPE with one cationic macroions is shown infigure 2.3 below. The linear polyelectrolyte chain is represented by using bead rod model, so as we see in figure 2.10 the linear chain is represented as a system of $N_{ch}$ beads connected by rigid bonds of the same length. The macroions are represented as a hard sphere model of radius R and with charge Q = Ze as in figure 2.10.

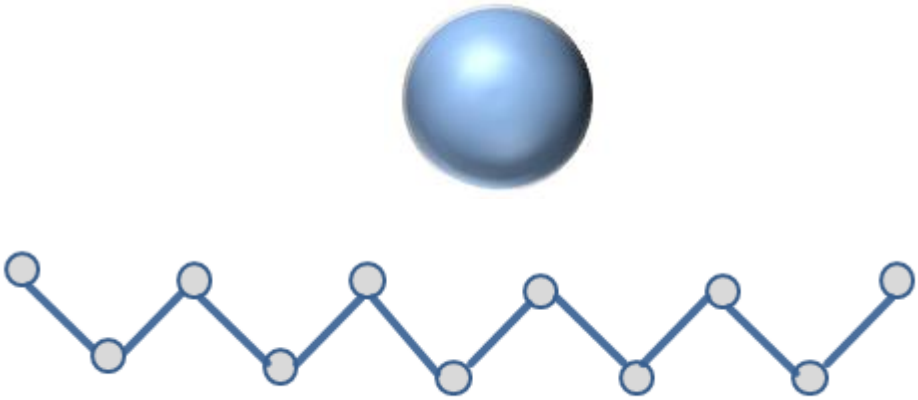

Figure 2.10 The freely jointed bead-rod model of LPE chain employed in this study. The macroions (dendrimers) are assumed to have hard sphere model.

# Chapter Three

# Results and discussions

## 3.1 Introduction

In this study the optimization method for finding the minimum of the total free energy for a system of cationic macroions that interact with LPE chain of contour length L is used by the essential tool of mathematics and modeling Maple 12 to find the optimal wrapping length of LPE chain around the macroions, the optimal length was found by taking the first derivative of the total equation and then solve it for length which is the optimal one. The linkers and tails are found by using some mathematical calculations. we also use the Origin lab program of version 8 for graphing and analyzing some of the theoretical results.

## 3.2 Effect of LPE chain length on the complexation.

The complexation between flexible LPE chain and oppositely charged spheres has been studied at variant chain length to understand the case of overcharging. The macroions spheres modeled as dendrimers of charge Z=24 and R=3.2 nm and LPE chain of radius a=0.4nm and total charge -48. Table 3.1 shows the theoretical predictions of the wrapping length of LPE on one maccroion for different lengths of LPE chain, once can see the following behavior (dotted line in figure.3.1); at small wrapping length which means that the difference between optimal wrapping length and neutralizing length i.e. $l_{opt} - l_{iso}$ is small, then the whole LPE chain collapses on the macroion. As the chain length L increases, the difference increases also and the whole LPE remains in the collapsed state. When L increases further, a first order phase transition happens and a tail with a finite length $L_T$ appears. The charge inversion can be calculated from the effective charge of the complex $Z_{compl}(e)$ , as we see the complex is overcharged for all optimal wrapping lengths, but we see that the overcharging increases until it reach a maximum value of wrapping length and then keep slightly constant, thus we can call this mechanism of charge inversion 'metallization' which means the elimination of self-energy. If we go now to the difference between the optimal length and the isoelectric length ( the same as neutralizing length $l_{iso} = Z * b$, where Z is the charge of LPE chain, and $b = \frac{1}{\eta}$). We notice that the difference has a positive value that is increasing until reach the maximum optimal length and then decreased again to become almost constant at the end. For this system we can see that for small wrapping length, all of the LPE chain is collapsed around the macroion, after that first order phase transition occurs which relates to the appearance of tail, for this system after $l_{opt} = 67.164$nm the tail is appearing and increasing in length as the chain length increased. In table.1 also, we notice that the number of turns increases by increasing the chain length until it reaches the maximum wrapping length and after that it almost constant, as we see in figure.3.2 (dotted line).

Table 3.1 Analytical model results for the interaction of LPE (charge -48e) with one macroion of radius R=3.2nm and total charge of 24e.

| Chain length L(nm) | Optimal wrapping length per one macroion $l_{opt}$ (nm) | $Z_{compl}(e)$ | $Diff = l_{opt} - l_{iso}$(nm) | tail length $L_T(nm)$ | No. of turns |
|---|---|---|---|---|---|
| 50 | 49.782 | -25.782 | 1.782 | 0.218 | 2.47 |
| 60 | 59.755 | -35.755 | 11.755 | 0.245 | 2.97 |
| 70 | 69.715 | -45.715 | 21.715 | 0.285 | 3.46 |
| 87 | 86.43 | -62.43 | 86.43 | 0.57 | 4.29 |
| 88 | 67.164 | -43.164 | 19.164 | 20.836 | 3.34 |
| 90 | 67.145 | -43.145 | 19.145 | 22.855 | 3.33 |
| 100 | 67.2559 | -43.256 | 19.2559 | 32.7441 | 3.33 |
| 102 | 67.2559 | -43.256 | 19.2559 | 34.7441 | 3.33 |
| 104 | 67.2559 | -43.256 | 19.2559 | 36.7441 | 3.33 |
| 110 | 67.2559 | -43.256 | 19.2559 | 42.7441 | 3.33 |
| 120 | 67.2559 | -43.256 | 19.2559 | 52.7441 | 3.33 |

Table 3.2 Analytical model results for the interaction of LPE (charge -48e) with two macroions each of radius R=3.2nm and charge of 24e.

| Chain length L(nm) | Optimal wrapping length per one macroion $l_{opt}$ (nm) | $Z_{compl}(e)$ | $Diff = l_{opt} - l_{iso}$(nm) | linker length $L_x(nm)$ | No. of turns per one macroion |
|---|---|---|---|---|---|
| 50 | 24.95 | -0.95 | 1.9 | 0.05 | 1.24 |
| 60 | 29.95 | -5.95 | 11.9 | 0.05 | 1.48 |
| 70 | 34.95 | -10.95 | 21.9 | 0.05 | 1.73 |
| 87 | 43.215 | -19.215 | 38.43 | 0.1425 | 2.15 |
| 88 | 43.95 | -19.95 | 39.9 | 0.025 | 2.18 |
| 90 | 44.95 | -20.95 | 41.9 | 0.05 | 2.23 |
| 100 | 49.95 | -20.95 | 51.9 | 0.05 | 2.48 |
| 102 | 41.5825 | -17.582 | 35.164 | 9.1475 | 2.06 |
| 104 | 41.5828 | -17.582 | 35.164 | 10.4175 | 2.06 |
| 110 | 41.5825 | -17.582 | 35.164 | 13.4175 | 2.06 |
| 120 | 41.5825 | -17.582 | 35.164 | 13.4157 | 2.06 |

Table 3.3 Analytical model results for the interaction of LPE (charge -48e) with three macroions each of radius R=3.2nm and charge of 24e.

| Chain length L(nm) | Optimal wrapping length per one macroion $l_{opt}$ (nm) | $Z_{compl}(e)$ | $Diff = l_{opt} - l_{iso}$(nm) | linker length $L_x(nm)$ | No. of turns |
|---|---|---|---|---|---|
| 50 | 15.409 | 8.591 | -1.773 | 1.257 | 0.766 |
| 60 | 18.383 | 5.617 | 7.149 | 1.617 | 0.914 |
| 70 | 21.93 | 2.07 | 17.79 | 1.403 | 1.09 |
| 87 | 25.334 | -1.334 | 28.002 | 3.666 | 1.26 |
| 88 | 25.5 | -1.5 | 28.5 | 3.833 | 1.268 |
| 90 | 26.09 | -2.09 | 30.27 | 3.91 | 1.29 |
| 100 | 29.886 | -5.886 | 41.658 | 3.447 | 1.48 |
| 102 | 30.446 | -6.446 | 43.338 | 3.554 | 1.51 |
| 104 | 30 | -6 | 42 | 4.667 | 1.49 |
| 110 | 30 | -6 | 42 | 6.667 | 1.49 |
| 120 | 30 | -6 | 42 | 6.667 | 1.49 |

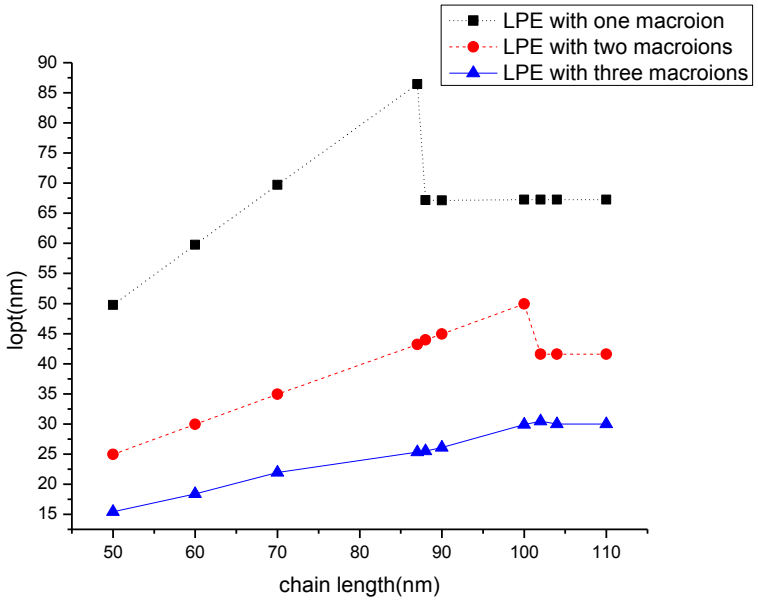


Figure 3.1. The length of wrapping LPE chain (per one macroion) versus the LPE length for the complex formed by one macroion and flexible LPE (dotted line), for two spherical macroions and flexible LPE (dashed line), for three spherical macroions and flexible LPE ( solid line). Macroion radius R=3.2nm, $Q_{macroion} = 24e$.

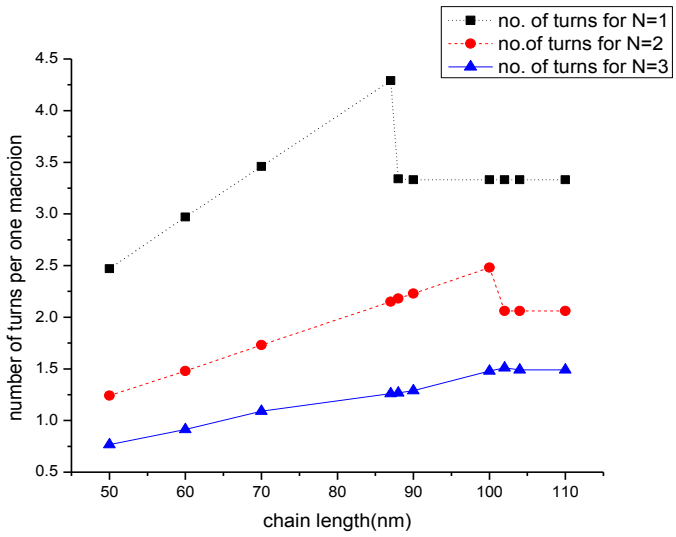


Figure.3.2: Effect of LPE chain length on the number of turns on the macroions in the case of one, two and three macroions, each with charge Z=24, and radius R=3.2 nm.

Table 3. 2 shows the optimal length that wrapped around two macroions each of total charge Z=24 and radius R=3.2. As we see from the table, optimal wrapping length per one macroion keeps increasing until it reached a maximum value which is equal to 49.95 nm at L= 100 nm, so in this regime, when the difference between optimal length and neutralizing length is small, the whole LPE chain collapses on the two macroions. After this maximum value the wrapping length per one macroion is reaching a maximum value and the whole LPE chain is still in the collapsed state. When the chain length increases more and more there is a transition state and linker will be formed between these two macroions. The effective charge of the complexation can be calculated by using $Z_{compl} = Z_{macroion} - Z_{conden}$, where $Z_{conden} = \frac{l_{opt}}{b}$ ,where b is the distance between two successive negative charges on the LPE chain, which is found by using the formula $b = \frac{1}{\eta}$, where $\eta$ is the linear charge density of LPE which is equal to Q/L. At the neutralizing length $\mathcal{L} = Z * b$, the total charge of the complex is zero, since the positive charge on the macroion is equal to the negative charge on the chian. To understand the case of overcharging for LPE wrapping around two macroions, our model predicts that there are two regimes for a complex configuration as a function of the LPE length. The chain is completely wound around two macroions which are close to each other at the region below some critical length, so; the overcharging increases with the lengthening of LPE. The appearance of linker and macroions start to separate takes place when the maximum overcharging degree is achieved and all nonadsorbed LPE monomers will participate in the formation of linker linker, and the tail appearance is unfavorable for this case, but it is favorable to appear in the case of one macroion. The difference between optimal wrapping length and isoelectric length in this case has a positive value that is increasing until reach the maximum optimal length and then decreased again to become almost constant at the end. If we have a look on figure 3.2 again we notice that the

number of turns keeps increasing until it reaches the maximum value of the optimal length, and we notice that the number of turns decreases by a little value, and this correspond to the formation of linker between these two macroions, and then it remains slightly constant.

The theoretical study of the comlexation of LPE with three macroions is shown in Table 3.3. Nevertheless, we did not see any discrepancy in what obtained earlier for the complexation of LPE with one or two macroions in the behavior of optimal wrapping length, that is at small values it completely collapsed on the macroions, after that when the chain length increases further, part of LPE chain collapsed on the three macroions, and then linkers formation appears. Now the effective charge of the complexation can be calculated which is found to be positive in values until reach optimal length per one macroion $l_{opt} = 21.93\text{nm}$ which means that the charge of the macroion is not reversed yet, and the overcharging is not achieved. After that the net charge of the macroion-LPE coplexation becomes negative which means that the complex is overcharged. If we go now to the difference between the optimal length and the isoelectric length, we notice that at the first the difference has a negative sign then becomes positive and has the same trend as in the previous two cases of LPE with one or two macroions. The negative sign indicates that the macroion is not completely neutralized by oppositely charged LPE chain. According to the number of turns, it increases until reach a maximum value and then has constant value.

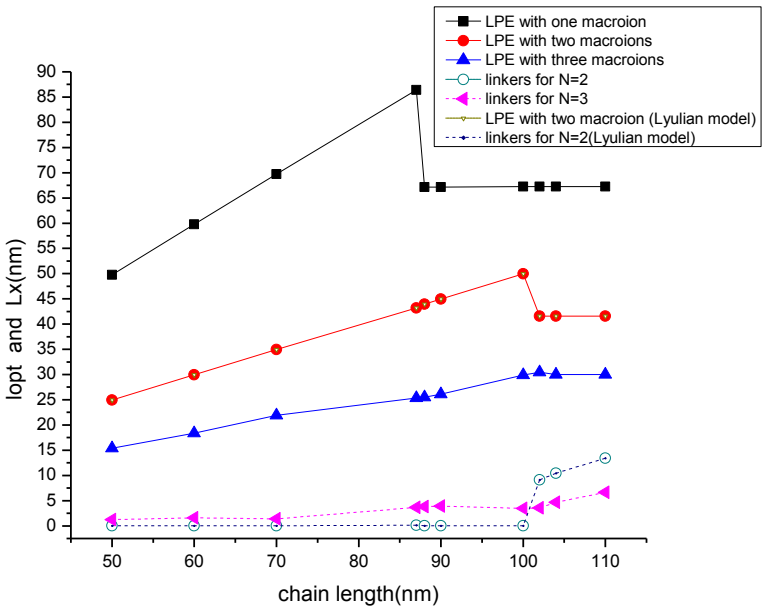


Figure.3.3 The formation of linkers for the complexes formed by two and three macroions with charge Z=24 and radius R=3.2nm with LPE chain with different lengths.

The current developed theory predicts that there are two regimes for a complex configuration as a function of the LPE length. Below some critical length, the chain is wound around two or three macroions which are close to each other. The overcharging increases with the lengthening of

LPE. When the maximum overcharging degree is achieved, the linker appears and macroions start to separate. All nonadsorbed LPE monomers are in the linker, and the tail appearance is unfavorable for these two cases (LPE with two or three macroions), but it is favorable to appear in the case of one macroion. For the complex formed by a single macroion, the tail appearance is a first-order phase transition and is accompanied by a sharp decrease of the amount of adsorbed monomers. In contrast to it, in the case of two and three macroions, the appearance of a linker does not change the length of the adsorbed part.

Figure .3.4 shows the theoretical prediction of the wrapping length of LPE on macroions for different lengths of LPE chain with one, two and three macroions to be compared with the predictions of shklovskii hard sphere model (Nguyen and Shklovskii, 2001) for LPE chain with one macroion and Lyuliian model (Lyulin, 2010) for LPE chain with two macroions. Upon increasing of the chain length the number of the condensed monomers (wrapping length) increases linearly until we reach to chain length which is critical and the number of the condensed monomers at this point is maximum *i.e.*, the overcharging of macroions is maximum. We point here that all studies are in agreement with each at $L < L_{citical}$ the macroions are always overcharged at all chain lengths, whereas at $L > L_{citical}$,, our model shows a saturation in the condensed monomers which shows agreement with the other two models. In general the saturation or little decrease in the condensed monomers of LPE chain is attributed to the increasing in the electrostatic repulsive free energy between chain monomers which is larger at maximum overcharging of macroions**.**

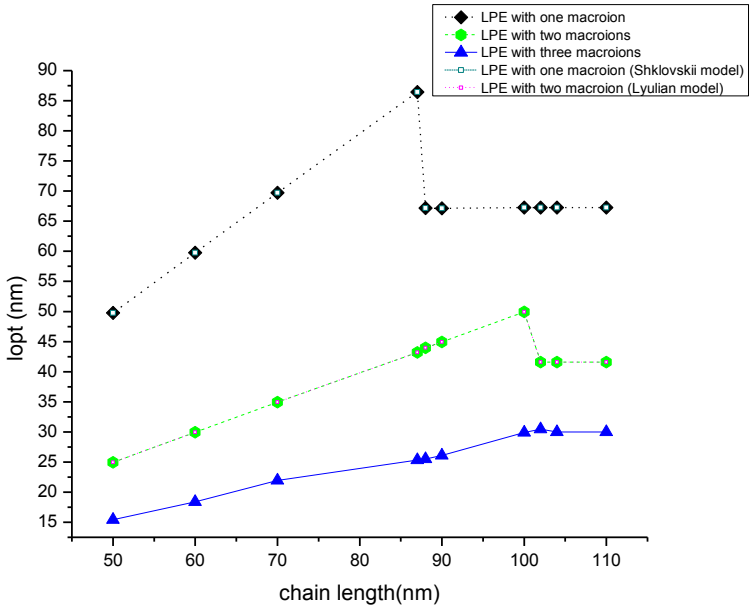


Figure 3.4. Comparison of the model developed by Shklovskii for LPE with one macroin, the model developed by Lyulian for LPE with two macroions, and the current model for LPE with three macroions. The macroions used as spherical complex with radius R=3.2nm and total charge of 24e.

The effect of the length of LPE chain, on the linker formed between $3G_x$-LPE chain complexes has been studied. In order to get stable LPE chain- $3G_3$complexes for different LPE lengths, the total free energy was minimized. In all cases the LPE exceeds the length needed to neutralize the $3G_3$ dendrimer. As it shown in Figure.3.5, the configuration of the complexes strongly depends on the length of the LPE chain. The total length of LPE divided into two parts, the optimal wrapping length per one macroion and the linker. The optimal wrapping length per one macroion increases with increasing LPE length until it reachs to the critical value of the chain length. Above this critical length, the linker appears and then increases with the increasing of chain length. Comparing with the result by LPE chain- $3G_3$ complexes, which shows also linker formation, this linker is shown to increase slowly with the increasing of the chain length. Schematic representation shows the effect of chain length on the linker and the optimal wrapping length obtained by the hard sphere model is shown in Figure 3.5

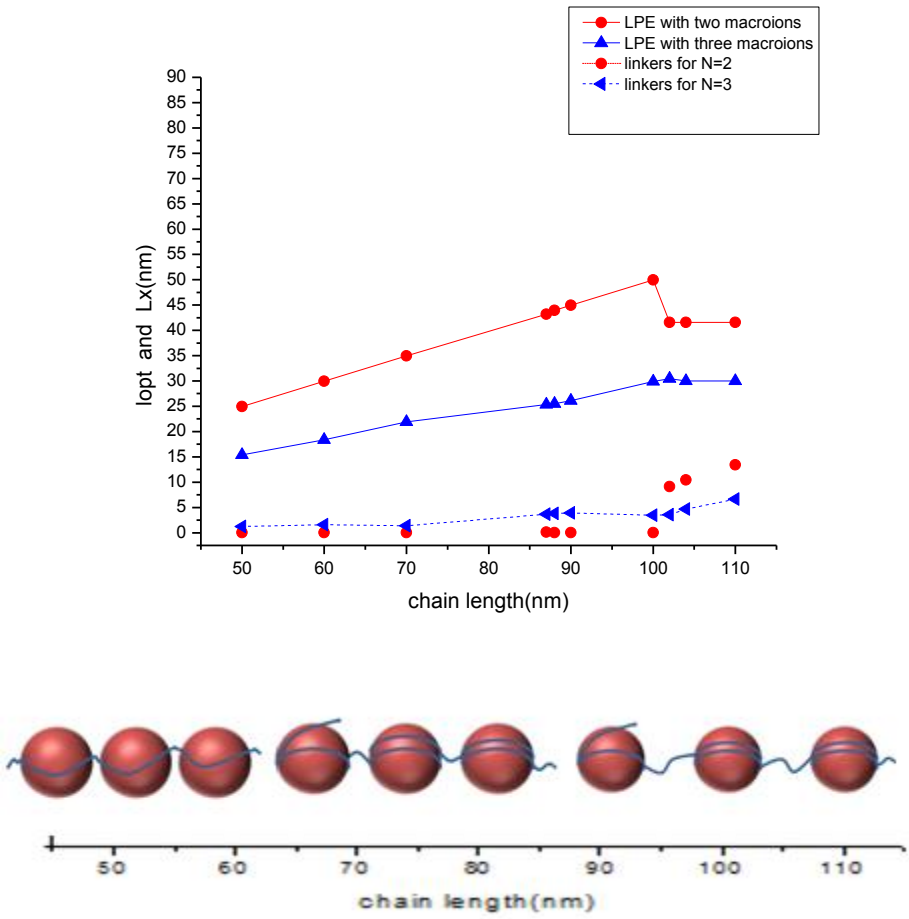


Figure.3.5 : The length of the wrapping chain on dendrimer as a function of chain length. A system of $3G_3$complexes with an oppositely charged flexible LPE of radius 0.4 nm and monomer spacing of 1nm.

### 3.3 Effect of dendrimer size on the complexation and the overcharging

The complexation between flexible LPE chain at variant chain length and an oppositely charged sphere has been studied at different radii and charges of hard spheres to understand the dependence of the case of overcharging on the variation of radius and charge of the dendrimer in the complex.

The value of the adsorbed charge and the lengths of unadsorbed LPE parts have been estimated by using numerical minimization method, calculations show that the most probable complex configuration is that with three dendrimers connected by two linkers without tails. Chain length dependence of the number of adsorbed LPE monomers (wrapping length) and number of monomers in the linkers ( unwrapping length) are presented in Figure. 3.6. For short LPE, the dendrimers are close to each other. LPE remains to be adsorbed on dendrimers up to some critical value of *L* where the linkers appears and dendrimers start to separate. All nonadsorbed LPE part goes into a linker. The value of the adsorbed charge does not change with the linker appearance and remains almost constant by further increase of the LPE length. Such a behavior is similar to the case of LPE with two macroions, but it is different from that for a complex comprised by one spherical macroion where the adsorbed charge sharply decreases with the tail appearance. The absence of the sharp change of the adsorbed charge after the linkers formation for the complex formed by three or two dendrimers shows that, in contrast to the case of one dendrimer, the first-order phase transition is absent.

It can also be seen that the maximum degree of the overcharging is observed in the complex comprised by a single dendrimer. Addition of another dendrimer decreases the value of the adsorbed charge per one dendrimer due to the electrostatic repulsion between them. Correspondingly, the linker appears at lower values of LPE length (per one dendrimer).

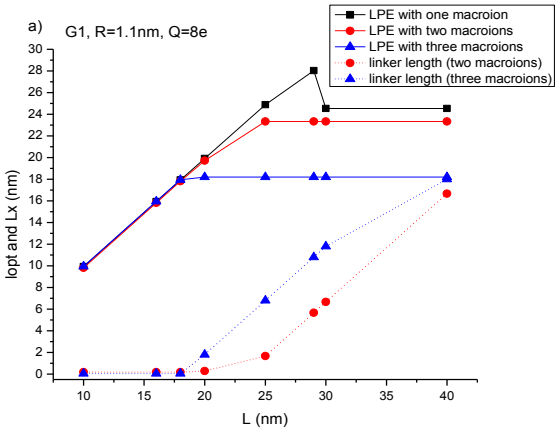


Figure.3.6a The wrapping length and the linker length as a function of the LPE length for the complex formed by one two and three spherical denrimers and flexible LPE, PAMAM dendrimers (ethylenediamine cores) of generations G1 has the radius R= 1.10 nm and charges of Q= 8.

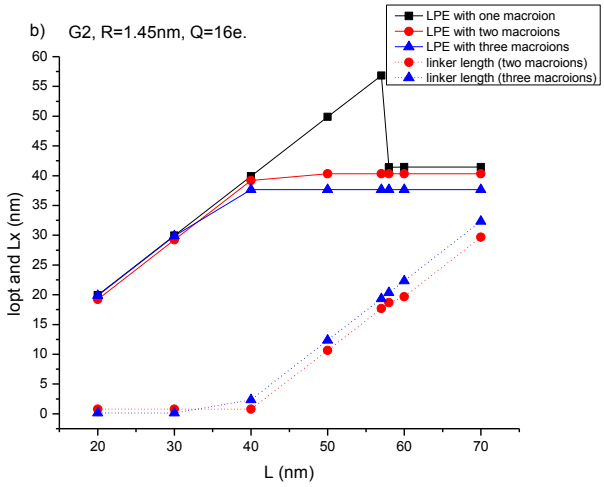


Figure.3.6b The wrapping length and the linker length as a function of the LPE length for the complex formed by one two and three spherical denrimers and flexible LPE, PAMAM dendrimers (ethylenediamine cores) of generations G2 has the radius R= 1.45 nm and charges of Q= 16.

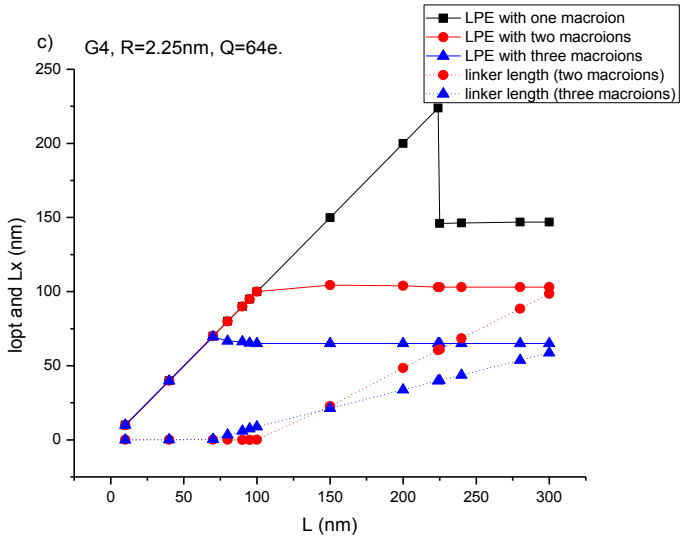


Figure.3.6c The wrapping length and the linker length as a function of the LPE length for the complex formed by one two and three spherical denrimers and flexible LPE, PAMAM dendrimers (ethylenediamine cores) of generations G4 has the radius R= 2.25 nm and charges of Q= 64.

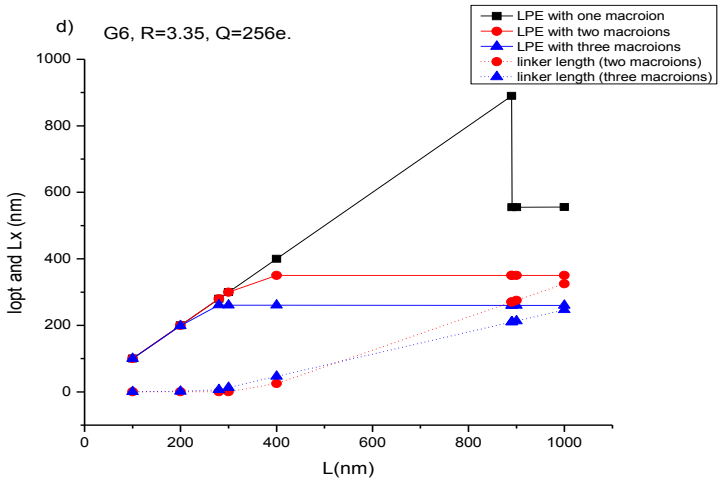


Figure.3.6d The wrapping length and the linker length as a function of the LPE length for the complex formed by one two and three spherical denrimers and flexible LPE, PAMAM dendrimers (ethylenediamine cores) of generations G6 has the radius R= 3.35 nm and charges of Q= 256.

Analytical tables below show the theoretical prediction of the wrapping length of LPE on dendrimers for different lengths of LPE chain with one, two, and three dendrimers at different values of radii and charges. Once can see the following behavior for the case of LPE with one dendrimer( tables: 3.4, 3.7, 3.10, 3.13) at small wrapping length the whole LPE chain collapses on the dendrimer. As the chain length L increases the difference increases also and the whole LPE remains in the collapsed state. When L increases further, a first order phase transition happens and a tail with a finite length $L_T$ appears. The charge inversion can be calculated from the effective charge of the complex $Z_{compl}(e)$ , as we see the complex is overcharged for all optimal wrapping lengths, but we see that the overcharging increases until it reachs a maximum value of wrapping length and then keeps slightly constant. For this system we can see the number of turns increases by increasing the chain length until it reaches the maximum wrapping length and after that it almost constant. The bending energy $F_{bending}(K_BT)$ is the elastic free energy required to bend a length of the chain of radius of curvature around sphere of radius R. As we see from the tables below, the bending free energy of LPE increases by increasing the chain length until the optimal length is becoming maximum, then the value of bending energy remains slightly constant.

If we keep on looking for the complexation of LPE with two dendrimers at different values of radius and charge (tables: 3. 5, 3.8, 3.11, 3.14), as we see from the table optimal wrapping length per one macroion keeps increasing until it reachs a maximum value and then keeps slightly constant, so in this regime the whole LPE chain collapses on the two dendrimers. When the chain length increases more and more there is a transition state and linker will be formed between these two dendrimers . At the neutralizing length $\mathcal{L} = Z * b,$ the total charge of the complex is zero,

since the positive charge on the dendrimer is equal to the negative charge on the chain. We notice that the number of turns are keep increasing until it reaches the maximum value of the optimal length, and we notice that the number of turns decreases by a little value, and this corresponds to the formation of linker between these two dendrimers, and then the number of turns remains slightly constant. In this case of LPE with two dendrimrs the bending free energy also keep increases until reach a maximum optimal wrapping length and then takes a constant value.

Tables( 3.6, 3.9, 3.12, 3.15) show The theoretical study of the comlexation of LPE with three dendrimers. The same trend is observed here as obtained earlier for the complexation of LPE with one or two dendrimers of optimal wrapping length, that at small values it completely collapsed on the dendrimers, after that when the chain length increases further, part of LPE chain collapsed on the three dendrimers, and then linkers formation appears. Now the effective charge of the complexation can be calculated which is found to be negative for all lengths, which means that the complex is overcharged. According to the number of turns, it increases until reach a maximum value and then keeps had constant value. By studying the case of LPE with three dendrimers, the bending free energy of LPE chain increases rapidly with increasing chain length until the optimal wrapping length reaches a maximum value, then the bending energy becomes constant.

Table 3.4 Analytical model results for the interaction of LPE with one dendrimer of radius R=1.1nm and charge of 8e.

| Chain length L(nm) | Optimal wrapping length per one macroion $l_{opt}$ (nm) | $Z_{compl}(e)$ | tail length $L_T(nm)$ | No. of turns | $F_{bending}$ ( $K_BT$) |
|---|---|---|---|---|---|
| 10 | 9.935 | -1.935 | 0.065 | 1.43 | 1.701 |
| 16 | 15.935 | -7.935 | 0.065 | 2.30 | 28.62 |
| 18 | 17.935 | -9.935 | 0.065 | 2.59 | 44.865 |
| 20 | 19.913 | -11.913 | 0.087 | 2.88 | 64.508 |
| 25 | 24.88 | -16.88 | 0.12 | 3.6 | 129.515 |
| 29 | 28.0274 | -20.027 | 0.9726 | 4.05 | 182.316 |
| 30 | 24.54 | -16.54 | 5.46 | 3.55 | 124.350 |

| | | | | | |
|---|---|---|---|---|---|
| 40 | 24.54 | -16.54 | 15.46 | 3.55 | 124.350 |

Table 3.5 Analytical model results for the interaction of LPE with two dendrimers each of radius R=1.1nm and charge of 8e.

| Chain length L(nm) | wrapping length per one macroion $l_{opt}$ (nm) | $Z_{compl}(e)$ | linker length $L_x(nm)$ | No. of turns | $F_{bending}$ ( $K_BT$) |
|---|---|---|---|---|---|
| 10 | 9.813 | -1.813 | 0.187 | 1.42 | 34.799 |
| 16 | 15.813 | -7.813 | 0.187 | 2.28 | 0.031 |
| 18 | 17.813 | -9.813 | 0.187 | 2.57 | 2.988 |
| 20 | 19.721 | -11.721 | 0.279 | 2.85 | 12.587 |
| 25 | 23.34 | -15.34 | 1.66 | 3.37 | 48.977 |
| 29 | 23.34 | -15.34 | 5.66 | 3.37 | 48.977 |
| 30 | 23.34 | -15.34 | 6.66 | 3.37 | 48.977 |
| 40 | 23.34 | -15.34 | 16.66 | 3.37 | 48.977 |

Table 3.6 Analytical model results for the interaction of LPE with three dendrimers each of radius R=1.1nm and charge of 8e.

| Chain length L(nm) | wrapping length per one macroion $l_{opt}$ (nm) | $Z_{compl}(e)$ | linker length $L_x(nm)$ | No. of turns | $F_{bending}$ ( $K_BT$) |
|---|---|---|---|---|---|
| 10 | 9.956 | -1.956 | 0.044 | 1.44 | 268.955 |
| 16 | 15.956 | -7.956 | 0.044 | 2.30 | 88.235 |
| 18 | 17.956 | -9.956 | 0.044 | 2.59 | 49.813 |

| | | | | | |
|---|---|---|---|---|---|
| 20 | 18.2 | -10.2 | 1.8 | 2.63 | 45.872 |
| 25 | 18.2 | -10.2 | 6.8 | 2.63 | 45.872 |
| 29 | 18.2 | -10.2 | 10.8 | 2.63 | 45.872 |
| 30 | 18.2 | -10.2 | 11.8 | 2.63 | 45.872 |
| 40 | 18.2 | -10.2 | 21.8 | 2.63 | 45.872 |

Table 3.7 Analytical model results for the interaction of LPE with one dendrimer of radius R=1.45nm and charge of 16e.

| Chain length L(nm) | Optimal length per one macroion $l_{opt}$(nm) | $Z_{compl}(e)$ | tail length $L_T(nm)$ | No. of turns | $F_{bending}$ ( $K_BT$) |
|---|---|---|---|---|---|
| 20 | 19.943 | -3.943 | 0.057 | 2.18 | 5.361 |
| 30 | 29.936 | -13.936 | 0.064 | 3.28 | 66.969 |
| 40 | 39.924 | -23.924 | 0.076 | 4.38 | 197.364 |
| 50 | 49.901 | -33.901 | 0.099 | 5.47 | 396.302 |
| 57 | 56.833 | -40.833 | 0.167 | 6.23 | 574.942 |
| 58 | 41.4223 | -25.4223 | 16.577 | 4.54 | 222.859 |
| 60 | 41.461 | -25.461 | 18.539 | 4.55 | 223.583 |
| 70 | 41.461 | -25.461 | 28.539 | 4.55 | 223.583 |

Table 3.8 Analytical model results for the interaction of LPE with two dendrimers each of radius R=1.45nm and charge of 16e.

| Chain length L(nm) | wrapping length per one macroion $l_{opt}$ (nm) | $Z_{compl}(e)$ | linker length $L_x(nm)$ | No. of turns | $F_{bending}$ ( $K_BT$) |
|---|---|---|---|---|---|
| 20 | 19.217 | -3.217 | 0.783 | 2.10 | 112.693 |
| 30 | 29.217 | -13.217 | 0.783 | 3.20 | 5.341 |
| 40 | 39.217 | -23.217 | 0.783 | 4.30 | 35.920 |
| 50 | 40.34 | -24.34 | 10.66 | 4.42 | 47.969 |
| 57 | 40.33 | -24.33 | 17.67 | 4.42 | 47.854 |
| 58 | 40.33 | -24.33 | 18.67 | 4.42 | 47.854 |
| 60 | 40.33 | -24.33 | 19.67 | 4.42 | 47.854 |
| 70 | 40.33 | -24.33 | 29.67 | 4.42 | 47.854 |

Table 3.9 Analytical model results for the interaction of LPE with three dendrimers each of radius R=1.45nm and charge of 16e.

| Chain length L(nm) | wrappinglength per one macroion $l_{opt}$ (nm) | $Z_{compl}(e)$ | linker length $L_x(nm)$ | No. of turns | $F_{bending}$ ( $K_BT$) |
|---|---|---|---|---|---|
| 20 | 19.87 | -3.87 | 0.13 | 2.18 | 818.583 |
| 30 | 29.87 | -13.87 | 0.13 | 3.27 | 340.031 |
| 40 | 37.66 | -21.66 | 2.34 | 4.13 | 110.602 |
| 50 | 37.66 | -21.66 | 12.34 | 4.13 | 110.602 |
| 57 | 37.66 | -21.66 | 19.34 | 4.13 | 110.602 |

| | | | | | |
|---|---|---|---|---|---|
| 58 | 37.66 | -21.66 | 20.34 | 4.13 | 110.602 |
| 60 | 37.66 | -21.66 | 22.34 | 4.13 | 110.602 |
| 70 | 37.66 | -21.66 | 32.34 | 4.13 | 110.602 |

Table 3.10 Analytical model results for the interaction of LPE with one dendrimer of radius R=2.25nm and charge of 64e.

| Chain length L(nm) | Optimal wrapping length per one macroion $l_{opt}$(nm) | $Z_{compl}(e)$ | tail length $L_T(nm)$ | No. of turns | $F_{bending}$ ( $K_BT$) |
|---|---|---|---|---|---|
| 70 | 69.968 | -23.968 | 0.032 | 4.95 | 647.232 |
| 80 | 79.97 | -33.97 | 0.03 | 5.65 | 909.369 |
| 90 | 89.97 | -43.97 | 0.03 | 6.36 | 1215.902 |
| 95 | 94.938 | -48.938 | 0.013 | 6.718 | 1384.712 |
| 100 | 99.901 | -53.901 | 0.099 | 7.07 | 1564.306 |
| 150 | 149.987 | -103.987 | 0.013 | 10.614 | 3989.448 |
| 200 | 199.938 | -153.938 | 0.062 | 14.14 | 7518.486 |
| 224 | 223.901 | -177.901 | 0.099 | 15.84 | 9605.072 |
| 225 | 146.07 | -100.07 | 78.93 | 10.33 | 3759.601 |
| 240 | 146.3223 | -100.3223 | 93.677 | 10.35 | 3774.200 |
| 280 | 146.8907 | -100.8907 | 133.109 | 10.39 | 3774.200 |
| 300 | 146.8907 | -100.8907 | 145.109 | 10.39 | 3774.200 |

Table 3.11 Analytical model results for the interaction of LPE with two dendrimers each of radius R=2.25nm and charge of Q= 64e

| Chain length L(nm) | Optimal length per one macroion $l_{opt}$(nm) | $Z_{compl}(e)$ | linker length $L_x(nm)$ | No. of turns | $F_{bending}$ ( $K_BT$) |
|---|---|---|---|---|---|
| 70 | 69.977 | -23.977 | 0.033 | 4.95 | 401.677 |
| 80 | 79.965 | -33.965 | 0.035 | 5.65 | 727.68 |
| 90 | 89.994 | -44.994 | 0.006 | 6.36 | 1141.55 |
| 95 | 94.987 | -48.987 | 0.013 | 6.72 | 1380.36 |
| 100 | 99.964 | -53.964 | 0.036 | 7.07 | 1639.75 |
| 150 | 104.347 | -58.347 | 22.826 | 7.38 | 1885.600 |
| 200 | 103.95 | -57.95 | 48.461 | 7.35 | 1863.013 |
| 224 | 103.078 | -57.078 | 60.461 | 7.29 | 1812.99 |
| 225 | 103.078 | -57.078 | 60.961 | 7.29 | 1812.99 |
| 240 | 103.078 | -57.078 | 68.461 | 7.29 | 1812.99 |
| 280 | 103.078 | -57.078 | 88.461 | 7.29 | 1812.99 |
| 300 | 103.078 | -57.078 | 98.461 | 7.29 | 1812.99 |

Table 3.12 Analytical model results for the interaction of LPE with three dendrimers each of radius R=2.25nm and charge of 64e.

| Chain length L(nm) | Optimal wrapping length per one macroion $l_{opt}$(nm) | $Z_{compl}(e)$ | linker length $L_x(nm)$ | No. of turns | $F_{bending}$ ( $K_BT$) |
|---|---|---|---|---|---|
| 70 | 69.563 | -23.563 | 0.437 | 4.9 | 307.975 |

| | | | | | |
|---|---|---|---|---|---|
| 80 | 66.666 | -20.666 | 3.335 | 4.7 | 232.279 |
| 90 | 66.276 | -20.276 | 5.931 | 4.69 | 222.674 |
| 95 | 65.275 | -19.275 | 7.4312 | 4.69 | 189.98 |
| 100 | 65 | -19 | 8.75 | 4.6 | 192.66 |
| 150 | 65 | -19 | 21.25 | 4.6 | 192.66 |
| 200 | 65 | -19 | 33.75 | 4.6 | 192.66 |
| 224 | 65 | -19 | 39.75 | 4.6 | 192.66 |
| 225 | 65 | -19 | 40 | 4.6 | 192.66 |
| 240 | 65 | -19 | 43.75 | 4.6 | 192.66 |
| 280 | 65 | -19 | 53.75 | 4.6 | 192.66 |
| 300 | 65 | -19 | 58.75 | 4.6 | 192.66 |

Table 3.13 Analytical model results for the interaction of LPE with one dendrimer of radius R=3.35nm and charge of 256e.

| Chain length L(nm) | Optimal wrapping length per one macroion $l_{opt}$(nm) | $Z_{compl}(e)$ | tail length $L_T(nm)$ | No. of turns | $F_{bending}$ ( $K_BT$) |
|---|---|---|---|---|---|
| 280 | 279.981 | -23.981 | 0.019 | 13.30 | 10400.89 |
| 300 | 299.96 | -43.96 | 0.31 | 14.25 | 12034.81 |
| 400 | 399.983 | -143.983 | 0.017 | 19.01 | 22006.6 |
| 890 | 889.945 | -633.945 | 0.017 | 42.29 | 113996.9 |
| 891 | 555.0109 | -299.01 | 335.989 | 26.37 | 43363.09 |
| 900 | 555.082 | -299.082 | 344.918 | 26.38 | 43374.53 |
| 1000 | 555.7866 | -299.7866 | 444.213 | 26.41 | 43487.99 |

Table 3.14 Analytical model results for the interaction of LPE with two dendrimers each of radius R=3.35nm and charge of 256e.

| Chain length L(nm) | Optimal wrapping length per one macroion $l_{opt}$(nm) | $Z_{compl}(e)$ | linker length $L_x(nm)$ | No. of turns | $F_{bending}$ ( $K_BT$) |
|---|---|---|---|---|---|
| 280 | 279.908 | -23.908 | 0.092 | 13.30 | 18345.78 |
| 300 | 299.454 | -43.454 | 0.546 | 14.23 | 21352.72 |
| 400 | 350.087 | -94.087 | 24.956 | 16.63 | 30202.78 |
| 890 | 350 | -94 | 270 | 16.63 | 30186.26 |
| 891 | 350 | -94 | 270.5 | 16.63 | 30186.26 |
| 900 | 350 | -94 | 275 | 16.63 | 30186.26 |
| 1000 | 350 | -94 | 325 | 16.63 | 30186.26 |

Table 3.15 Analytical model results for the interaction of LPE with three dendrimes each of radius R=3.35nm and charge of 256e.

| Chain length L(nm) | Optimal wrapping length per one macroion $l_{opt}$(nm) | $Z_{compl}(e)$ | linker length $L_x(nm)$ | No. of turns | $F_{bending}$ ( $K_BT$) |
|---|---|---|---|---|---|
| 280 | 261.5 | -5.5 | 6.166 | 12.42 | 20409.96 |
| 300 | 260.7 | -4.7 | 13.1 | 12.39 | 20257.29 |
| 400 | 260.5 | -4.5 | 46.5 | 12.38 | 20219.21 |
| 890 | 260 | -4 | 210 | 12.35 | 20124.17 |
| 891 | 260 | -4 | 210.3 | 12.35 | 20124.17 |
| 900 | 260 | -4 | 213.3 | 12.35 | 20124.17 |
| 1000 | 260 | -4 | 246.66 | 12.35 | 20124.17 |

The variation of radii and charges of the macroions in the complexes shows that in all cases of G1, G2, G4 and G6 they have the same trend and behavior of how LPE is wrapping around the three dendrimers; at the beginning all LPE chain wrapped on the dendrimers until reached a maximum value and at the end the wrapping degree becomes almost constant. The effect of dendrimer generation is shown in figure 3.7 below. The complexation of LPE with one dendrimer is shown in figure 3.7(a) as we notice as the generation increases the optimal wrapping length (maximum point) increase, for G1 it was $l_{opt}$ =28.0274nm, for G2 ($l_{opt} = 56.833nm$), G4 ($l_{opt} = 223.901nm$), and for G6 ($l_{opt} = 889.945nm$), this increasing of $l_{opt}$ by increasing the generation of dendrimer is due to the increasing of size by increasing the radius and due to increasing in the charge, so more monomers are needed to be condensed on the dendrimers to reach the optimal value. As we see in figure 3.7 (b) which describes the interaction of LPE with two dendrimers for different generations and the optimal wrapping degreefor G1, G2, G4 and G6 is 23.34nm, 40.34nm, 104.374nm, and 350.087nm respectively, which increases by increases the generation as in the case of LPE with one dendrimer. The case of LPE with three dendrimers of different generations is shown in figure 3.7 (c) which shows the same behavior as in the two cases of LPE with one and two dendrimers, that the optimal wrapping length increases by increasing the generation which was calculated to be $l_{opt} = 18.2nm$ for G1, $l_{opt} = 37.66nm$ for G2, $l_{opt}$=65.275nm for G4 and $l_{opt} = 260.5nm$ for G6.

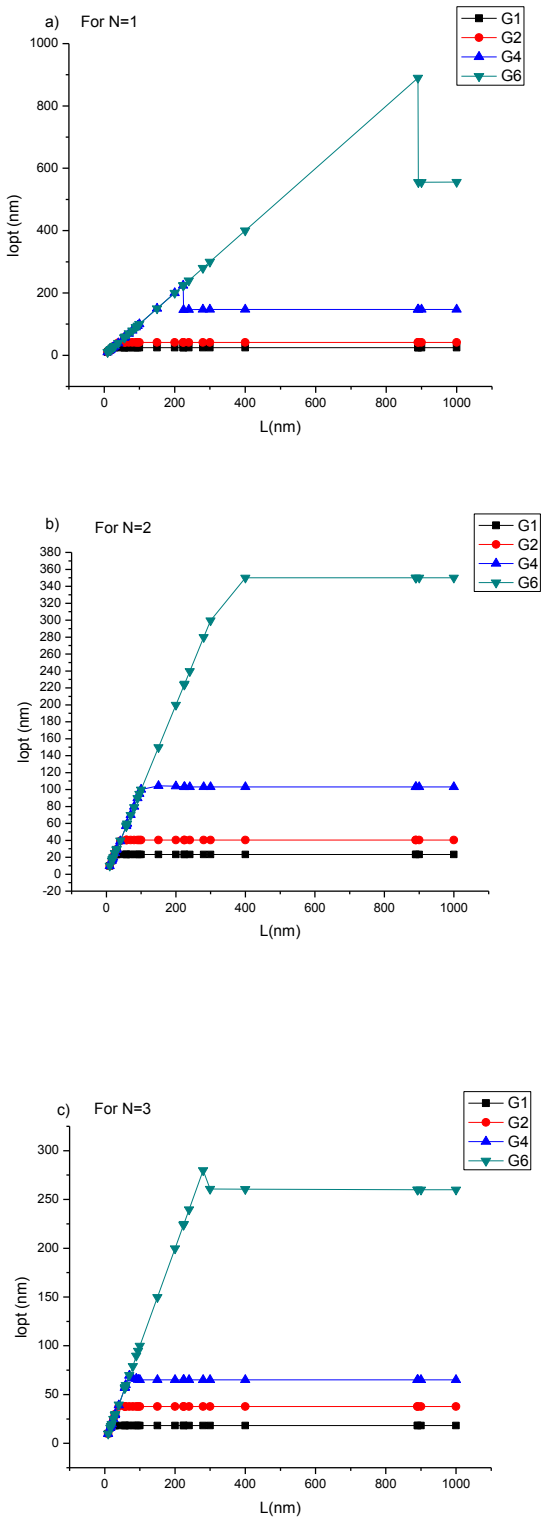


Figure 3.7 The length of the wrapping LPE chain on dendrimer as a function of chain length for different generations. LPE with N=1 (a) N=2 (b) and N=3 (c) each case studied with G1, G2, G4 and G6 dendrimers.

### 3.4 Effect of LPE chain length on the wrapping length of LPE chain on many PAMAM dendrimers –comparsion between our model and Shklovskii N-spher model

In order to compare with Shclovskii model for the complexation of N spheres[48] with one LPE chain, the complexation of flexible LPE chain and an oppositely charged three spheres has been studied. The three spheres modeled a PAMAM dendrimer G3 each has a charge Z=24 and R=3.2nm and LPE chain of radius a=0.4nm. Both table 3.16 with Figure 3.8 show the theoretical prediction of the wrapping length of LPE on three dendrimers for different lengths of LPE chain by assuming N equals to three (three dendrimers). Upon increasing of the chain length the wrwpping lengt increases linearly until we reach to chain length which is critical and the number of the condensed monomers at this point is maximum i.e., the overcharging of the dendrimers is maximum, this critical point is equal to 30.446nm in our model and equals to 28.565nm in Shklovskii model. In general the decrease in the wrapping length of LPE chain is attributed to the increasing in the electrostatic repulsive free energy between chain monomers which is larger at maximum overcharging of dendrimer.

In this study we expect to have two graphs that are coincidence on each other since both models (our model and Shklovskii N-sphere model) had been developed for one LPE chain interacts with N-charged spheres, but what we have get is little different from our expectation by a value around 1nm less than our model. This difference due to the assumptions that Shklovskii did in his model, such as: when he derived the total free energy of one period of the complex (interaction energy) he multiplied it with N, so he neglected the difference between the end spheres with those in the middle of the LPE, this is justified for a reasonably large value of N in his model, but in our model we didn't neglect them since we worked on N=3 spheres. In his model he assumed that the linker length is much larger than the radius of each sphere$L_x >$ R, this assumption leads to the simplification of his total equation by keeping only terms of the highest order in the large parameter $\frac{L_x}{R}$, but in our equation we didn't make any approximations, we just took our equation as we get it.

Table 3.16 The complexation of flexibleLPE (charge -48e) with three macroions each of radius R=3.2nm and charge of 24e.

| Chain length L(nm) | Optimal length per one macroion $l_{opt}$(nm) | | linker length $L_x(nm)$ | |
|---|---|---|---|---|
| | Our model | Shklovskii model | Our model | Shklovskii model |
| 50 | 15.409 | 14.923 | 1.257 | 1.743 |
| 60 | 18.383 | 17.546 | 1.617 | 2.454 |
| 70 | 21.93 | 20.323 | 1.403 | 3.01 |
| 87 | 25.334 | 24.376 | 3.666 | 4.624 |
| 88 | 25.5 | 24.54 | 3.833 | 4.793 |
| 90 | 26.09 | 25.176 | 3.91 | 4.824 |
| 100 | 29.886 | 27.989 | 3.447 | 5.344 |
| 102 | 30.446 | 28.656 | 3.554 | 5.344 |

| | | | | |
|---|---|---|---|---|
| 104 | 30 | 28.001 | 4.667 | 6.66 |
| 110 | 30 | 28.001 | 6.667 | 8.66 |
| 120 | 30 | 28.001 | 6.667 | 8.66 |

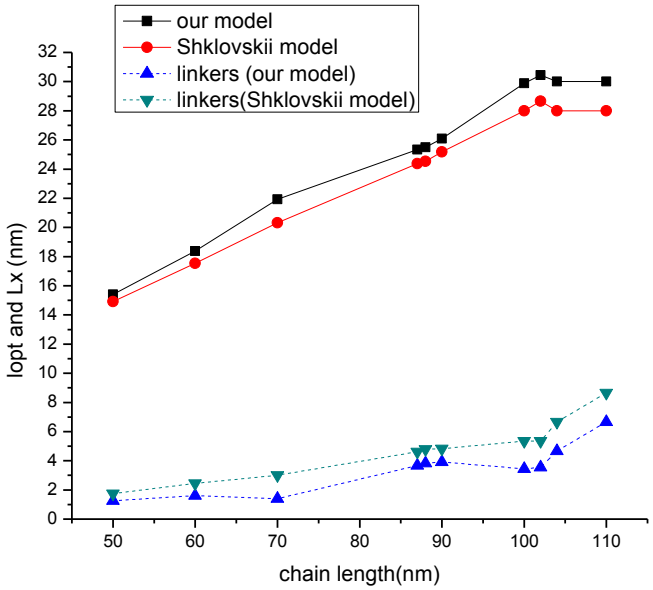


Figure.3.8 : The wrapping length of the LPE chain on dendrimer as a function of chain length and the linker appeared in the interaction. A system of $3G_3$complexes with an oppositely charged flexible LPE of radius 0.4nm.

Shklovskii N-spheres model [48] also used here to study the complexation of flexible LPE chain of different lengths with four, five and six ammonia cord PAMAM dendrimers of G3 with charge of 24e in solution with low salt concentration (10 mM) and high salt concentration (90 mM). Figure 3.9 shows the optimal wrapping length per one macroion as a function of chain length at both low and high salt concentration. In both cases, the behavior of length wrapped around dendrimers is the same, that at the beginning upon increasing of the chain length the wrapping length increase linearly until we reach to chain length which is critical, and each case has it's critical length, after that the wrapping length decreases to reach a constant value at the end. As shown in figure 3.9, at high salt concentration the LPE chain become more wrapped around dendrimers, where the saturation in the number of condensed monomers of LPE chain at high salt concentration means that the complex conformation at higher salt concentration shows a strong binding interaction in contrast to low salt concentration.

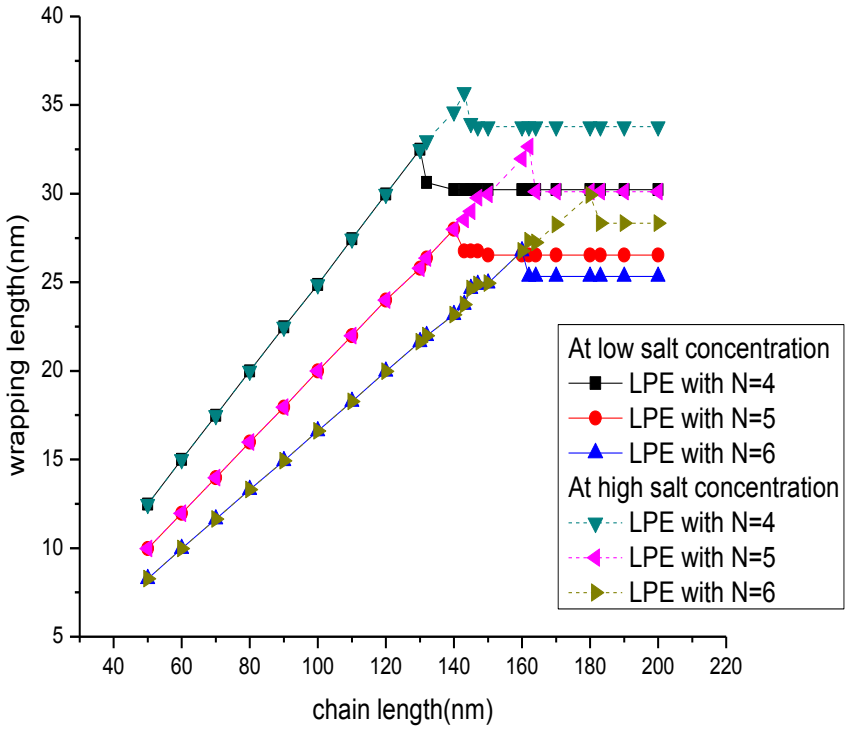


Figure 3.9 The wrapping length of LPE chain on four, five, and six ammonia cord PAMAM dendrimers G3 each of charge 24e as a function of chain length at different salt concentration. At high salt concentration complex conformation shows strong binding interaction in contrast to low salt concentration.

The optimal wrapping length of LPE wrapped per one macroion, and the linker formed between two successive macroions when the chain length increases from 50 to 233 nm at low salt concentration (10 mM) and high salt concentration(90 mM) are analytically studied by using Shklovskii N-sphere model, for a complexation formed between one LPE with N=1,2,3,….,9 and 10 dendrimers of G3 with radius R=3.2nm and total charge of 24e. Table 3.17 with figure 3.10 show the optimal wrapping length per one macroion for the ten cases at low salt concentration to be linearly increased by increasing the chain length until we reach a critical value which is specified for each N spheres. After this critical point the behavior is similar for all of the cases again to be decreased and finally reached almost a constant value. This behavior is attributed to that the whole monomers of LPE have been wrapped around dendrimers at the first, and then after the overcharging happened tails will start to be appeared in the case of LPE with N=1, and linkers will take place in the case of N>1.

The aggregate formed between LPE with N=1,2,….,9,10 also studied at high salt concentration by using the same model. At high salt concentration the same behavior as in the case at low salt

concentration as shown in table 3.18 and figure 3.11. The important thing to be noticed between the two cases of low and high salt concentration that at high salt concentration the LPE chain become more wrapped around dendrimers, where the saturation in the number of condensed monomers of LPE chain at high salt concentration means that the complex conformation at higher salt concentration shows a strong binding interaction in contrast to low salt concentration.

Table 3.17: Analytical model results for the optimal wrapping length at low salt concentration for the interaction between LPE with N=1,2,3…..,9,10 ammonia cord PAMAM dendrimers of G3 with radius R=3.2nm and total charge of 24e, by using Shklovskii N-sphere model.

| Chain length L(nm) | Optimal length per one macroion $l_{opt}$(nm) | | | | | | | | | |
|---|---|---|---|---|---|---|---|---|---|---|
| | N=1 | N=2 | N=3 | N=4 | N=5 | N=6 | N=7 | N=8 | N=9 | N=10 |
| **50** | **49.876** | **24.494** | **14.923** | **12.474** | **9.977** | **8.263** | **7.128** | **6.327** | **5.445** | **4.798** |
| **60** | **59.699** | **29.743** | **17.546** | **14.997** | **11.971** | **9.966** | **8.894** | **7.435** | **6.906** | **5.478** |
| **65** | **64.678** | **32.435** | **21.76** | **16.143** | **12.143** | **10.675** | **9.285** | **8.715** | **7.417** | **6.457** |
| **67** | **59.887** | **33.39** | **22.26** | **16.698** | **13.654** | **11.321** | **9.54** | **8.347** | **7.42** | **6.78** |
| **70** | **59.766** | **34.89** | **23.323** | **17.497** | **13.975** | **11.633** | **9.96** | **8.752** | **7.753** | **6.987** |
| **78** | **59.766** | **38.94** | **25.45** | **19.29** | **15.576** | **12.89** | **11.125** | **9.735** | **8.653** | **7.78** |
| **80** | **59.766** | **35.765** | **26.6** | **19.987** | **15.976** | **13.296** | **11.41** | **9.98** | **8.87** | **7.899** |
| **102** | **59.766** | **35.743** | **35.656** | **25.37** | **20.375** | **16.799** | **14.453** | **12.347** | **11.139** | **10.157** |
| **104** | **59.766** | **35.743** | **28.001** | **25.995** | **20.679** | **17.33** | **14.587** | **12.799** | **11.553** | **10.398** |
| **110** | **59.766** | **35.743** | **28.001** | **27.456** | **21.98** | **18.264** | **15.711** | **13.69** | **12.71** | **10.98** |
| **120** | **59.766** | **35.743** | **28.001** | **29.987** | **23.99** | **19.98** | **17.08** | **14.94** | **13.23** | **11.95** |
| **130** | **59.766** | **35.743** | **28.001** | **32.499** | **25.799** | **21.63** | **18.552** | **16.231** | **14.42** | **12.87** |
| **132** | **59.766** | **35.743** | **28.001** | **27.625** | **26.36** | **21.98** | **18.771** | **16.543** | **14.87** | **13.022** |
| **140** | **59.766** | **35.743** | **28.001** | **27.625** | **27.998** | **23.166** | **19.914** | **17.425** | **15.366** | **13.99** |
| **143** | **59.766** | **35.743** | **28.001** | **27.625** | **26.769** | **23.75** | **20.21** | **17.988** | **15.87** | **14.54** |
| **150** | **59.766** | **35.743** | **28.001** | **27.625** | **26.531** | **24.95** | **21.4** | **18.725** | **16.64** | **15.012** |
| **160** | **59.766** | **35.743** | **28.001** | **27.625** | **26.541** | **26.77** | **22.87** | **19.57** | **17.55** | **15.9** |

| | | | | | | | | | | |
|---|---|---|---|---|---|---|---|---|---|---|
| **162** | **59.766** | **35.743** | **28.001** | **27.625** | **26.532** | **25.327** | **23.12** | **19.99** | **17.98** | **16.2** |
| **170** | **59.766** | **35.743** | **28.001** | **27.625** | **26.532** | **25.325** | **24.21** | **21.187** | **18.83** | **16.95** |
| **180** | **59.766** | **35.743** | **28.001** | **27.625** | **26.532** | **25.325** | **25.655** | **22.844** | **19.485** | **17.759** |
| **183** | **59.766** | **35.743** | **28.001** | **27.625** | **26.532** | **25.325** | **23.873** | **22.932** | **20.33** | **18.23** |
| **190** | **59.766** | **35.743** | **28.001** | **27.625** | **26.532** | **25.325** | **23.873** | **20.76** | **20.977** | **18.88** |
| **195** | **59.766** | **35.743** | **28.001** | **27.625** | **26.532** | **25.325** | **23.873** | **20.66** | **21.642** | **19.43** |
| **197** | **59.766** | **35.743** | **28.001** | **27.625** | **26.532** | **25.325** | **23.873** | **20.66** | **21.83** | **19.67** |
| **205** | **59.766** | **35.743** | **28.001** | **27.625** | **26.532** | **25.325** | **23.873** | **20.66** | **22.799** | **20.49** |
| **209** | **59.766** | **35.743** | **28.001** | **27.625** | **26.532** | **25.325** | **23.873** | **20.66** | **21.54** | **20.987** |
| **215** | **59.766** | **35.743** | **28.001** | **27.625** | **26.532** | **25.325** | **23.873** | **20.66** | **21.54** | **21.487** |
| **220** | **59.766** | **35.743** | **28.001** | **27.625** | **26.532** | **25.325** | **23.873** | **20.66** | **21.54** | **21.947** |
| **222** | **59.766** | **35.743** | **28.001** | **27.625** | **26.532** | **25.325** | **23.873** | **20.66** | **21.54** | **19.234** |
| **230** | **59.766** | **35.743** | **28.001** | **27.625** | **26.532** | **25.325** | **23.873** | **20.66** | **21.54** | **19.233** |

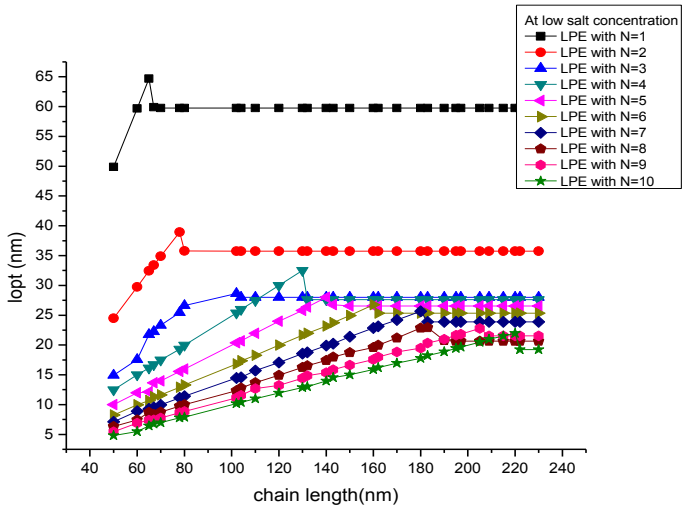


Figure 3.10: Optimal wrapping length per one macroion with different LPE chain lengths at low salt concentration for the interaction between LPE with N=1,2,3…..,9,10 ammonia cord PAMAM dendrimers of G3 with radius R=3.2nm and total charge of 24e, by using Shklovskii N-sphere model.

Table 3.18: Analytical model results for the optimal wrapping length at high salt concentration for the interaction between LPE with N=1,2,3…..,9,10 ammonia cord PAMAM dendrimers of G3 with radius R=3.2nm and total charge of 24e, by using Shklovskii N-sphere model.

| Chain length L(nm) | Optimal length per one macroion $l_{opt}$(nm) | | | | | | | | | |
|---|---|---|---|---|---|---|---|---|---|---|
| | N=1 | N=2 | N=3 | N=4 | N=5 | N=6 | N=7 | N=8 | N=9 | N=10 |
| **50** | **49.876** | **24.494** | **14.923** | **12.474** | **9.977** | **8.263** | **7.128** | **6.327** | **5.445** | **4.798** |
| **60** | **59.699** | **29.743** | **17.546** | **14.997** | **11.971** | **9.966** | **8.894** | **7.435** | **6.906** | **5.478** |
| **65** | **64.678** | **32.435** | **21.76** | **16.143** | **12.143** | **10.675** | **9.285** | **8.715** | **7.417** | **6.457** |
| **67** | **66.89** | **33.39** | **22.26** | **16.698** | **13.654** | **11.321** | **9.54** | **8.347** | **7.42** | **6.78** |
| **70** | **62.233** | **34.89** | **23.323** | **17.497** | **13.975** | **11.633** | **9.96** | **8.752** | **7.753** | **6.987** |
| **78** | **62.233** | **38.94** | **25.45** | **19.29** | **15.576** | **12.89** | **11.125** | **9.735** | **8.653** | **7.78** |
| **80** | **62.233** | **39.887** | **26.6** | **19.987** | **15.976** | **13.296** | **11.41** | **9.98** | **8.87** | **7.899** |
| **83** | **62.233** | **36.213** | **27.583** | **20.625** | **16.48** | **13.733** | **11.771** | **10.3** | **9.15** | **8.24** |
| **102** | **62.233** | **36.213** | **33.956** | **25.37** | **20.375** | **16.799** | **14.453** | **12.347** | **11.139** | **10.157** |
| **104** | **62.233** | **36.213** | **36.556** | **25.995** | **20.679** | **17.33** | **14.587** | **12.799** | **11.553** | **10.398** |
| **110** | **62.233** | **36.213** | **30.459** | **27.456** | **21.98** | **18.264** | **15.711** | **13.69** | **12.71** | **10.98** |
| **120** | **62.233** | **36.213** | **30.459** | **29.987** | **23.99** | **19.98** | **17.08** | **14.94** | **13.23** | **11.95** |
| **130** | **62.233** | **36.213** | **30.459** | **32.499** | **25.799** | **21.63** | **18.552** | **16.231** | **14.42** | **12.87** |
| **132** | **62.233** | **36.213** | **30.459** | **32.875** | **26.36** | **21.98** | **18.771** | **16.543** | **14.87** | **13.022** |
| **140** | **62.233** | **36.213** | **30.459** | **29.116** | **27.998** | **23.166** | **19.914** | **17.425** | **15.366** | **13.99** |
| **143** | **62.233** | **36.213** | **30.459** | **29.116** | **28.514** | **23.75** | **20.21** | **17.988** | **15.87** | **14.54** |
| **150** | **62.233** | **36.213** | **30.459** | **29.116** | **27.165** | **24.95** | **21.4** | **18.725** | **16.64** | **15.012** |
| **160** | **62.233** | **36.213** | **30.459** | **29.116** | **27.165** | **26.77** | **22.87** | **19.57** | **17.55** | **15.9** |
| **162** | **62.233** | **36.213** | **30.459** | **29.116** | **27.165** | **26.93** | **23.12** | **19.99** | **17.98** | **16.2** |
| **170** | **62.233** | **36.213** | **30.459** | **29.116** | **27.165** | **26.021** | **24.21** | **21.187** | **18.83** | **16.95** |
| **180** | **62.233** | **36.213** | **30.459** | **29.116** | **27.165** | **26.021** | **25.655** | **22.844** | **19.485** | **17.759** |
| **183** | **62.233** | **36.213** | **30.459** | **29.116** | **27.165** | **26.021** | **26.105** | **22.932** | **20.33** | **18.23** |

| | | | | | | | | | | |
|---|---|---|---|---|---|---|---|---|---|---|
| **190** | **62.233** | **36.213** | **30.459** | **29.116** | **27.165** | **26.021** | **24.576** | **23.697** | **20.977** | **18.88** |
| **195** | **62.233** | **36.213** | **30.459** | **29.116** | **27.165** | **26.021** | **24.576** | **21.657** | **21.642** | **19.43** |
| **197** | **62.233** | **36.213** | **30.459** | **29.116** | **27.165** | **26.021** | **24.576** | **21.657** | **21.83** | **19.67** |
| **205** | **62.233** | **36.213** | **30.459** | **29.116** | **27.165** | **26.021** | **24.576** | **21.657** | **22.799** | **20.49** |
| **209** | **62.233** | **36.213** | **30.459** | **29.116** | **27.165** | **26.021** | **24.576** | **21.657** | **23.166** | **20.987** |
| **215** | **62.233** | **36.213** | **30.459** | **29.116** | **27.165** | **26.021** | **24.576** | **21.657** | **22.132** | **21.487** |
| **220** | **62.233** | **36.213** | **30.459** | **29.116** | **27.165** | **26.021** | **24.576** | **21.657** | **22.132** | **21.947** |
| **222** | **62.233** | **36.213** | **30.459** | **29.116** | **27.165** | **26.021** | **24.576** | **21.657** | **22.132** | **22.18** |
| **230** | **62.233** | **36.213** | **30.459** | **29.116** | **27.165** | **26.021** | **24.576** | **21.657** | **22.132** | **22.98** |
| **233** | **62.233** | **36.213** | **30.459** | **29.116** | **27.165** | **26.021** | **24.576** | **21.657** | **22.132** | **20.786** |

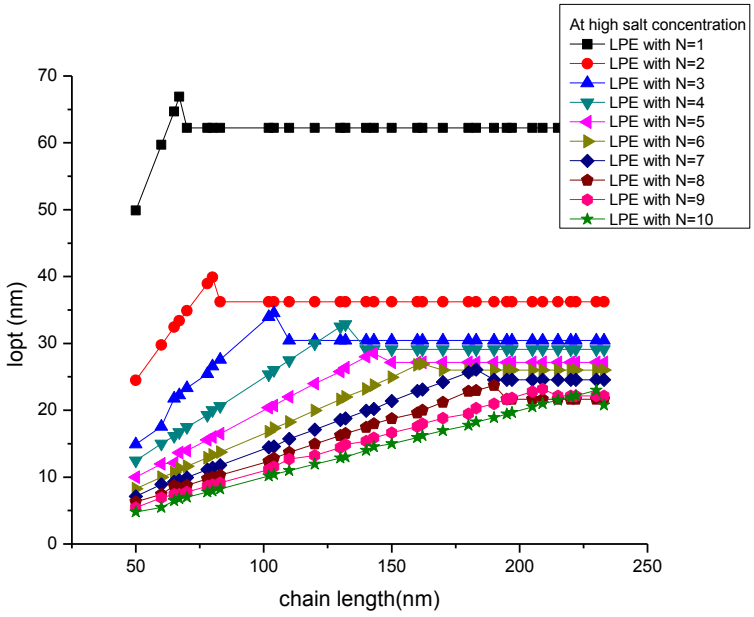


Figure 3.11: Optimal wrapping length per one macroion with different LPE chain length at high salt concentration for the interaction between LPE with N=1,2,3…..,9,10 ammonia cord PAMAM dendrimers of G3 with radius R=3.2nm and total charge of 24e, by using Shklovskii N-sphere model.

The effect of the chain length of LPE on the linker formed between NG3 – LPE chain complexs have been studied for N=2,3,….,9,10 macroions at low and high salt concentration. The total free energy in Shklovskii N-sphere model for these two cases (low and high salt concentration) was

minimized in order to get stable LPE chain-NG3 complexes for different LPE lengths. In all cases the LPE exceeds the length needed to neutralize the NG3 dendrimers. The total length of LPE divideds into two parts, the optimal wrapping length and the linker. The behavior of optimal wrapping length per one macroion was shown in figures above (figure 3.10 and 3.11). The behavior of the linker length is shown in figure 3.12 at low salt concentration, and in figure 3.13 at high salt concentration for LPE interacts with N=2,3,…,9,10 dendrimers. At the beginning of the interaction the linker starts to appear and keeps increasing as we increase chain length. The point to be discussed is the effect of salt concentration on linker length. Tables 3.19 and 3.20 show the value of linker length at low and high salt concentration respectively, as we see in these two tables with the help of figures 3.12 and 3.13 for low and high salt concentration recpectively, that in more salty solution, we have the largest wrapping length of LPE chain around dendrimers, as a result the linker formed between complexes in smaller than the linker length formed in low salty solution.

Table 3.19: Analytical model results for the linker length between two successive macroions at low salt concentration for the interaction between LPE with N=1,2,3…..,9,10 ammonia cord PAMAM dendrimers of G3 with radius R=3.2nm and total charge of 24e, by using Shklovskii N-sphere model.

| **Chain length L(nm)** | **linker length $L_X$(nm)** | | | | | | | | | |
|---|---|---|---|---|---|---|---|---|---|---|
| | **N=1 Tail length** | **N=2** | **N=3** | **N=4** | **N=5** | **N=6** | **N=7** | **N=8** | **N=9** | **N=10** |
| **50** | **0.124** | **0.506** | **0.74** | **0.026** | **0.023** | **0.07** | **0.017** | **0.075** | **0.023** | **0.0798** |
| **60** | **0.301** | **0.257** | **0.454** | **0.03** | **0.029** | **0.034** | **0.322** | **0.065** | **0.098** | **0.0478** |
| **65** | **0.322** | **0.065** | **0.93** | **0.107** | **0.857** | **0.158** | **0.147** | **0.059** | **0.033** | **0.0457** |
| **67** | **3.556** | **0.11** | **0.73** | **0.051** | **0.254** | **0.154** | **0.314** | **0.028** | **0.023** | **0.078** |
| **70** | **5.17** | **0.11** | **0.91** | **0.03** | **0.25** | **0.336** | **0.43** | **0.02** | **0.023** | **0.0987** |
| **78** | **9.117** | **0.06** | **0.55** | **0.42** | **0.24** | **0.11** | **0.178** | **0.015** | **0.034** | **0.078** |
| **80** | **1.117** | **4.235** | **0.66** | **0.13** | **0.24** | **0.373** | **0.18** | **0.201** | **0.053** | **0.0899** |
| **102** | **21.117** | **15.257** | **5.344** | **0.13** | **0.25** | **0.201** | **0.118** | **0.403** | **0.233** | **0.0157** |
| **104** | **22.117** | **16.257** | **6.66** | **0.501** | **0.121** | **0.33** | **0.27** | **0.201** | **0. 432** | **0.0398** |
| **110** | **25.117** | **19.257** | **8.66** | **0.44** | **0.23** | **0.69** | **0.328** | **0.601** | **0.71** | **0.098** |
| **120** | **29.617** | **24.257** | **11.99** | **0.13** | **0.11** | **0.23** | **0.628** | **0.52** | **0.23** | **0.95** |
| **130** | **34.617** | **29.257** | **15.33** | **0.13** | **0.201** | **0.36** | **0.19** | **0.19** | **0.42** | **0.87** |

| | | | | | | | | | | |
|---|---|---|---|---|---|---|---|---|---|---|
| **132** | **35.617** | **30.257** | **15.99** | **2.375** | **0.35** | **0.201** | **0.68** | **0.43** | **0.87** | **0.22** |
| **140** | **39.617** | **34.257** | **18.66** | **4.778** | **0.401** | **0.167** | **0.68** | **0.75** | **0.366** | **0.99** |
| **143** | **41.617** | **35.757** | **19.66** | **5.528** | **1.831** | **0.833** | **0.218** | **0.63** | **0.87** | **0.54** |
| **150** | **44.617** | **39.257** | **21.99** | **7.278** | **3.469** | **0.503** | **0.285** | **0.84** | **0.64** | **0. 12** |
| **160** | **49.617** | **44.257** | **25.332** | **9.778** | **5.459** | **1.36** | **0.19** | **0.43** | **0.227** | **0.01** |
| **162** | **51.117** | **45.257** | **25.999** | **10.278** | **5.868** | **1.673** | **0.022** | **0.26** | **0.02** | **0.04** |
| **170** | **54.617** | **49.257** | **28.66** | **12.278** | **7.468** | **3.008** | **0.075** | **0.063** | **0.058** | **0.05** |
| **180** | **59.617** | **54.257** | **31.999** | **14.778** | **9.468** | **4.675** | **0.059** | **0.056** | **0.515** | **0.241** |
| **183** | **61.617** | **55.757** | **32.999** | **15.528** | **10.068** | **5.175** | **2.269** | **0.243** | **0.03** | **0.07** |
| **190** | **64.617** | **59.257** | **35.332** | **17.278** | **11.468** | **6.341** | **3.268** | **3.09** | **0.134** | **0.12** |
| **195** | **67.617** | **61.757** | **36.999** | **18.528** | **12.468** | **7.175** | **3.98** | **3.715** | **0.024** | **0.07** |
| **197** | **68.617** | **62.757** | **37.665** | **19.028** | **12.868** | **7.508** | **4.269** | **3.965** | **0.0588** | **0.03** |
| **205** | **72.617** | **66.757** | **40.332** | **21.028** | **14.468** | **8.841** | **5.412** | **4.965** | **0.021** | **0.01** |
| **209** | **74.617** | **68.757** | **41.665** | **22.028** | **15.268** | **9.508** | **5.984** | **5.465** | **1.682** | **0.087** |
| **215** | **77.617** | **71.757** | **43.665** | **23.528** | **16.468** | **10.508** | **6.841** | **6.215** | **2.34** | **0.022** |
| **220** | **80.117** | **74.257** | **45.332** | **24.778** | **17.468** | **11.341** | **7.555** | **6.84** | **2.904** | **0.053** |
| **222** | **81.117** | **75.257** | **45.999** | **25.278** | **17.868** | **11.675** | **7.84** | **7.09** | **3.126** | **2.966** |
| **230** | **85.115** | **79.257** | **48.665** | **27.278** | **19.468** | **13.008** | **8.98** | **8.09** | **4.015** | **3.767** |

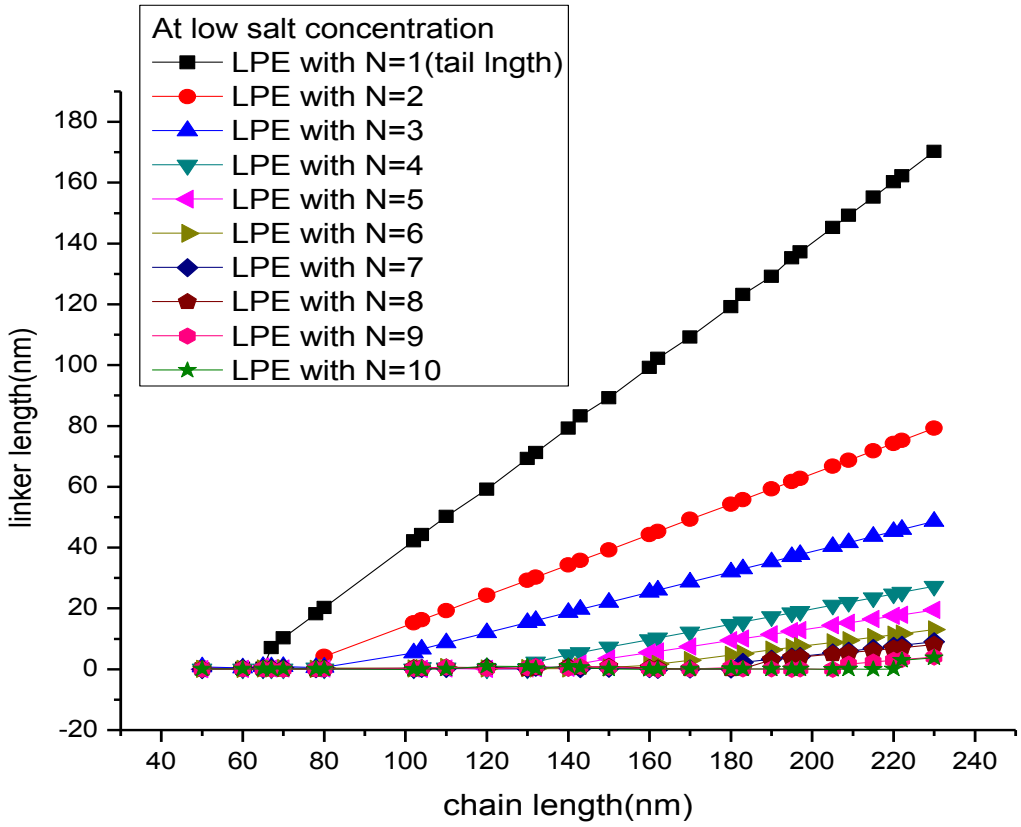


Figure 3.12: linker length between two successive macroions at low salt concentration for the interaction between LPE with N=1,2,3…..,9,10 ammonia cord PAMAM dendrimers of G3 with radius R=3.2nm and total charge of 24e, by using Shklovskii N-sphere model.

Table 3.20: Analytical model results for the linker length between two successive macroions at high salt concentration for the interaction between LPE with N=1,2,3…..,9,10 ammonia cord PAMAM dendrimers of G3 with radius R=3.2nm and total charge of 24e, by using Shklovskii N-sphere model.

| **Chain length L(nm)** | **linker length $L_X$(nm)** | | | | | | | | | |
|---|---|---|---|---|---|---|---|---|---|---|
| | **N=1 (tail)** | **N=2** | **N=3** | **N=4** | **N=5** | **N=6** | **N=7** | **N=8** | **N=9** | **N=10** |
| **50** | **0.124** | **0.506** | **0.74** | **0.026** | **0.023** | **0.07** | **0.017** | **0.075** | **0.023** | **0.0798** |
| **60** | **0.301** | **0.257** | **0.454** | **0.03** | **0.029** | **0.034** | **0.322** | **0.065** | **0.098** | **0.0478** |
| **65** | **0.322** | **0.065** | **0.93** | **0.107** | **0.857** | **0.158** | **0.147** | **0.059** | **0.033** | **0.0457** |
| **67** | **7.113** | **0.11** | **0.73** | **0.051** | **0.254** | **0.154** | **0.314** | **0.028** | **0.023** | **0.078** |

| | | | | | | | | | | |
|---|---|---|---|---|---|---|---|---|---|---|
| **70** | **5.17** | **0.11** | **0.91** | **0.03** | **0.25** | **0.336** | **0.43** | **0.02** | **0.023** | **0.0987** |
| **78** | **9.117** | **0.06** | **0.55** | **0.42** | **0.24** | **0.11** | **0.178** | **0.015** | **0.034** | **0.078** |
| **80** | **10.117** | **4.235** | **0.66** | **0.13** | **0.24** | **0.373** | **0.18** | **0.201** | **0.053** | **0.0899** |
| **83** | **11.49** | **5.287** | **0.836** | **0.125** | **0.12** | **0.103** | **0.086** | **0.75** | **0.072** | **0.06** |
| **102** | **19.88** | **14.787** | **0.344** | **0.13** | **0.25** | **0.201** | **0.118** | **0.403** | **0.233** | **0.0157** |
| **104** | **20.88** | **15.787** | **0.556** | **0.501** | **0.121** | **0.33** | **0.27** | **0.201** | **0. 432** | **0.0398** |
| **110** | **23.88** | **18.787** | **6.207** | **0.44** | **0.23** | **0.69** | **0.328** | **0.601** | **0.71** | **0.098** |
| **120** | **28.88** | **23.787** | **9.541** | **0.13** | **0.11** | **0.23** | **0.628** | **0.52** | **0.23** | **0.95** |
| **130** | **33.88** | **28.787** | **12.874** | **0.13** | **0.201** | **0.36** | **0.19** | **0.19** | **0.42** | **0.87** |
| **132** | **34.88** | **29.787** | **13.541** | **2.375** | **0.35** | **0.201** | **0.68** | **0.43** | **0.87** | **0.22** |
| **140** | **38.88** | **33.787** | **16.207** | **3.884** | **0.401** | **0.167** | **0.68** | **0.75** | **0.366** | **0.99** |
| **143** | **40.38** | **35.287** | **17.207** | **4.634** | **1.831** | **0.833** | **0.218** | **0.63** | **0.87** | **0.54** |
| **150** | **43.88** | **38.787** | **19.541** | **6.384** | **2.835** | **0.503** | **0.285** | **0.84** | **0.64** | **0. 12** |
| **160** | **48.88** | **43.787** | **22.874** | **8.884** | **4.835** | **1.36** | **0.19** | **0.43** | **0.227** | **0.01** |
| **162** | **49.88** | **44.787** | **23.541** | **9.384** | **5.235** | **1.673** | **0.022** | **0.26** | **0.02** | **0.04** |
| **170** | **53.88** | **48.787** | **26.207** | **11.384** | **6.835** | **2.312** | **0.075** | **0.063** | **0.058** | **0.05** |
| **180** | **58.88** | **53.787** | **29.541** | **13.884** | **8.835** | **3.979** | **0.059** | **0.056** | **0.515** | **0.241** |
| **183** | **60.38** | **55.287** | **30.541** | **14.634** | **9.435** | **4.479** | **2.269** | **0.243** | **0.03** | **0.07** |
| **190** | **63.88** | **58.787** | **32.874** | **16.384** | **10.835** | **5.645** | **2.566** | **1.09** | **0.134** | **0.12** |
| **195** | **66.38** | **61.287** | **34.541** | **17.634** | **11.835** | **6.479** | **3.281** | **2.718** | **0.024** | **0.07** |
| **197** | **67.38** | **62.287** | **35.207** | **18.134** | **12.235** | **6.812** | **3.566** | **2.968** | **0.0588** | **0.03** |
| **205** | **71.38** | **66.287** | **37.874** | **20.134** | **13.835** | **8.145** | **4.709** | **3.968** | **0.021** | **0.01** |
| **209** | **73.38** | **68.287** | **39.207** | **21.134** | **14.635** | **8.812** | **5.281** | **4.468** | **1.182** | **0.087** |
| **215** | **76.38** | **71.287** | **41.207** | **22.634** | **15.835** | **9.812** | **6.138** | **5.218** | **1.756** | **0.022** |
| **220** | **78.88** | **73.787** | **42.874** | **23.884** | **16.835** | **10.645** | **6.852** | **5.843** | **2.321** | **0.053** |
| **222** | **79.88** | **74.787** | **43.541** | **24.384** | **17.235** | **10.979** | **7.138** | **6.093** | **2.534** | **1.02** |

| | | | | | | | | | | |
|---|---|---|---|---|---|---|---|---|---|---|
| **230** | **83.88** | **78.787** | **46.207** | **26.384** | **18.835** | **12.312** | **8.281** | **7.093** | **3.423** | **2.13** |
| **233** | **85.383** | **80.287** | **47.207** | **27.134** | **19.435** | **12.812** | **8.709** | **7.468** | **3.756** | **3.541** |

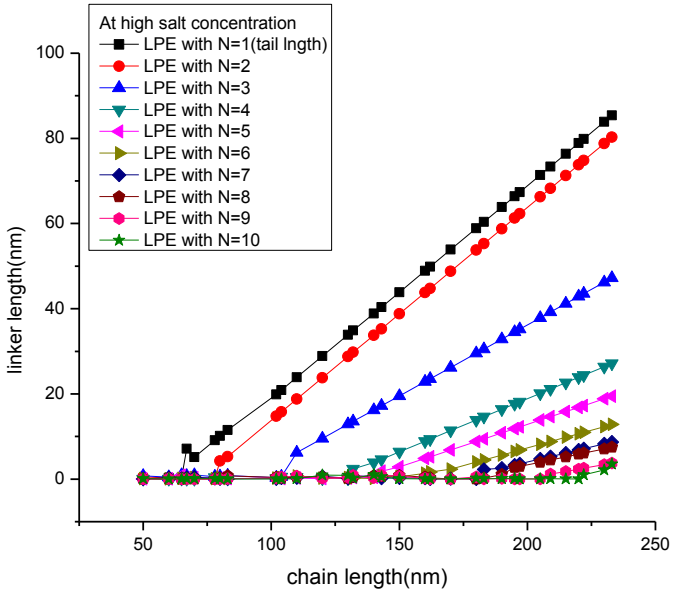


Figure 3.13: linker length between two successive macroions at high salt concentration for the interaction between LPE with N=1,2,3…..,9,10 ammonia cord PAMAM dendrimers of G3 with radius R=3.2nm and total charge of 24e, by using Shklovskii N-sphere model.

The critical wrapping length per one macroion of LPE chain as a function number of macroions participate in the reaction is studied by using Shklovskii N-sphere model. As a result of the interaction between LPE with N=1,2,…,9,10 macroions at different LPE chain length we notice that at each number of macroions there is a critical wrapping length, as the number of macroions participate in the interaction increases the critical wrapping length per one macroion decreases as we see in figure 3.14. The critical wrapping length was observed at low and at high salt concentration which have the same behavior of decreasing by increasing the number of macroions, but salty solution shows strong binding interaction in contrast to low salt concentration, so as we see in figure 3.14, the critical wrapping length at high salt concentration is little more than at low salt concentration. I also studied how the linker varies with number of macroions participate in the interaction at chain length L=233nm as shown in figure 3.15, with increasing the number of macroions the linker length decreases, and as we see at low and high salt concentration the two curves have the same trend, but at high salt concentration linker length is less by a little value than at low salt concentration, this is due to strong binding energy at high salt concentration.

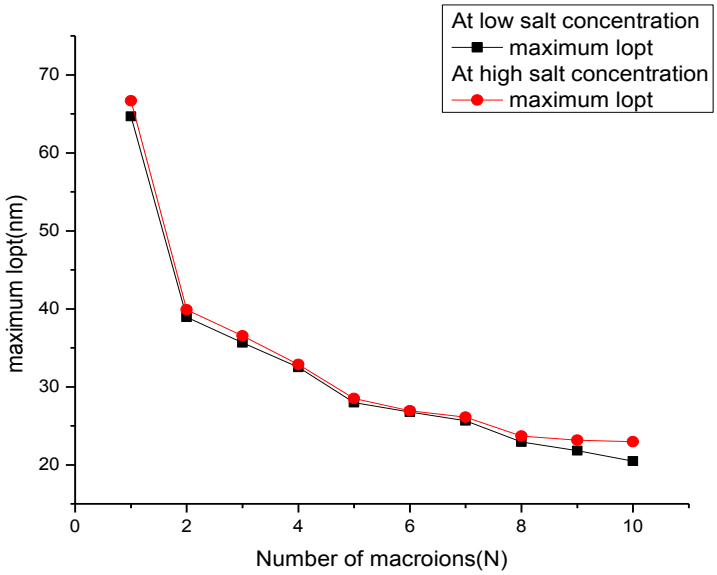


Figure 3.14: Maximum optimal wrapping length per one macroion at both low and high salt concentration as a function of the number of macroions for the interaction between LPE with N=1,2,3…..,9,10 ammonia cord PAMAM dendrimers of G3 with radius R=3.2nm and total charge of 24e, by using Shklovskii N-sphere model.

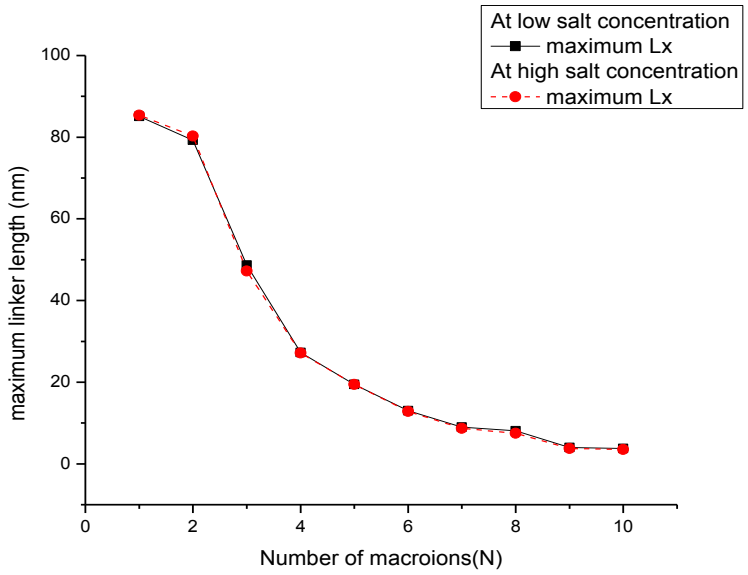


Figure 3.15: The linker length between two successive macroions at both low and high salt concentration as a function of the number of macroions at LPE length of 233nm observed by the interaction between LPE with N=1,2,3…..,9,10 ammonia cord PAMAM dendrimers of G3 with radius R=3.2nm and total charge of 24e, by using Shklovskii N-sphere model.

In the following system which describes the interaction between LPE of length varying from 233 to 550nm with large number of macroions such as N=10,15,20,25,30,35,and 40 each macroion of G3 with radius R=3.2nm and charge 24e, the optimal wrapping length is studied as a function of the LPE chain length at both low salt concentration (10 mM) and high salt concentration (90 mM). As shown in figure 3.16 and analytical results in table 3.21, at low salt concentration the optimal wrapping length per one macroion is linearly increased by increasing the chain length until we reach a critical value which is specified for each N spheres. After this critical point the behavior is similar for all of the cases again to be decreased and finally reached almost a constant value. At high salt concentration as shown in table 3.22 and figure 3.17, the same behavior as in the case at low salt concentration. The difference between the two cases of low and high salt concentration that at high salt concentration the LPE chain become more wrapped around dendrimers, where the saturation in the number of condensed monomers of LPE chain at high salt concentration means that the complex conformation at higher salt concentration shows a strong binding interaction in contrast to low salt concentration.

Table 3.21: Analytical model results for the optimal wrapping length at low salt concentration for the interaction between LPE with N=10,15,20,30,35,40 ammonia cord PAMAM dendrimers of G3 with radius R=3.2nm and total charge of 24e, by using Shklovskii N-sphere model.

| Chain length L(nm) | Optimal length per one macroion $l_{opt}$(nm) | | | | | | |
|---|---|---|---|---|---|---|---|
| | N=10 | N=15 | N=20 | N=25 | N=30 | N=35 | N=40 |
| **215** | **21.487** | **14.332** | **10.749** | **8.599** | **7.166** | **6.142** | **5.374** |
| **220** | **21.947** | **14.638** | **10.979** | **8.783** | **7.319** | **6.273** | **5.48** |
| **222** | **19.234** | **14.74** | **11.06** | **8.848** | **7.373** | **6.32** | **5.53** |
| **250** | **19.234** | **16.63** | **12.475** | **9.98** | **8.31** | **7.12** | **6.23** |
| **270** | **19.233** | **18.26** | **13.95** | **11.36** | **9.63** | **8.4** | **7.475** |
| **273** | **19.233** | **17.636** | **13.625** | **10.9** | **9.08** | **7.785** | **6.812** |
| **280** | **19.233** | **17.636** | **14.22** | **11.192** | **9.31** | **7.98** | **6.98** |
| **340** | **19.233** | **17.636** | **16.975** | **13.58** | **11.316** | **9.7** | **8.487** |
| **345** | **19.233** | **17.636** | **14.987** | **13.788** | **11.49** | **9.84** | **8.617** |
| **390** | **19.233** | **17.636** | **14.987** | **15.587** | **12.989** | **11.133** | **9.742** |
| **410** | **19.233** | **17.636** | **14.987** | **16.392** | **13.66** | **11.708** | **10.237** |
| **412** | **19.233** | **17.636** | **14.987** | **14.102** | **13.89** | **12.01** | **10.45** |

| | | | | | | | |
|---|---|---|---|---|---|---|---|
| **430** | **19.233** | **17.636** | **14.987** | **14.102** | **14.316** | **12.271** | **10.737** |
| **434** | **19.233** | **17.636** | **14.987** | **14.102** | **13.23** | **12.38** | **10.84** |
| **455** | **19.233** | **17.636** | **14.987** | **14.102** | **13.23** | **12.982** | **11.35** |
| **460** | **19.233** | **17.636** | **14.987** | **14.102** | **13.23** | **11.21** | **11.49** |
| **480** | **19.233** | **17.636** | **14.987** | **14.102** | **13.23** | **11.21** | **11.996** |
| **485** | **19.233** | **17.636** | **14.987** | **14.102** | **13.23** | **11.21** | **10.57** |
| **500** | **19.233** | **17.636** | **14.987** | **14.102** | **13.23** | **11.21** | **10.57** |
| **550** | **19.233** | **17.636** | **14.987** | **14.102** | **13.23** | **11.21** | **10.57** |

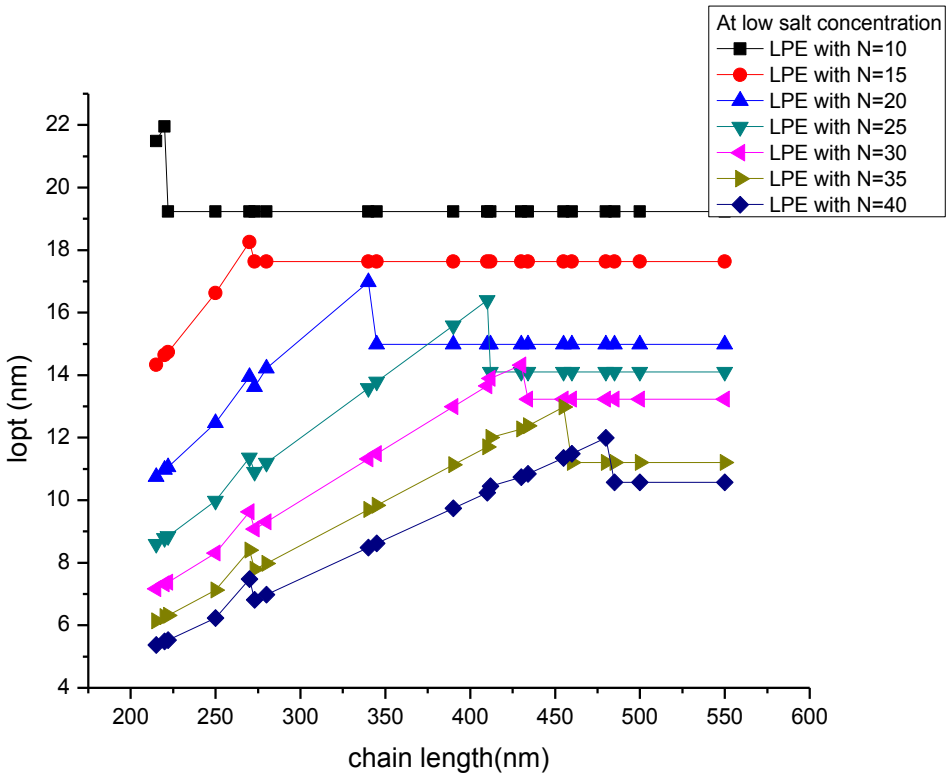


Figure 3.16: Optimal wrapping length per one macroion at low salt concentration for the interaction between LPE with =10,15,20,30,35,40 ammonia cord PAMAM dendrimers of G3 with radius R=3.2nm and total charge of 24e, by using Shklovskii N-sphere model.

Table 3.22: Analytical model results for the optimal wrapping length at high salt concentration for the interaction between LPE with N=10,15,20,30,35,40 ammonia cord PAMAM dendrimers of G3 with radius R=3.2nm and total charge of 24e, by using Shklovskii N-sphere model.

| Chain length L(nm) | Optimal length per one macroion $l_{opt}$(nm) | | | | | | |
|---|---|---|---|---|---|---|---|
| | N=10 | N=15 | N=20 | N=25 | N=30 | N=35 | N=40 |
| **215** | **21.487** | **14.332** | **10.749** | **8.599** | **6.166** | **6.142** | **5.374** |
| **220** | **21.947** | **14.638** | **10.979** | **8.783** | **7.019** | **6.273** | **5.48** |
| **222** | **22.18** | **14.74** | **11.06** | **8.848** | **7.173** | **6.32** | **5.53** |
| **230** | **22.98** | **15.33** | **11.475** | **8.98** | **7.31** | **6.42** | **5.623** |
| **233** | **20.786** | **15.5** | **11.629** | **9.303** | **7.75** | **6.645** | **5.814** |
| **270** | **20.786** | **18.26** | **13.95** | **11.36** | **9.63** | **8.4** | **7.475** |
| **273** | **20.786** | **18.936** | **13.625** | **10.9** | **9.08** | **7.785** | **6.812** |
| **280** | **20.786** | **18.001** | **14.22** | **11.192** | **9.31** | **7.98** | **6.98** |
| **340** | **20.786** | **18.001** | **16.975** | **13.58** | **11.316** | **9.7** | **8.487** |
| **350** | **20.786** | **18.001** | **17.445** | **13.788** | **11.49** | **9.84** | **8.617** |
| **355** | **20.786** | **18.001** | **16.345** | **13.956** | **12.02** | **9.96** | **8.72** |
| **390** | **20.786** | **18.001** | **16.345** | **15.587** | **12.989** | **11.133** | **9.742** |
| **410** | **20.786** | **18.001** | **16.345** | **16.392** | **13.66** | **11.708** | **10.237** |
| **425** | **20.786** | **18.001** | **16.345** | **16.902** | **13.89** | **12.01** | **10.45** |
| **430** | **20.786** | **18.001** | **16.345** | **15.012** | **14.316** | **12.271** | **10.737** |
| **434** | **20.786** | **18.001** | **16.345** | **15.012** | **14.45** | **12.38** | **10.84** |
| **440** | **20.786** | **18.001** | **16.345** | **15.012** | **12.83** | **12.982** | **11.35** |
| **460** | **20.786** | **18.001** | **16.345** | **15.012** | **12.83** | **13.128** | **11.49** |
| **465** | **20.786** | **18.001** | **16.345** | **15.012** | **12.83** | **11.51** | **11.996** |
| **485** | **20.786** | **18.001** | **16.345** | **15.012** | **12.83** | **11.51** | **12.112** |
| **490** | **20.786** | **18.001** | **16.345** | **15.012** | **12.83** | **11.51** | **10.86** |
| **500** | **20.786** | **18.001** | **16.345** | **15.012** | **12.83** | **11.51** | **10.86** |

| | | | | | | | |
|---|---|---|---|---|---|---|---|
| **550** | **20.786** | **18.001** | **16.345** | **15.012** | **12.83** | **11.51** | **10.86** |

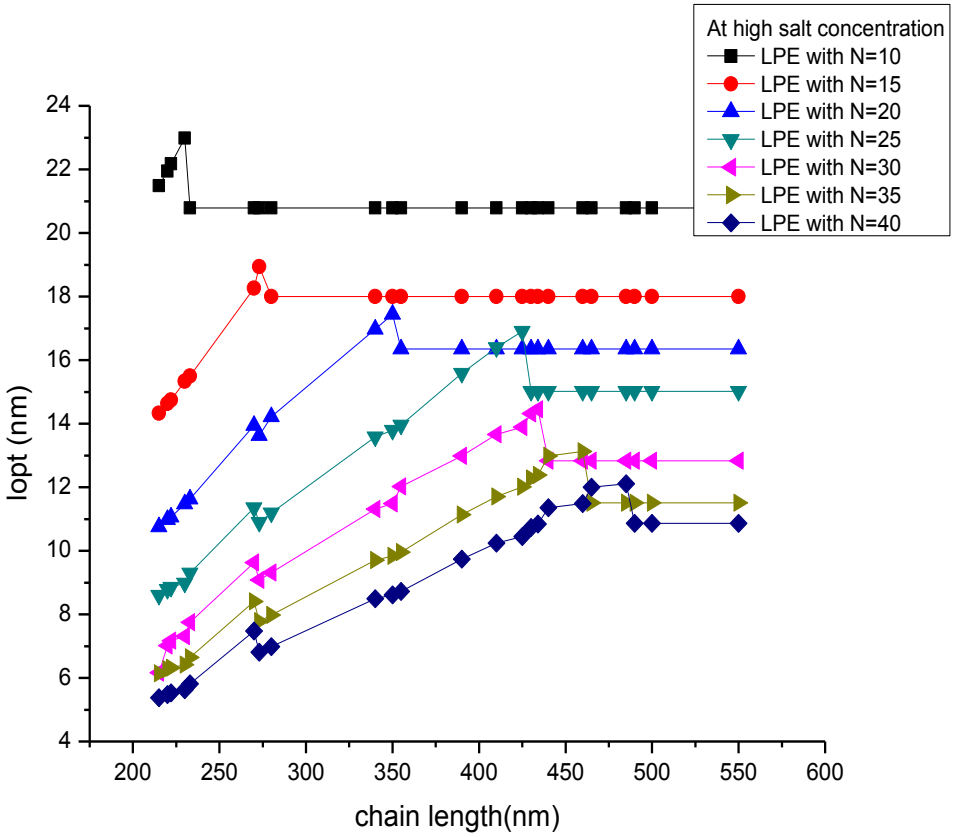


Figure 3.17: Optimal wrapping length per one macroion at high concentration for the interaction between LPE with =10,15,20,30,35,40 ammonia cord PAMAM dendrimers of G3 with radius R=3.2nm and total charge of 24e, by using Shklovskii N-sphere model.

The effect of the chain length of LPE on the linker formed between NG3 – LPE chain complexs have been studied for N=10,15,20,25,30,35,40 macroions at low and high salt concentration. The total length of LPE divides into two parts, the optimal wrapping length and the linker. The behavior of optimal wrapping length per one macroion was shown in figures above (figure 3.16 and 3.17). The behavior of the linker length is shown in figure 3.18 at low salt concentration, and in figure 3.19 at high salt concentration for LPE interacts with N=10,15,20,25,30,35,40 dendrimers. At the beginning of the interaction the linker start to appear and keep increasing as we increase chain length. Tables 3.23 and 3.24 show the value of linker length at low and high salt concentration respectively, as we see in these two tables with the help of figures 3.18 and 3.19, we have the largest wrapping length of LPE chain around dendrimers in more salty solution, as a result the linker formed between complexes is smaller than the linker length formed in low salty solution.

Table 3.23: Analytical model results for the linker length between two successive macroions at low salt concentration for the interaction between LPE with N=10,15,20,30,35,40 ammonia cord PAMAM dendrimers of G3 with radius R=3.2nm and total charge of 24e, by using Shklovskii N-sphere model.

| Chain length L(nm) | **linker length $L_x$ (nm)** | | | | | | |
|---|---|---|---|---|---|---|---|
| | N=10 | N=15 | N=20 | N=25 | N=30 | N=35 | N=40 |
| **215** | **0.023** | **0.098** | **0.0749** | **0.0599** | **0.0166** | **0.0142** | **0.0374** |
| **220** | **0.13** | **0.087** | **0.0979** | **0.0783** | **0.0319** | **0.0273** | **0.048** |
| **222** | **2.966** | **0.12** | **0.06** | **0.0848** | **0.0373** | **0.032** | **0.53** |
| **250** | **5.766** | **0.32** | **0.0475** | **0.098** | **0.31** | **0.012** | **0.23** |
| **270** | **7.767** | **0.123** | **0.095** | **0.036** | **0.63** | **0.04** | **0.475** |
| **273** | **8.067** | **0.564** | **0.0625** | **0.09** | **0.08** | **0.0785** | **0.812** |
| **280** | **8.767** | **1.031** | **0.22** | **0.192** | **0.31** | **0.98** | **0.98** |
| **340** | **14.767** | **2.031** | **0.975** | **0.058** | **0.316** | **0.7** | **0.487** |
| **345** | **15.276** | **5.364** | **2.263** | **0.788** | **0.49** | **0.84** | **0.617** |
| **390** | **19.767** | **8.364** | **4.413** | **0.587** | **0.989** | **0.133** | **0.742** |
| **410** | **21.767** | **9.687** | **5.513** | **0.392** | **0.66** | **0.708** | **0.237** |
| **412** | **21.967** | **9.98** | **5.613** | **2.378** | **0.89** | **0.01** | **0.45** |
| **430** | **23.767** | **11.031** | **6.513** | **3.098** | **0.316** | **0.271** | **0.737** |
| **434** | **24.167** | **11.297** | **6.713** | **3.258** | **1.236** | **0.38** | **0.84** |
| **455** | **26.267** | **12.697** | **7.763** | **4.098** | **1.93** | **0.982** | **0.35** |
| **460** | **26.767** | **13.031** | **8.013** | **4.298** | **2.103** | **1.932** | **0.98** |
| **480** | **28.767** | **14.364** | **9.013** | **5.098** | **2.77** | **2.504** | **0.996** |
| **485** | **29.267** | **14.697** | **9.263** | **5.298** | **2.936** | **2.64** | **1.555** |
| **500** | **30.767** | **15.697** | **10.013** | **5.898** | **3.436** | **3.075** | **1.93** |
| **550** | **35.767** | **19.031** | **12.513** | **7.898** | **5.103** | **4.504** | **3.18** |

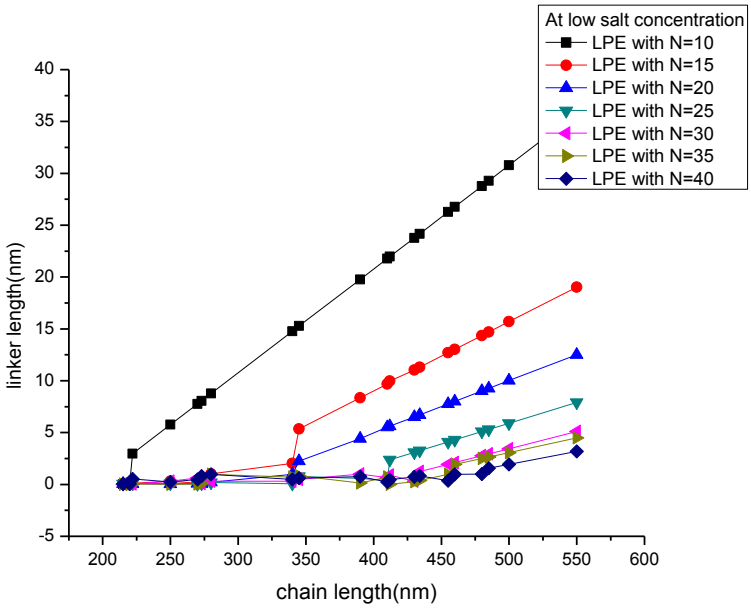


Figure 3.18: linker length between two successive macroions at low salt concentration for the interaction between LPE with =10,15,20,30,35,40 ammonia cord PAMAM dendrimers of G3 with radius R=3.2nm and total charge of 24e, by using Shklovskii N-sphere model

Table 3.24: Analytical model results for the linker length between two successive macroions at high salt concentration for the interaction between LPE with N=10,15,20,30,35,40 ammonia cord PAMAM dendrimers of G3 with radius R=3.2nm and total charge of 24e, by using Shklovskii N-sphere model.

| Chain length L(nm) | **linker length $L_x$ (nm)** | | | | | | |
|---|---|---|---|---|---|---|---|
| | N=10 | N=15 | N=20 | N=25 | N=30 | N=35 | N=40 |
| **215** | **0.023** | **0.098** | **0.0749** | **0.0599** | **0.0166** | **0.0142** | **0.0374** |
| **220** | **0.13** | **0.087** | **0.0979** | **0.0783** | **0.0319** | **0.0273** | **0.048** |
| **222** | **0.966** | **0.12** | **0.06** | **0.0848** | **0.0373** | **0.032** | **0.53** |
| **230** | **0.98** | **0.32** | **0.0475** | **0.098** | **0.31** | **0.012** | **0.23** |
| **233** | **2.514** | **0.123** | **0.095** | **0.036** | **0.63** | **0.04** | **0.475** |
| **270** | **6.214** | **0.564** | **0.0625** | **0.09** | **0.08** | **0.0785** | **0.812** |
| **273** | **6.514** | **0.131** | **0.22** | **0.192** | **0.31** | **0.98** | **0.98** |
| **280** | **7.214** | **0.665** | **0.975** | **0.058** | **0.316** | **0.7** | **0.487** |

| | | | | | | | |
|---|---|---|---|---|---|---|---|
| **340** | **13.214** | **4.665** | **0.263** | **0.788** | **0.49** | **0.84** | **0.617** |
| **350** | **14.214** | **5.332** | **0.413** | **0.587** | **0.989** | **0.133** | **0.742** |
| **355** | **14.714** | **5.665** | **1.405** | **0.392** | **0.66** | **0.708** | **0.237** |
| **390** | **18.214** | **7.999** | **3.155** | **2.378** | **0.89** | **0.01** | **0.45** |
| **410** | **20.214** | **9.332** | **4.155** | **0. 98** | **0.316** | **0.271** | **0.737** |
| **425** | **21.714** | **10.332** | **4.905** | **0.958** | **0.236** | **0.38** | **0.84** |
| **430** | **22.214** | **10.665** | **5.155** | **2.188** | **0.93** | **0.982** | **0.35** |
| **434** | **22.786** | **10.932** | **5.355** | **2.348** | **0.903** | **0.932** | **0.98** |
| **440** | **22.214** | **11.332** | **5.655** | **2.588** | **1.836** | **0.904** | **0.996** |
| **460** | **25.214** | **12.665** | **6.655** | **3.388** | **2.503** | **0.964** | **0.955** |
| **465** | **25.714** | **12.999** | **6.905** | **3.588** | **2.67** | **1.775** | **0.93** |
| **485** | **27.714** | **14.332** | **7.905** | **4.388** | **3.336** | **2.347** | **0.918** |
| **490** | **28.214** | **14.665** | **8.155** | **4.588** | **3.503** | **2.49** | **1.39** |
| **500** | **29.214** | **15.332** | **8.655** | **4.988** | **3.836** | **2.775** | **1.64** |
| **550** | **34.214** | **18.665** | **11.155** | **6.988** | **3.836** | **4.204** | **2.89** |

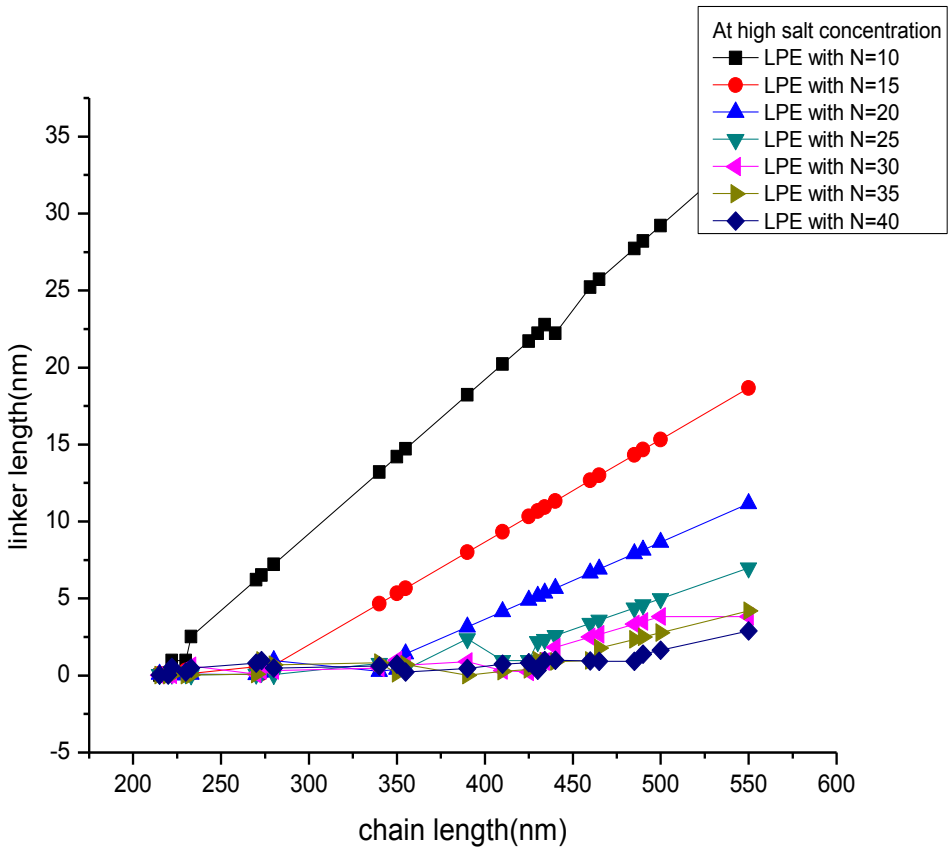


Figure 3.19: linker length between two successive macroions at high salt concentration for the interaction between LPE with N =10,15,20,30,35,40 ammonia cord PAMAM dendrimers of G3 with radius R=3.2nm and total charge of 24e, by using Shklovskii N-sphere model.

The interaction between LPE with N =10,15,20,30,35,40 macroions at different LPE chain length was used to study the effect of increasing the number of macroions on the maximum wrapping length (critical value). We notice that at each number of macroions participating in the interaction with LPE chain, there is a critical wrapping length, as the number of macroions increases the critical wrapping length per one macroion decreases as we see in figure 3.20. The critical wrapping length was observed at low and at high salt concentration which have the same behavior of decreasing by increasing the number of macroions, but salty solution shows strong binding interaction in contrast to low salt concentration, so as we see in figure 3.20, the critical wrapping length at high salt concentration is little more than at low salt concentration. I also studied how the linker varies with number of macroions participate in the interaction at chain length L=550nm as shown in figure 3.21, with increasing the number of macroions the linker length decreases, and as we see at low and high salt concentration the two curves have the same trend, but at high salt concentration linker length is less by a little value than at low salt concentration, this is due to strong binding energy at high salt concentration.

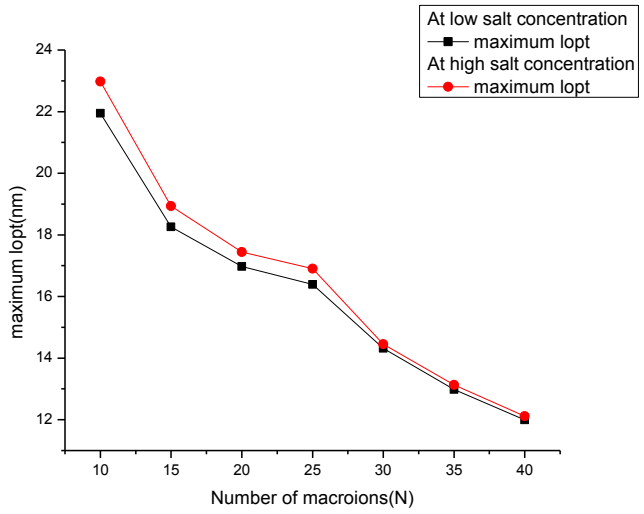


Figure 3.20: The critical wrapping length per one macroion at both low and high salt concentration as a function of the number of macroions for the interaction between LPE with N =10,15,20,30,35,40ammonia cord PAMAM dendrimers of G3 with radius R=3.2nm and total charge of 24e, by using Shklovskii N-sphere model.

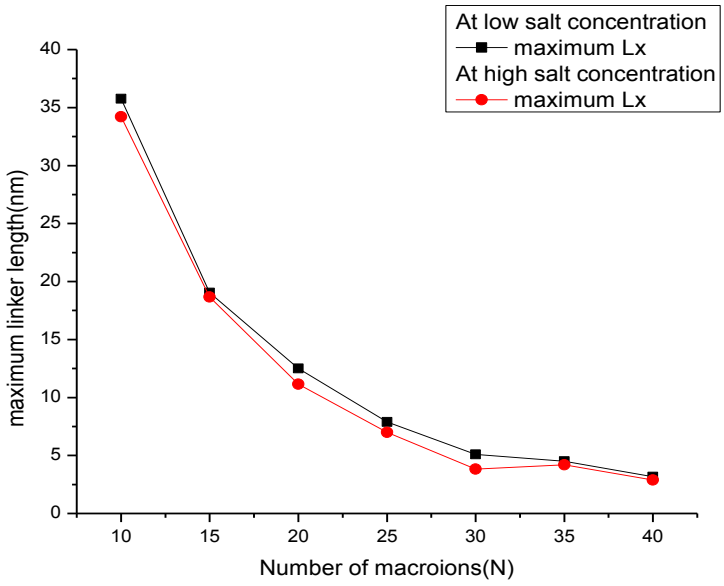


Figure 3.21: The linker length between two successive macroions at both low and high salt concentration as a function of the number of macroions at LPE length of 233nm observed by the interaction between LPE with N=10,15,20,30,35,40ammonia cord PAMAM dendrimers of G3 with radius R=3.2nm and total charge of 24e, by using Shklovskii N-sphere model.

### 3.5 Simulation details

Computational resources are utilized to mimic the experiments, it is more efficient to study the LPE-macroion complex using computer simulations which achieve various length and time scales on the basis of the potential function (force field) and coarse-grained (CG) degree of models. Brownian dynamics (BD) simulation is the method used here to investigate the properties of the complexation of LPE with three oppositely charged macroions.

All the following BD simulations were carried out using BD-BOX program which utilized Ermak-MacCammon algorithm with 20fs time step to find the Brownian trajectories of the particles solvated in water with viscosity 0.01 Poise, dielectric constant of 78.54 and 1:1salt concentration of 90 mM.

As long as we are interested in a study of the properties of LPE-macroion complex, we want to concentrate on the case of LPE interacts with three macroions. Here we used dendrimers of G2 to represent the macroions modeled by a positively charged sphere.

#### 3.5.1 Radius of gyration

In general, the radius of gyration can be defined as a length that represents the distance in a rotating system between the point about which it is rotating and the point to or from which a transfer of energy has the maximum effect. We calculated the radius of gyration $R_g$ for the complex as a whole which isthe average distance of all beads from their common center of gravity, or a point where a chain will be in a balanced position when placed on top of an imaginary tip. The radius of gyration for the complex versus time is shown in figure 3.22 which is calculated for LPE with three dendrimers of G2.

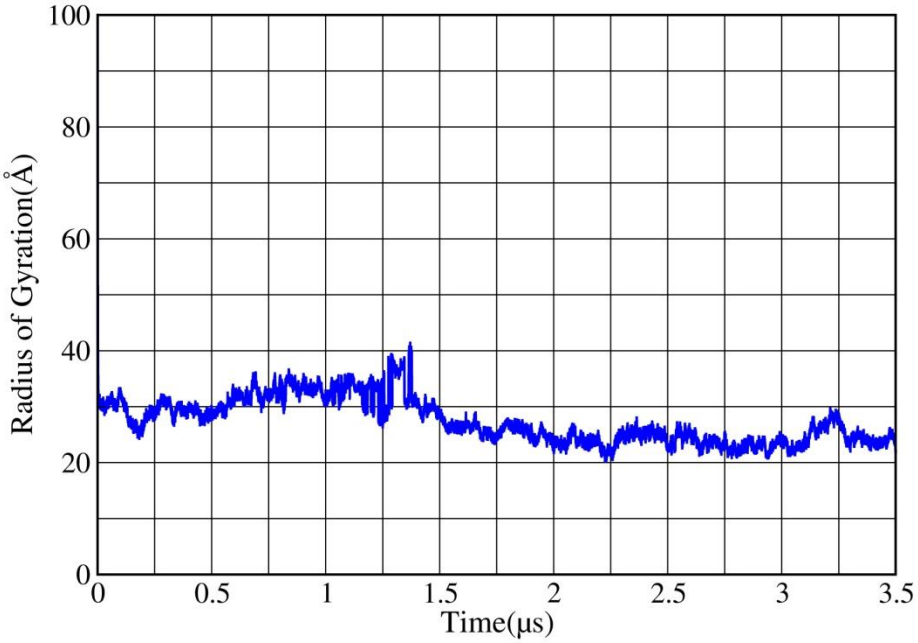


Figure 3.22 Radius of gyration for a complex of LPE with three oppositely charged drndrimers of G2.

As shown in Figure 3.22, the value of the radius of gyration can be understood by notice that two different regimes are observed. First $R_g$ slowly increases with time( which means increases by increasing condenced monomers on the dendrimer) until some value, where we can say that all chain monomers are adsorbed onto the dendrimers, and only small tails are formed. With further increase of time, the total charge of a chain exceeds the total charge of the dendrimers, so the value of the $R_g$ decreases since the condenced monomers reach the optimal value and no need for more monomers, and linkers are more favorable to appear. So we can conclude that the radius of gyration increases until the formation of the complex (maximum number of monomers condense on the dendrimers) after that the radius of gyration decreases.

When a total charge of a whole LPE chain exceeds the total charge of the three dendrimers, the chain of the complex is in a compact folded conformation with linkers and one or two tails appear, as shown in the snapshots in figure 3.23 for complexes formed by 100 beads (each bead has a diameter of $2nm$)of LPE with three dendrimers of G2. It is shown that the configuration of a complex is strongly depends on the number of condensed monomers. We recognize in figure 3.23 the region of chain lengths where dendrimers are close to each other and form a joint macroions with linker at time1.4μs (figure 3.23a). After a duration of about 3.3μs the linkers between dendrimers exist (figure 3.23b). If we let the complex reach a stable case after a time of about 3.5μs, the linkers become nearly constant and the tails appear (figure 3.23c).

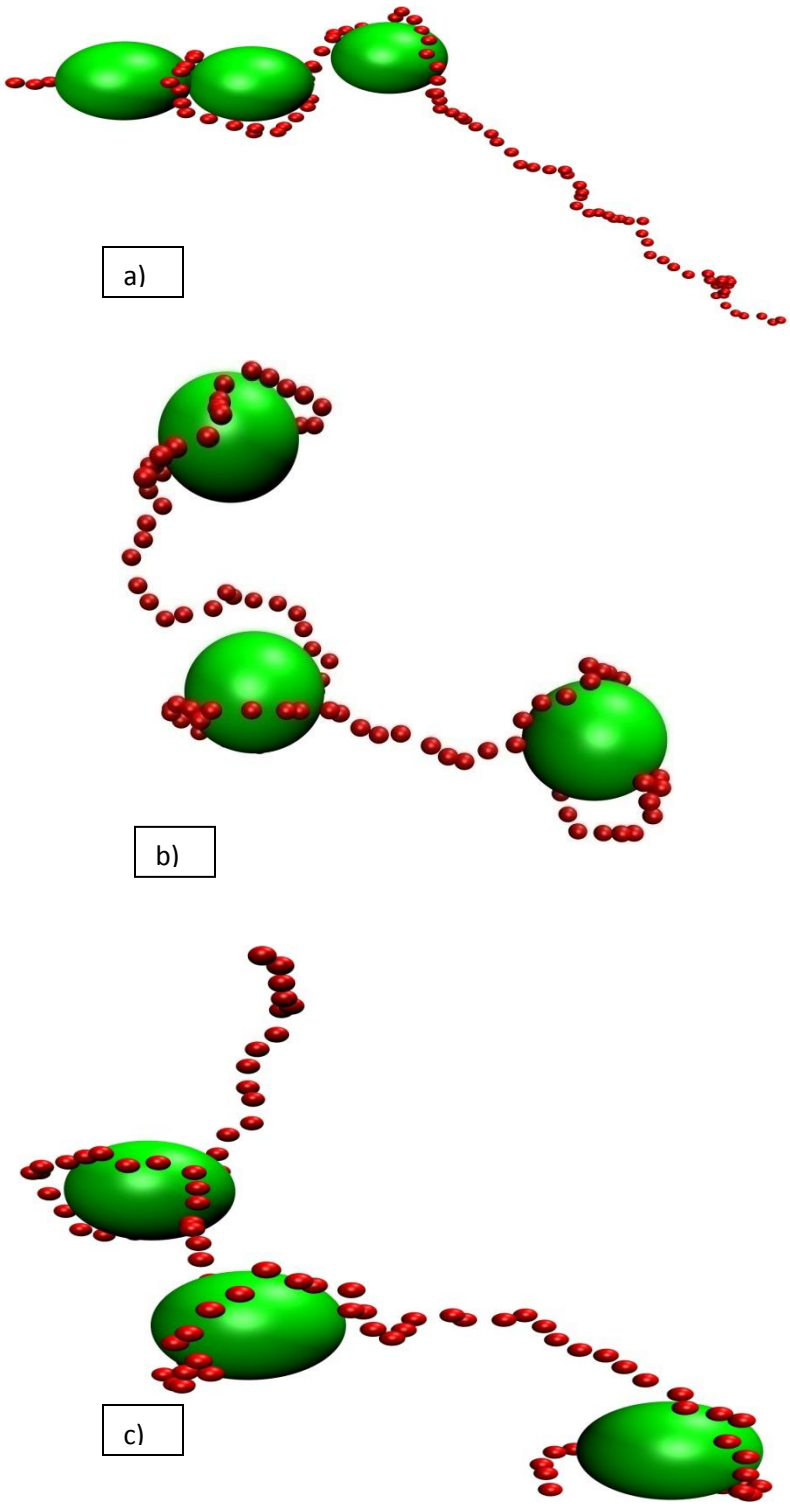


Figure 3.23 Typical snapshots of a complex formed by LPE of 100 beads each with diameter of $2nm$ and three G2 dendrimers, taken at different times (a) 1.4μs (b) 3.3 μs (c) 3.5μs.

For the case of a complex formed by three dendrimers of G2 each of radius 1.45nm, and charge of 16e with LPE chain varies from 20 to 100 nm, a semiquantitative agreement of simulation results with prediction of correlation theory developed by us for the complex formed by N solid spherical macroions and using N to be three dendrimers, has been observed below in figure 3.24.

Figure 3.24 compares the theoretical predictions for the overcharging and the linker length with the simulation results for 3G2 complexes. It is seen that the local criterion of adsorption gives qualitative agreement with the theory predictions but the degree of the overcharging is little higher than the theoretical value. Developed theory predicts that there are two regimes for a complex configuration as a function of the LPE length. Below some critical length, the chain is wound around three macroions which are close to each other. The overcharging increases with the lengthening of LPE. When the maximum overchargingdegree is achieved, the two linkers appear and macroions start to separate.

The developed theory predicts also that all nonadsorbed LPE monomers belong to the linkers. Its length increases monotonously after the maximum of adsorption is achieved. However, our simulations show the release of a remarkable tail which coexists with the two linkers. Therefore, the length of the two linkers occurs to be bit little smaller than the theoretical one in this region of the LPE length.

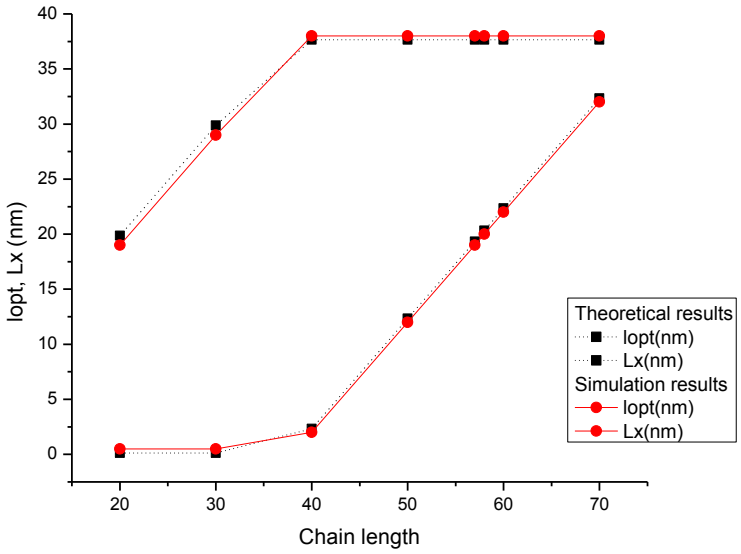


Figure 3.24 Comparison of the simulated amount of the adsorbed LPE monomers ($l_{opt}$) and number of LPE monomers in linker ($L_X$) with theoretical predictions. Dotted lines represent theoretical results and solid lines represent simulation results for both optimal wrapping length per one macroion, and linker length between two successive macroions.

### 3.5.2 Distance between dendrimer and LPE beads

The dynamics of the LPE- three dendrimers complexes are studied by analyzing the distance between the dendrimer and each LPE participating in the complex all the time. In detail, the complexes are extracted at the final step of simulation at 7μs by detecting the number and positions of the LPE beads that are forming the complex for each dendrimer bead. Figure 3.25 shows a complex at the first time step of simulation, $d_i$ is the distance between the center of the dendrimer and the distance of the ith DNA bead taking part in the complex. I calculated the averages of these distances for all complexes formed and taking the average through all frames.

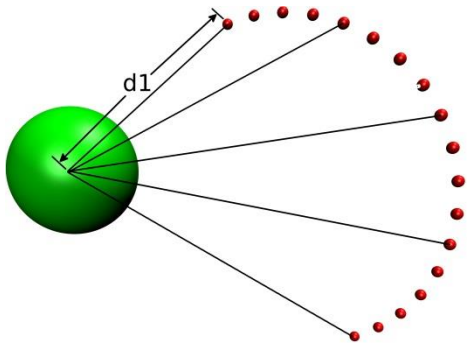


Figure 3.25: illustrative figure of the LPE-dendrimer complex at the first time step of simulation.

Figure 3.26 below exhibits the expected behavior of the LPE wrapping on three G2 dendrimers through complex formation. At the initial μs, the LPE becomes closer to the dendrimer but the wrapping starts at 2.5 μs. During this time of simulation, the LPE reaches its minimum distance from the dendrimer which is 32Å. After that the LPE makes several energetic and random movements to find its optimal wrapping patterns on the dendrimer surface.

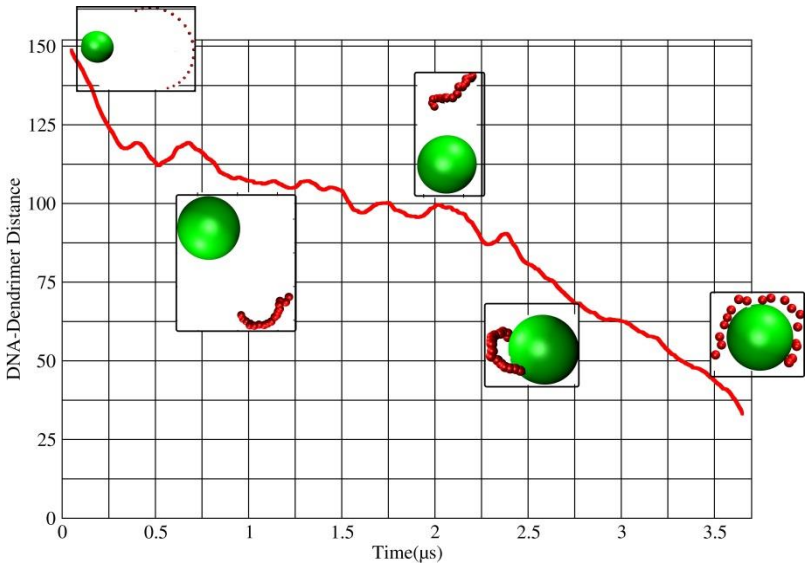


Figure 3.26: The distance between the LPE and dendrimer

### 3.5.3 The Effect of Salt Concentration

The salt concentration is taken into consideration through the inverse of Debye screening length $k^{-1} = (8\pi c_s l_B)^{-\frac{1}{2}}$, where $l_B = \frac{e^2}{\varepsilon k_B T}$ is the Bjerrum length, $k_B T$ is the thermal energy and $c_s$ is the salt concentration. Increasing the salt concentration has the same effects as increasing pH or increasing the negative charges in the salt which weakens the attractions between the negative charges on the LPE and the positive charges on the dendrimer.

We carried out various BD simulations for generations 2 and 4 at different salt concentrations as shown in table 3.25 below. In this part we use a LPE of 200 Å length(of 100 beads each of 2Å diameter) with three dendrimers of generation 2, and we used a LPE of 300 Å length(of 150 beads each of 2Å diameter) with three dendrimers of generation 4.

Table 3.25 Details of BD simulations for generations 2 and 4 at different salt concentrations. A chain of 100 beads (200 Å length), and 150 beads (300 Å length) were used for G2 and G4 respectively.

| Generation | No of LPE beads | No of dendrimer beads | Salt Concentration (mM) | $k^{-1}$(Å) | Length of simulation (μs) |
|---|---|---|---|---|---|
| 2 | 100 | 3 | 10 | 30 | 7 |
| 2 | 100 | 3 | 90 | 10 | 7 |
| 4 | 150 | 3 | 10 | 30 | 16 |
| 4 | 150 | 3 | 90 | 10 | 16 |
| 4 | 150 | 3 | $9x10^6$ | 0.033 | 1.2 |

Our BD simulations reveal that for G2 dendrimer, the LPE wrapping starts faster at high concentration, and upon increasing the concentration of salt the LPE chain become more wrapped around dendrimers(less distance between DNA-Dendrimers) where the saturation in the number of condenced monomers of LPE at the end of the interaction is due to the finite length of the LPE. There are no differences between the behavior of G4 dendrimers in the salts of concentrations 10 and 90 mM, as illustrated in figures 3.27 and 3.28 below, so one can conclude that for lower denderimer generations (namely G2) upon increasing of salt concentration the number of condenced monomers on dendrimers increases considerably, whereas for higher generations (G4) the number of condence monomers on dendrimers doesn't change significantly, which means that the aggregate formed from the complexation between LPE chain and dendrimers of higher generations seemed to be more neutralized because more and more DNA charges being get more neutralized by higher generations, this trend is found in agreement with recent theoritecal study (Qamhieh and Abu-Khaleel, 2014, see ref. [57] )and with experimental study (Carnerup, et al., 2011, see ref. [15] ).

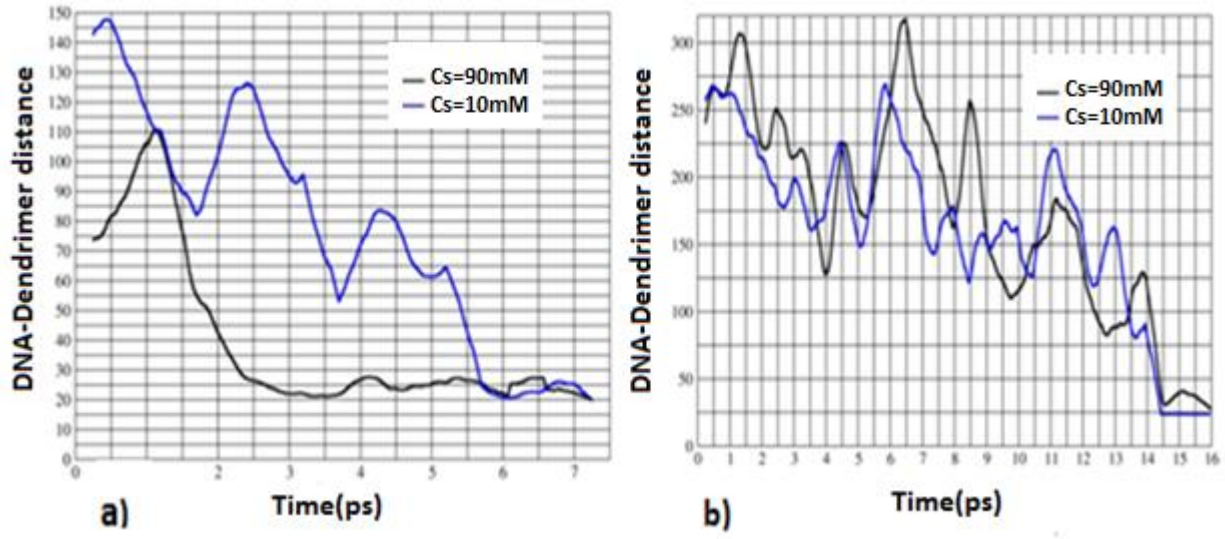


Figure 3.27 The average distance between DNA and a) G2dendrimer and b) G4 dendrimer vs. time of the simulation.

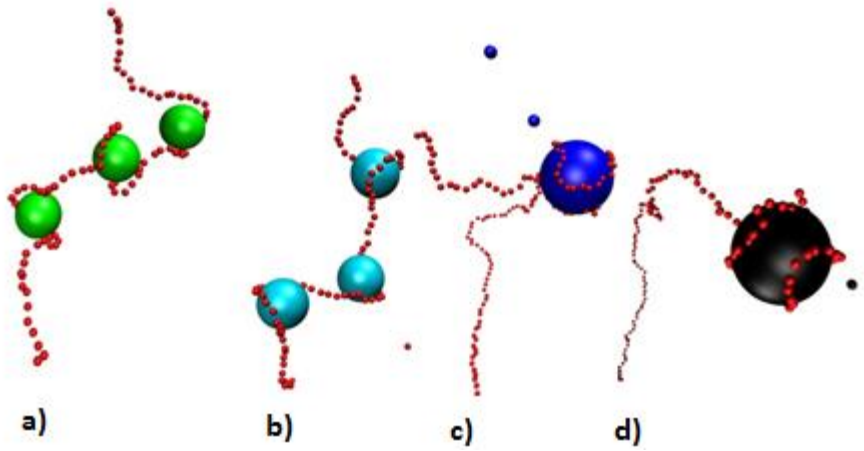


Figure 3.28: ( a) and (b) G2-DNAcomplexes at salt concentrations 10mM(green) and 90mM(cyan) respectively. (c) and (d)areG4-DNA complexes at salt concentrations 10mM(blue) and 90mM(black) respectively.

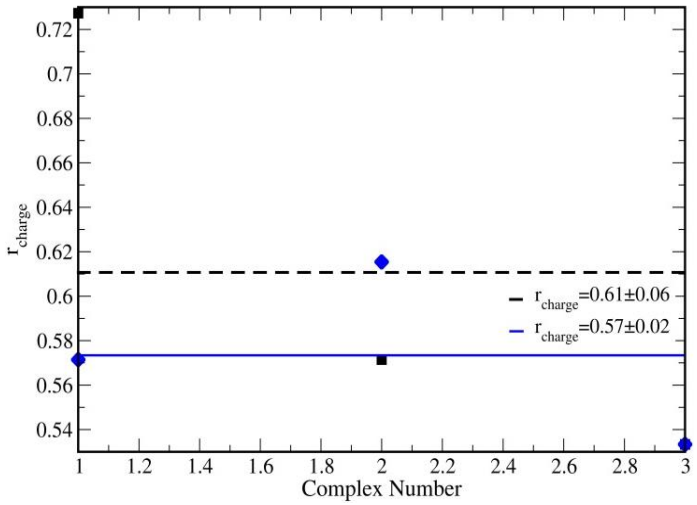


Figure 3.29 :the charge ratio of the DNA-G2 dendrimer complex at salt concentration of 10mM (blue) and 90mM(black).

Figure 3.29 presents the charge ratio of the complexes formed from DNA and G2 dendrimer at two values of salt concentration(10mM and 90mM)where the charge ratio here is defined as the charge of dendrimer over the charge of DNA for each complex. The BD simulations result shows that $r_{charge} = 0.57 \pm 0.02$ at salt concentration of 10mM, and $r_{charge} = 0.61 \pm 0.06$ at high salt concentration (90mM). As a conclusion increasing the salt concentration leads to increase the ionic screening effects which decrease the attractions between DNA and dendrimer.

# Chapter Four

# Conclusions and Future Work

## Chapter Four

### Conclusions and Future work

Theoretical prediction of the wrapping length of LPE on maccroions for different lengths of LPE chain with one and multi macroions showed that at short LPE chain length the whole LPE chain collapses on the macroions. When L increases further, a first order phase transition happens and a tail with a finite length appeared in the case of one macroion, and a linker appeared in the case of two or three macroions.

The complex was overcharged for all optimal wrapping lengths, but we noticed that the overcharging increased until it reached a maximum value of wrapping length and then kept slightly constant. The optimal wrapping length increases with increasing LPE length until it reachs to the critical value of the chain length. Above this critical length, the linker appears and then increases with the increasing of chain length.

As the generation increased, the optimal wrapping length (maximum point) increased. This increasing of $l_{opt}$ by increasing the generation of dendrimer was due to the increasing of size by increasing the radius and due to increasing in the charge, so more monomers were needed to be condensed on the dendrimers to reach the optimal value.

The calculated radius of gyration $R_g$ for the complex as a whole increases until the formation of the complex (maximum number of monomers condense on the dendrimers), after that the radius of gyration decreases.

The dynamics of the LPE- three dendrimers complexes showed that at initial μs, the LPE becomes closer to the dendrimer but the wrapping starts at 2.5 μs. During the time of simulation, the LPE reaches its minimum distance from the dendrimer which is 32Å. After that the LPE makes several energetic and random movements to find its optimal wrapping patterns on the dendrimer surface.

In conclusion, the model presented for complexation of LPE with one and multi spheres is suitable to represent the complexation of DNA with dendrimers. As a lot of our results are in agreement with a series of computer simulations carried out.

The present analytical study has a great practical significance and promises to be an exciting area for further research in gene therapy. We expect that more results could be obtained by this new developed model. Despite of this, for future work minor modifications could be inserted on the developed model to study the cases of LPE with multi spheres (more than N=3) ; this can be done by work on the developed model by make some approximations and simplifications on the total derived equation, also more developed computer system should be used to be able to deal with such complicated equation and get results in short time.

**Appendix A: Shklovskii model**

In this appendix we present the model developed by ShKlovskii and co-workers (Shklovskii 2000) which studied the polyelectrolyte/ macroion complex using analytical model. He assumed hard sphere of macroion, with radius R and charge 100e distributed on the surface of the sphere. The polyelectrolyte will be considered as a chain of N joined hard spherical beads each with charge –e, and radius a = $0.2l_B$, where $l_B$ is the Bjerum length which is equal to $l_B$= 7.12 $A^0$, so that; the total length of the PE is L, where L>>R. The linear charge density of PE is $\eta$, but we will assume it weakly charged, so that $\eta \ll \eta_c$ , where $\eta_c$ obtained from Onsager-Manning critical linear density $\eta_c = \frac{k_B T D}{e}$, where $k_B$ is Boltzmann constant, T is the temperature, and D is the dielectric constant of water.

This model of the complexation is shown in FigA.1, he placed the complexation of PE/Macroion in both, salt-free solution and in salty solution separately. This was done to calculate the net charge of the complexation $Q^*$, and to calculate the charge inversion ration $\frac{|Q^*|}{Q}$, where Q is the positive charge of the macroion, and $Q^*$ is the negative net charge of the complexation, whose absolute value is as large as( some % value) of the bare positive charge.

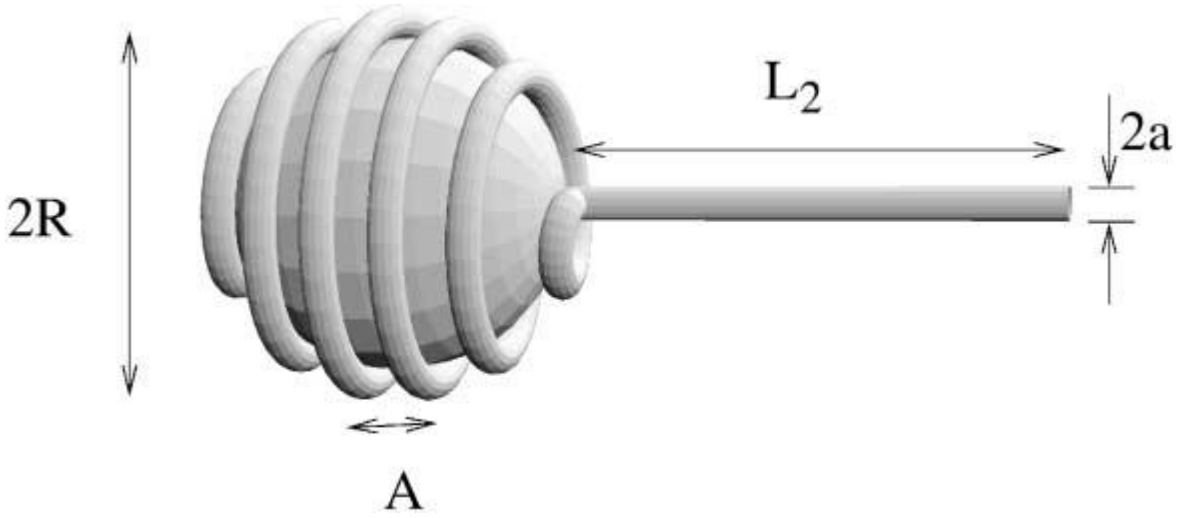


Figure A.1. The PE winds around a spherical macroion. Due to their Coulomb repulsion, neighboring turns lie parallel to each other. Locally, they resemble a one-dimensional Wigner crystal with the lattice constant A.

Shklovskii model for electrostatic complexation which assumes the macroion as a hard sphere, and his goal is to calculate the net charge of the complex $Q^* = Q - L_1\eta = (\mathcal{L} - L_1)\eta$ , Where $\mathcal{L}$ is the neutralizing length$\mathcal{L} = \frac{Q}{\eta}$ ,and the charge inversion ratio $\frac{|Q^*|}{Q}$.

For the salt-free solution in which all Coulomb interactions are not screened. The total energy of the macroion with the PE solenoid wound around it,$F_1$,can be written as a sum of the Coulomb energy of its net charge plus the self-energy of PE:

$$F_1 = L_1 ln\left(\frac{R}{a}\right) - L_1 ln\left(\frac{L_1}{R}\right) + \frac{(L_1-\mathcal{L})^2}{2R} \quad \text{(A.1)}$$

Where $L_1$ is the length of the PE molecule wrapped around the hard sphere( macroion).

Shklovskiiwrote all energies in units of $\frac{\eta^2}{D}$, where D is dielectric constant of water (thus, all energies have the dimensionality of length. The first two terms of eq.1 is called $F_{elastic}(L_1)$ , which represents the elastic (bending) free energy required to bend $L_1$ of the chain of radius a around hard sphere of radius R. The third term of eq.1, is called $F_{compl}(L_1)$, which represents the electrostatic charging free energy of a spherical complex.

Shklovskii studied the effect of the chain length for two tails configuration, firstly; for one tail configuration. In which, the total free energy of the system is the sum of that of the spherical complex, the self-energy of the tail and their interaction. This gives

$$F = F_1 + L_2 ln\left(\frac{L_2}{a}\right) + (L_1 - \mathcal{L}) ln\left(\frac{L_2+R}{R}\right) \quad \text{(A.2)}$$

The first term in equation A.2 is described above, the second term is called $F_{chain}(L_2)$ , which describes the electrostatic free energy of the remaining chain length $L_2$ . the last term in equation A. 2 is called $F_{compl-chain}(L_1)$ , which is the electrostatic free energy of the interaction between the complex and the reminder of the chain (unwrapped part).

Secondly; for two tail configuration; The free energy of the system can be written similar to equation A.2, keeping in mind that we have two tails instead of one, each with length$\frac{L_2}{2}$

$$F = F_1 + L_2 ln\left(\frac{L_2}{2a}\right) + 2(L_1 - \mathcal{L}) ln\left(\frac{L_2+2R}{2R}\right) + (L_2 + 2R) ln\left(\frac{L_2+2R}{2R}\right) - (L_2 + 4R) ln\left(\frac{L_2+4R}{4R}\right) \quad \text{(A.3)}$$

The last two terms describe the interaction between the tails.

Shklovskii had described configurations with one tail and two tails separately. One should ask which of them is realized at a given L. Numerical calculations show that, when L is not very large, the overcharged, one-tail configuration is lower in energy. At a very large value of L, the complex undergoes a first-order phase transition to a two-tails configuration and becomes undercharged.

In practical situations, there is always a finite salt concentration in a water solution. One, therefore, has to take the finite screening length $r_s$ into account. For any reasonable $r_s$ and all Coulomb interactions responsible for the transition from one to two tails are screened out. Therefore, in a salty solution the two-tail configuration disappears.

The total form of the equation that Shklovskii did can be written as the following:

$$F(L_1) = F_{compl}(L_1) + F_{chain}(L_2) + F_{compl-chain}(L_1) + F_{elastic}(L_1) \quad \text{(A.4)}$$

The first term in equation A.4, $F_{compl}(L_1)$ represents the charging free energy of the complex of charge $Z(L_1)e$, the second term $F_{chain}(L_2)$, is the total entropic free energy of the remaining chain of length ( $L_2$ ). The third term $F_{compl-chain}(L_1)$, it represents the interaction free energy between the complex and the free chain of un-wrapped length of ($L_2$), and the last term $F_{elastic}(L_1)$, is the elastic (bending) free energy required to bend $L_1$ of the chain of radius of curvature around sphere of radius R.

**Appendix B: Shklovskii N-sphere model**

In this appendix we present the model developed by ShKlovskii and co-workers (Shklovskii 2001) which studied the polyelectrolyte with N-sphere complex. In the case of weak screening, the free energy of the complex of a PE with length *L* and charge density $\eta$winding consequently around *N* oppositely charged spheres of charge *q* and radius *R* as shown in figure B.1.we assume the complex is in a low salt concentration the screening radius $r_D$ is larger than the distance between two neighboring spheres (x+2R).Taking into account that the length of the PE segment that winds around each sphere is $(\frac{\boldsymbol{L}}{\boldsymbol{N}} - \boldsymbol{x})$, we have

$$F(N,x) = \frac{Q^{*2}}{DN(x+2R)} ln\mathbf{N} + Nf(x) \qquad \text{B.1}$$

Here D is the dielectric constant of water. The first term is the macroscopic self-energy of the necklace, and the second term accounts for the total energy of one period of the necklace. It is calculated as the energy of a Wigner–Seitzcell consisting of a sphere with two PE tails of length $\frac{x}{2}$.

$$f(x) = \frac{q^{*2}}{2RD} - \frac{2q^*\eta}{D} ln\frac{x+2R}{2R} + (x+2R)\frac{\eta^2}{D} ln\frac{x+2R}{2R} - (x+4R)\frac{\eta^2}{D} ln\frac{x+4R}{4R} + \left(\frac{L}{N} - x\right)\frac{\eta^2}{D} ln\frac{A}{a} + x\frac{\eta^2}{D} ln\frac{x}{2a} \qquad \text{B.2}$$

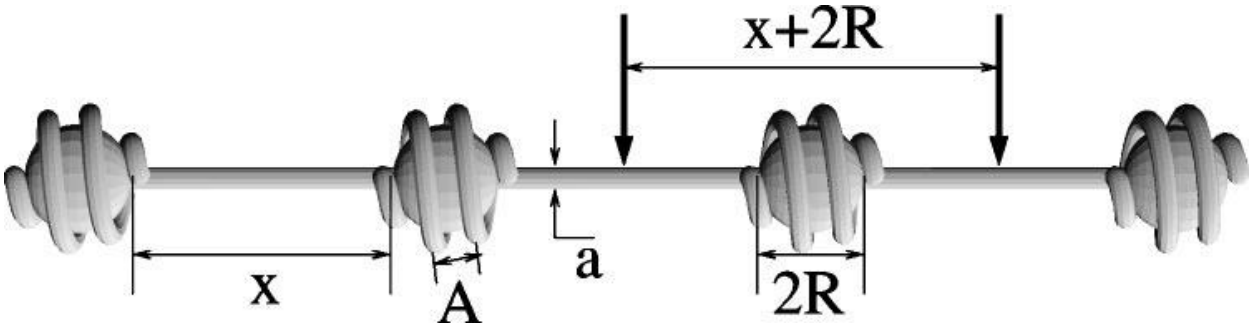


Figure B.1. The beads-on-a-string complex of a negative PE molecule and many positive spheres. On the surface of each sphere, due to the Coulomb repulsion, neighboring PE turns lie parallel to each other. Locally, they resemble an one-dimensional Wigner crystal with the lattice constant *A*. At a larger scale, charged spheres repel each other and form another one-dimensional Wigner crystal along the PE with lattice constant *x*+2*R*. A Wigner–Seitz cell of this crystal is shown by the thick arrows.

At a length scale greater than its period *x*+2*R*, the complex is a uniform rod of length *N*(*x*+2*R*) and charge density $\frac{Q^*}{N(x+2R)}$. The logarithmic divergence of this energy is cut off at small distances by *x*+2*R* and at large distances by the length$\mathbf{N}(x+2R) = \min\{r_D, N(x+2R)\}$, where $N(x+2R)$ is the rod length. The first terms in equation B.2 accounts for the self-energy of the adsorbed sphere with net charge $q^*$ at the PE. The second term accounts for the interaction of the sphere with the tails,the third and fourth terms account for the interaction between the tails. The fifth and sixth terms are, respectively, the self-energies of the PE wound around the macroion (which is screened at distance *A* between turns) and of the two straight tails with length $\frac{x}{2}$. It

should be noted that writing down the second of equation B.1 as Nf(x)we have neglected the difference between the end spheres with those in the middle of the PE. This is justified for a reasonably large value of N. It should also be noted that we neglected the entropy of the PE monomers in the tails and at the spheres surface.

Approximating $A \cong R^2/(L/N - x)$ and keeping only terms of the highest orderin the large parameter $\frac{x}{R}$, one can rewrite these equationsas

$$F(N,x) = \frac{\boldsymbol{\delta^2}}{x} N ln\mathbf{N} + Nf(x) \qquad \text{B.3}$$

$$f(x) = \frac{(\boldsymbol{\delta+x})^2}{2R} - 2(\delta + x) ln\frac{x}{R} - \left(\frac{L}{N} - x\right) ln\frac{\left(\frac{L}{N}-x\right)}{R^2} + x ln\frac{x}{2a} \qquad \text{B.4}$$

where we introduce the PE length needed to neutralize one sphere$\mathcal{L} = \frac{q}{\eta}$ and $\delta = \mathcal{L} - \frac{L}{N} = \frac{Q^*}{N\eta}$. So that,$q^* = \eta(\delta + x)$. The energies is written in units of $\frac{\eta^2}{D}$, hence has the dimensionality of length. At a given *N*, the optimal distance *x* can be calculated by minimizing the free energy *F*(*N*,*x*) with respect to *x*. This gives, to the leading terms

$$\frac{\partial F}{\partial x} = -\frac{\delta^2}{x^2} ln\big(N(x + 2R)\big) + \frac{\delta+x}{R} - ln\frac{x}{R} + ln\frac{\frac{L}{N}-x}{R} = 0 \qquad \text{B.5}$$

The physical meaning of each term in equation B.5 is quite clear. When one brings a unit length of the PE from thesphere surface to their tails, thereby increasing *x*, the four terms of equation B.5 are, respectively, the lowering in the system's macroscopic energy (with increasing *x*), the potential energy cost due to the attraction of the PE to the sphere, the potential energy gained due to the repulsion of two PE tails of each sphere and finally the cost in the correlation energy at the surface of the sphere.

Until now, we assumed the salt concentration is small enough so that the screening radius $r_D$is larger than the distance between neighboring spheres, *x*. In the case ofhigher salt concentration when $r_D \ll x$, our theory needs some modifications. First, the macroscopic energy term [thefirst term in equation B.1] has to be replaced by the sum of repulsionenergies of neighboring spheres. When R$\ll r_D \ll x$, itstill has the form of interaction of two pointlike charges.

$$F(N,x) = N\frac{q^{*2}}{x+2R} e^{\frac{-(x+2R)}{r_D}} + Nf(x) \qquad \text{B.6}$$

At the same time, all the logarithmic factors in equation B.2 for $f(x)$ are cut off at $r_D$instead of *x*. Correspondingly, equation B.5 [which is the result of the minimization of *F*(*N*,*x*) with respect to *x* at a given *N*] should be replaced by

$$\frac{\partial F}{\partial x} = -\frac{(\delta+x)^2}{x r_D} e^{-x/r_D} + \frac{\delta+x}{R} - ln\frac{r_D}{R} + ln\frac{\frac{L}{N}-x}{R} = 0 \qquad \text{B.7}$$

## Refrences


[1] Cao, Q., & Bachmann, M. (2013). Electrostatic complexation of linear polyelectrolytes with soft spherical nanoparticles. *Chemical Physics Letters*,*586*, 51-55.

[2] Nrmak, D. L., &McCammon, J. A. (1978). Brownian dynamics with hydrodynamic interactions. *The Journal of chemical physics*, *69*(4), 1352-1360

[3] Ainalem, M. L., Carnerup, A. M., Janiak, J., Alfredsson, V., Nylander, T., &Schillén, K. (2009). Condensing DNA with poly (amido amine) dendrimers of different generations: means of controlling aggregate morphology. *Soft Matter*,*5*(11), 2310-2320.

[4] Cao, Q., & Bachmann, M. (2013). Electrostatic complexation of linear polyelectrolytes with soft spherical nanoparticles. *Chemical Physics Letters*,*586*, 51-55.

[5] Carnerup, A. M., Ainalem, M. L., Alfredsson, V., & Nylander, T. (2011). Condensation of DNA using poly (amido amine) dendrimers: effect of salt concentration on aggregate morphology. *Soft Matter*, *7*(2), 760-768.

[6] Jonsson, M., &Linse, P. (2001). Polyelectrolyte–macroion complexation. II. Effect of chain flexibility. *The Journal of Chemical Physics*, *115*(7), 3406-3418.

[7] Lyulin, S. V., Darinskii, A. A., &Lyulin, A. V. (2005). Computer simulation of complexes of dendrimers with linear polyelectrolytes. *Macromolecules*, *38*(9), 3990-3998.

[8] Lyulin, S., Karatasos, K., Darinskii, A., Larin, S., & Lyulin, A. (2008). Structural effects in overcharging in complexes of hyperbranched polymers with linear polyelectrolytes. *Soft Matter*, *4*(3), 453-457.

[9] Anderson, D. P. An, Yuehuei, Adjunct Associate Professor, Bioengineering. MD, Harbin Medical University (China), 1983; MM, Beijing Medical University (China), 1986 Anderson, Daniel Morgan, Lecturer, Parks, Recreation, and Tourism Management. BS, Western Illinois University, 1997.

[10] Nguyen, T. T., &Shklovskii, B. I. (2001). Complexation of a polyelectrolyte with oppositely charged spherical macroions: giant inversion of charge. *The Journal of Chemical Physics*, *114*(13), 5905-5916.

[11] Örberg, M. L., Schillén, K., &Nylander, T. (2007). Dynamic light scattering and fluorescence study of the interaction between double-stranded DNA and poly (amido amine) dendrimers. *Biomacromolecules*, *8*(5), 1557-1563

[12] Qamhieh, K., Nylander, T., &Ainalem, M. L. (2009). Analytical model study of dendrimer/DNA complexes. *Biomacromolecules*, *10*(7), 1720-1726.

[13] Netz, R. R., &Joanny, J. F. (1999). Complexation between a semiflexible polyelectrolyte and an oppositely charged sphere. *Macromolecules*, *32*(26), 9026-9040.

[14] Schiessel, H., Gelbart, W. M., & Bruinsma, R. (2001). DNA folding: structural and mechanical properties of the two-angle model for chromatin. *Biophysical Journal*, *80*(4), 1940-1956.

[15] Carnerup, A. M., Ainalem, M. L., Alfredsson, V., &Nylander, T. (2011). Condensation of DNA using poly (amido amine) dendrimers: effect of salt concentration on aggregate morphology. *Soft Matter*, *7*(2), 760-768.

[16] Nguyen, T. T., &Shklovskii, B. I. (2001). Complexation of a polyelectrolyte with oppositely charged spherical macroions: giant inversion of charge. *The Journal of Chemical Physics*, *114*(13), 5905-5916.

[17] Lyulin, S. V., Darinskii, A. A., &Lyulin, A. V. (2005). Computer simulation of complexes of dendrimers with linear polyelectrolytes. *Macromolecules*, *38*(9), 3990-3998.

[18] Nguyen, T. T., &Shklovskii, B. I. (2001). Complexation of a polyelectrolyte with oppositely charged spherical macroions: giant inversion of charge. *The Journal of Chemical Physics*, *114*(13), 5905-5916.

[19] Paul, A., Shao, W., Abbasi, S., Shum-Tim, D., & Prakash, S. (2012). PAMAM dendrimer-baculovirusnanocomplex for microencapsulated adipose stem cell-gene therapy: in vitro and in vivo functional assessment. *Molecular pharmaceutics*, *9*(9), 2479-2488.

[20] Overturf, K., Al-Dhalimy, M., Tanguay, R., Brantly, M., Ou, C. N., Finegold, M., &Grompe, M. (1996). Hepatocytes corrected by gene therapy are selected in vivo in a murine model of hereditary tyrosinaemia type I. *Nature genetics*,*12*(3), 266-273.

[21] Williams, B. A., Lin, L., Lindsay, S. M., &Chaput, J. C. (2009). Evolution of a histone H4-K16 acetyl-specific DNA aptamer. *Journal of the American Chemical Society*, *131*(18), 6330-6331.

[22] McMurray, C. T., Small, E. W., & Van Holde, K. E. (1991). Binding of ethidium to the nucleosome core particle. 2. Internal and external binding modes.*Biochemistry*, *30*(23), 5644-5652.

[23] Ainalem, M. L., &Nylander, T. (2011). DNA condensation using cationic dendrimers—morphology and supramolecular structure of formed aggregates.*Soft Matter*, *7*(10), 4577-4594.

[24] Chang, H. Y., Lin, Y. L., Sheng, Y. J., &Tsao, H. K. (2013). Structural Characteristics and Fusion Pathways of Onion-Like Multilayered Polymersome Formed by Amphiphilic Comb-Like Graft Copolymers. *Macromolecules*, *46*(14), 5644-5656.

[25] Jain, K. K. (Ed.). (2014). *Drug delivery system*.Humana Press/Springer.

[26] Likens, G. E., Bormann, F. H., Johnson, N. M., Fisher, D. W., & Pierce, R. S. (1970). Effects of forest cutting and herbicide treatment on nutrient budgets in the Hubbard Brook watershed-ecosystem. *Ecological monographs*, *40*(1), 23-47.

[27] Netz, R. R., &Joanny, J. F. (1999). Complexation between a semiflexible polyelectrolyte and an oppositely charged sphere. *Macromolecules*, *32*(26), 9026-9040.

[28] Qamhieh, K., Nylander, T., &Ainalem, M. L. (2009). Analytical model study of dendrimer/DNA complexes. *Biomacromolecules*, *10*(7), 1720-1726.

[29] Hayakawa, K., Santerre, J. P., &Kwak, J. C. (1983). The binding of cationic surfactants by DNA. *Biophysical chemistry*, *17*(3), 175-181.

[30] Overturf, K., Al-Dhalimy, M., Tanguay, R., Brantly, M., Ou, C. N., Finegold, M., &Grompe, M. (1996). Hepatocytes corrected by gene therapy are selected in vivo in a murine model of hereditary tyrosinaemia type I. *Nature genetics*,*12*(3), 266-273.

[31] Kikuchi, I. S., & Carmona-Ribeiro, A. M. (2000). Interactions between DNA and synthetic cationic liposomes. *The Journal of Physical Chemistry B*, *104*(13), 2829-2835.

[32] Wagner, K., Harries, D., May, S., Kahl, V., Rädler, J. O., & Ben-Shaul, A. (2000). Direct evidence for counterion release upon cationic lipid-DNA condensation. *Langmuir*, *16*(2), 303-306.

[33] Qamhieh, K., Nylander, T., Black, C. F., Attard, G. S., Dias, R. S., &Ainalem, M. L. (2014). Complexes formed between DNA and poly (amido amine) dendrimers of different generations–modelling DNA wrapping and penetration.*Physical Chemistry Chemical Physics*, *16*(26), 13112-13122.

[34] Bhattacharya, S., & Mandal, S. S. (1997). Interaction of surfactants with DNA. Role of hydrophobicity and surface charge on intercalation and DNA melting.*BiochimicaetBiophysicaActa (BBA)-Biomembranes*, *1323*(1), 29-44.

[35] Lasic, D. D., &Papahadjopoulos, D. (Eds.). (1998). *Medical applications of liposomes*.Elsevier.

[36] Braun, C. S., Vetro, J. A., Tomalia, D. A., Koe, G. S., Koe, J. G., & Russell Middaugh, C. (2005). Structure/function relationships of polyamidoamine/DNA dendrimers as gene delivery vehicles. *Journal of pharmaceutical sciences*,*94*(2), 423-436.

[37] Eichman, J. D., Bielinska, A. U., Kukowska-Latallo, J. F., & Baker, J. R. (2000). The use of PAMAM dendrimers in the efficient transfer of genetic material into cells. *Pharmaceutical science & technology today*, *3*(7), 232-245.

[38] Hellweg, T., Henry-Toulmé, N., Chambon, M., & Roux, D. (2000). Interaction of short DNA fragments with the cationic polyelectrolyte poly (ethylene imine): a dynamic light scattering study. *Colloids and Surfaces A: Physicochemical and Engineering Aspects*, *163*(1), 71-80.

[39] Ainalem, M. L., Bartles, A., Muck, J., Dias, R. S., Carnerup, A. M., Zink, D., &Nylander, T. (2014). DNA Compaction Induced by a Cationic Polymer or Surfactant Impact Gene Expression and DNA Degradation. *PloS one*, *9*(3), e92692.

[40] Ainalem, M. L., Carnerup, A. M., Janiak, J., Alfredsson, V., Nylander, T., &Schillén, K. (2009). Condensing DNA with poly (amido amine) dendrimers of different generations: means of controlling aggregate morphology. *Soft Matter*,*5*(11), 2310-2320.

[41] Schiessel, H. (2003). Charged rosettes at high and low ionic strengths.*Macromolecules*, *36*(9), 3424-3431.

[42] Schiessel, H., Gelbart, W. M., & Bruinsma, R. (2001). DNA folding: structural and mechanical properties of the two-angle model for chromatin. *Biophysical Journal*, *80*(4), 1940-1956.

[43] Nguyen, T. T., &Shklovskii, B. I. (2001). Complexation of a polyelectrolyte with oppositely charged spherical macroions: giant inversion of charge. *The Journal of Chemical Physics*, *114*(13), 5905-5916.

[44] Nguyen, T. T., &Shklovskii, B. I. (2001). Complexation of DNA with positive spheres: phase diagram of charge inversion and reentrant condensation. *The Journal of Chemical Physics*, *115*(15), 7298-7308.

[45] Grosberg, A. Y., Nguyen, T. T., &Shklovskii, B. I. (2002). Colloquium: the physics of charge inversion in chemical and biological systems. *Reviews of modern physics*, *74*(2), 329.

[46] Lyulin, S. V., Darinskii, A. A., &Lyulin, A. V. (2005). Computer simulation of complexes of dendrimers with linear polyelectrolytes. *Macromolecules*, *38*(9), 3990-3998.

[47] Lyulin, S., Karatasos, K., Darinskii, A., Larin, S., & Lyulin, A. (2008). Structural effects in overcharging in complexes of hyperbranched polymers with linear polyelectrolytes. *Soft Matter*, *4*(3), 453-457.

[48] Eichman, J. D., Bielinska, A. U., Kukowska-Latallo, J. F., & Baker, J. R. (2000). The use of PAMAM dendrimers in the efficient transfer of genetic material into cells. *Pharmaceutical science & technology today*, *3*(7), 232-245.

[49] Svenson, S., &Tomalia, D. A. (2005). Dendrimers in biomedical applications—reflections on the field. *Advanced drug delivery reviews*, *57*(15), 2106-2129.

[50] Tomalia, D. A. (2005). Birth of a new macromolecular architecture: dendrimers as quantized building blocks for nanoscale synthetic polymer chemistry.*Progress in Polymer Science*, *30*(3), 294-324.

[51] Lee, I., Athey, B. D., Wetzel, A. W., Meixner, W., & Baker, J. R. (2002). Structural molecular dynamics studies on polyamidoaminedendrimers for a therapeutic application: effects of pH and generation. *Macromolecules*, *35*(11), 4510-4520.

[52] Bohinc, K., Iglič, A., Maset, S., & May, S. (2010, January). The interaction between charged macroions induced by rod-like ions.In *World Congress on Medical Physics and Biomedical Engineering, September 7-12, 2009, Munich, Germany* (pp. 329-331). Springer Berlin Heidelberg.

[53] Ausio, J., & Van Holde, K. E. (1986). Histone hyperacetylation: its effects on nucleosome conformation and stability. *Biochemistry*, *25*(6), 1421-1428.

[54] Boe, S., Longva, A. S., &Hovig, E. (2008). Evaluation of various polyethylenimine formulations for light-controlled gene silencing using small interfering RNA molecules. *Oligonucleotides*, *18*(2), 123-132.

[55] Kukowska-Latallo, J. F., Candido, K. A., Cao, Z., Nigavekar, S. S., Majoros, I. J., Thomas, T. P., ... & Baker, J. R. (2005). Nanoparticle targeting of anticancer drug improves therapeutic response in animal model of human epithelial cancer. *Cancer research*, *65*(12), 5317-5324.

[56] Haensler, J., &Szoka Jr, F. C. (1993). Polyamidoamine cascade polymers mediate efficient transfection of cells in culture. *Bioconjugate chemistry*, *4*(5), 372-379.

[57] Lee, C. C., MacKay, J. A., Fréchet, J. M., &Szoka, F. C. (2005). Designing dendrimers for biological applications. *Nature biotechnology*, *23*(12), 1517-1526.

[58] Williams, B. A., Lin, L., Lindsay, S. M., &Chaput, J. C. (2009). Evolution of a histone H4-K16 acetyl-specific DNA aptamer. *Journal of the American Chemical Society*, *131*(18), 6330-6331.

[59] Dautzenberg, H., Jaeger, W., Kötz, J., Philipp, B., Seidel, C., &Stscherbina, D. (1994). Polyelectrolytes: formation, characterization and application.

[60] Li, Y., Wang, S., Wang, Z., Qian, X., Fan, J., Zeng, X., ...&Ju, D. (2014). Cationic poly (amidoamine) dendrimers induced cyto-protective autophagy in hepatocellular carcinoma cells. *Nanotechnology*, *25*(36), 365101.

[61] Padilla De Jesús, O. L., Ihre, H. R., Gagne, L., Fréchet, J. M., & Szoka, F. C. (2002). Polyester dendritic systems for drug delivery applications: in vitro and in vivo evaluation. *Bioconjugate chemistry*, *13*(3), 453-461.

[62] Mourey, T. H., Turner, S. R., Rubinstein, M., Fréchet, J. M. J., Hawker, C. J., & Wooley, K. L. (1992). Unique behavior of dendritic macromolecules: intrinsic viscosity of polyether dendrimers. *Macromolecules*, *25*(9), 2401-2406.

[63] Padilla De Jesús, O. L., Ihre, H. R., Gagne, L., Fréchet, J. M., & Szoka, F. C. (2002). Polyester dendritic systems for drug delivery applications: in vitro and in vivo evaluation. *Bioconjugate chemistry*, *13*(3), 453-461.

[64] Adronov, A., Gilat, S. L., Frechet, J. M., Ohta, K., Neuwahl, F. V., & Fleming, G. R. (2000). Light harvesting and energy transfer in laser-dye-labeled poly (aryl ether) dendrimers. *Journal of the American Chemical Society*, *122*(6), 1175-1185. [65] Tomalia, D. A. (2005). Birth of a new macromolecular architecture: dendrimers as quantized building blocks for nanoscale synthetic polymer chemistry.*Progress in Polymer Science*, *30*(3), 294-324.

[65] Gilat, S. L., Adronov, A., & Frechet, J. M. (1999). Light harvesting and energy transfer in novel convergently constructed dendrimers. *AngewandteChemie International Edition*, *38*(10), 1422-1427.

[66] Roberts, J. C., Bhalgat, M. K., &Zera, R. T. (1996). Preliminary biological evaluation of polyamidoamine (PAMAM) StarburstTMdendrimers. *Journal of biomedical materials research*, *30*(1), 53-65.

[67] Malik, N., Wiwattanapatapee, R., Klopsch, R., Lorenz, K., Frey, H., Weener, J. W., ... & Duncan, R. (2000). Dendrimers:: Relationship between structure and biocompatibility in vitro, and preliminary studies on the biodistribution of 125I-labelled polyamidoaminedendrimers in vivo. *Journal of Controlled Release*,*65*(1), 133-148.

[68] Kukowska-Latallo, J. F., Candido, K. A., Cao, Z., Nigavekar, S. S., Majoros, I. J., Thomas, T. P., ... & Baker, J. R. (2005). Nanoparticle targeting of anticancer drug improves therapeutic response in animal model of human epithelial cancer. *Cancer research*, *65*(12), 5317-5324.

[69] Haensler, J., &Szoka Jr, F. C. (1993). Polyamidoamine cascade polymers mediate efficient transfection of cells in culture. *Bioconjugate chemistry*, *4*(5), 372-379.

[70] Zieliński,Długosz, M., P., &Trylska, J. (2011). Brownian dynamics simulations on CPU and GPU with BD_BOX. *Journal of computational chemistry*, *32*(12), 2734-2744.

[71] Bourne, N., Stanberry, L. R., Kern, E. R., Holan, G., Matthews, B., & Bernstein, D. I. (2000). Dendrimers, a new class of candidate topical microbicides with activity against herpes simplex virus infection. *Antimicrobial agents and chemotherapy*, *44*(9), 2471-2474.

[72] Briñas, R. P., Troxler, T., Hochstrasser, R. M., &Vinogradov, S. A. (2005). Phosphorescent oxygen sensor with dendritic protection and two-photon absorbing antenna. *Journal of the American Chemical Society*, *127*(33), 11851-11862.

[73] Choyke, P. L., & Kobayashi, H. (2006).Functional magnetic resonance imaging of the kidney using macromolecular contrast agents. *Abdominal imaging*, *31*(2), 224-231.

[74] Dunphy, I., Vinogradov, S. A., & Wilson, D. F. (2002). Oxyphor R2 and G2: phosphors for measuring oxygen by oxygen-dependent quenching of phosphorescence. *Analytical biochemistry*, *310*(2), 191-198.

[75] Bloomfield, V. A. (1996). DNA condensation. *Current opinion in structural biology*, *6*(3), 334-341.

[76] Boe, S., Longva, A. S., &Hovig, E. (2008). Evaluation of various polyethylenimine formulations for light-controlled gene silencing using small interfering RNA molecules. *Oligonucleotides*, *18*(2), 123-132.

[77] Boe, S., Longva, A. S., &Hovig, E. (2008). Evaluation of various polyethylenimine formulations for light-controlled gene silencing using small interfering RNA molecules. *Oligonucleotides*, *18*(2), 123-132.

[78] Barratt, E. S., Stanford, M. S., Kent, T. A., & Alan, F. (1997). Neuropsychological and cognitive psychophysiological substrates of impulsive aggression. *Biological psychiatry*, *41*(10), 1045-1061.

[79] Förster, S., & Schmidt, M. (1995). Polyelectrolytes in solution.In *Physical Properties of Polymers* (pp. 51-133).Springer Berlin Heidelberg.

[80] Salamone, J. C. (Ed.). (1998). *Concise polymeric materials encyclopedia* (Vol. 1).CRC press.

[81] Williams, B. A., Lin, L., Lindsay, S. M., &Chaput, J. C. (2009). Evolution of a histone H4-K16 acetyl-specific DNA aptamer. *Journal of the American Chemical Society*, *131*(18), 6330-6331.

[82] Strauss, J. K., & Maher, L. J. (1994). DNA bending by asymmetric phosphate neutralization. *Science*, *266*(5192), 1829-1834.

[83] Strauss, J. K., & Maher, L. J. (1994). DNA bending by asymmetric phosphate neutralization. *Science*, *266*(5192), 1829-1834.

[84] Simpson, R. T. (1990). Nucleosome positioning can affect the function of a cis-acting DMA elementin vivo.

[85] Qamhieh, K., &Khaleel, A. A. (2014). Analytical model study of complexation of dendrimer as an ion penetrable sphere with DNA. *Colloids and Surfaces A: Physicochemical and Engineering Aspects*, *442*, 191-198.

[86] Yager, T. D., McMurray, C. T., & Van Holde, K. E. (1989). Salt-induced release of DNA from nucleosome core particles. *Biochemistry*, *28*(5), 2271-2281.

[87] Dubin, P. L., Rigsbee, D. R., Gan, L. M., & Fallon, M. A. (1988).Equilibrium binding of mixed micelles to oppositely charged polyelectrolytes.*Macromolecules*, *21*(8), 2555-2559.

[88] McGhee, J. D., Wood, W. I., Dolan, M., Engel, J. D., &Felsenfeld, G. (1981). A 200 base pair region at the 5′ end of the chicken adult β-globin gene is accessible to nuclease digestion. *Cell*, *27*(1), 45-55.

[89] Carnerup, A. M., Ainalem, M. L., Alfredsson, V., &Nylander, T. (2011). Condensation of DNA using poly (amido amine) dendrimers: effect of salt concentration on aggregate morphology. *Soft Matter*, *7*(2), 760-768.

[90] Lasic, D. D., &Papahadjopoulos, D. (Eds.). (1998). *Medical applications of liposomes*.Elsevier.

[91] Jonsson, M., &Linse, P. (2001). Polyelectrolyte–macroion complexation. I. Effect of linear charge density, chain length, and macroion charge. *The Journal of Chemical Physics*, *115*(7), 3406-3418.

[92] Lyulin, S. V., Darinskii, A. A., &Lyulin, A. V. (2005). Computer simulation of complexes of dendrimers with linear polyelectrolytes. *Macromolecules*, *38*(9), 3990-3998.

[93] Nrmak, D. L., &McCammon, J. A. (1978). Brownian dynamics with hydrodynamic interactions. *The Journal of chemical physics*, *69*(4), 1352-1360

[94] Zieliński,Długosz, M., P., &Trylska, J. (2011). Brownian dynamics simulations on CPU and GPU with BD_BOX. *Journal of computational chemistry*, *32*(12), 2734-2744.

**الملخص**

لقد تمت دراسة عملية الترابط بين عدد من الدندريمر ( dendrimer) والحمض النووي باستخدام نموذج نظري جديد يصف التفاعل بين (LPE chain) ومجموعة من الكرات الصلبة، وقد وجد أنه في حالة وجود دينديريمر واحد، اثنان أو ثلاثة فإن الجزء الملتف من (LPE chain) على هذه الدينديريمرز يزداد بزيادة طول ( LPE chain) حتى يصل إلى قيمة عظمى ليثبت في النهاية عند قيمة ثابتة. في هذا النموذج وجد أن الذيل يظهر في حالة وجود دينديريمر واحد وفي حالة وجود أكثر من واحد فإنه يتكون (linker between two dendrimers) ومن الجدير بالذكر هنا أنّه عندما يتكون هذا الترابط بين الدينديريمر وLPE فإن الدينديريمر يكون (overcharged) عند جميع الأطوال.

بالإضافة إلى هذا النموذج النظري، فقد تم استخدام طريقة محاكاة (Brownain Dynamic Simulation) لدراسة التفاعل بين ثلاثة دينديريمرز مع LPE، وقد وجد أن نصف قطر الالتفاف (Radius of gyration ) لهذا التفاعل يزداد بزيادة طول LPE حتى يصل إلى قيمة ثابتة في نهاية التفاعل. لقد تمت دراسة التفاعل هذا أيضا عن طريق ايجاد المسافة بين دينديريمرز و LPE beads وقد وجد أن هذه المسافة تقل بزيادة التفاعل حتى تصل أقل قيمة لها في نهاية التفاعل.